Diabetologia Springer

Systems biology of the IMIDIA biobank from organ donors and pancreatectomized patients defines a novel transcriptomic signature of type 2 diabetes islets

Journal:	*Diabetologia*
Manuscript ID	Draft
Manuscript Type:	Article
Keywords:	3.02.01 Islets, 3.01.03 Genetics of type 2 diabetes, 4.02 Microarray, 4.11 Biological statistics, 2.10 Human

SCHOLARONE™
Manuscripts

For Peer Review

Systems biology of the IMIDIA biobank from organ donors and pancreatectomized patients defines a novel transcriptomic signature of type 2 diabetes islets

Michele Solimena[1,2,3,*], Anke M. Schulte[4,*], Lorella Marselli[5], Florian Ehehalt[1,2,6], Daniela Richter[1,2], Manuela Kleeberg[1,2,6], Hassan Mziaut[1,2], Klaus-Peter Knoch[1,2], Julia Parnis[7], Marco Bugliani[5], Afshan Siddiq[8], Anne Jörns[9], Frédéric Burdet[10], Robin Liechti[10], Mara Suleiman[5], Daniel Margerie[4], Farooq Syed[5], Marius Distler[6], Robert Grützmann[11], Enrico G. Petretto[21], Aida Moreno-Moral[21], Carolin Wegbrod[1,2], Anke Sönmez[1,2], Katja Pfriem[1,2], Anne Friedrich[1,2], Jörn Meinel[12], Claes B. Wollheim[13], Gustavo B. Baretton[12], Raphael Scharfmann[14], Everson Nogoceke[15], Ezio Bonifacio[1,2,16], Dorothée Sturm[1,2,6], Birgit Meyer-Puttlitz[4], Ugo Boggi[5], Hans-Detlev Saeger[1,2,6], Franco Filipponi[5], Mathias Lesche[17], Paolo Meda[13], Andreas Dahl[17], Leonore Wigger[10], Ioannis Xenarios[10], Mario Falchi[8], Bernard Thorens[18], Jürgen Weitz[1,2,6], Krister Bokvist[19], Sigurd Lenzen[9], Guy A. Rutter[7], Philippe Froguel[8,20,21], Manon von Bülow[4], Mark Ibberson[10,*], Piero Marchetti[5,*]

Affiliations

[1]Paul Langerhans Institute Dresden of the Helmholtz Center Munich at University Hospital Carl Gustav Carus and Faculty of Medicine, TU Dresden, 01307 Dresden, Germany.

[2]German Center for Diabetes Research (DZD e.V.), 85764 Neuherberg, Germany.

[3]Max Planck Institute of Molecular Cell Biology and Genetics, 01307 Dresden, Germany.

[4]Sanofi-Aventis Deutschland GmbH, 65926 Frankfurt am Main, Germany.

[5]Department of Clinical and Experimental Medicine, University of Pisa, 56126 Pisa, Italy.

[6]Department of Visceral-Thoracic-Vascular Surgery, University Hospital Carl Gustav Carus and Faculty of Medicine, TU Dresden, 01307 Dresden, Germany.

For Peer Review

[7]Section of Cell Biology and Functional Genomics, Division of Diabetes, Endocrinology and Metabolism, Imperial Centre for Translational and Experimental Medicine, Imperial College London, London W12 0NN, UK.

[8]Department of Genomics of Common Disease, School of Public Health, Imperial College London, Hammersmith Hospital, London W12 0NN, UK.

[9]Institute of Clinical Biochemistry, Hannover Medical School, 30625 Hannover, Germany.

[10]Vital-IT Group, Swiss Institute of Bioinformatics, 1015 Lausanne, Switzerland.

[11] Department of Surgery, University Hospital of Erlangen, 91054 Erlangen, Germany.

[12]Department of Pathology, University Hospital Carl Gustav Carus and Faculty of Medicine, TU Dresden, 01307 Dresden, Germany.

[13]Department of Cell Physiology and Metabolism, Geneva University Medical Center, 41211 Geneva, Switzerland.

[14]INSERM, U1016, Institut Cochin, Faculté de Médecine, Université Paris Descartes, Sorbonne Paris Cité, Paris 75014, France.

[15]F. Hoffmann-La Roche Ltd, Roche Innovation Center Basel, Basel, Switzerland.

[16]Center for Regenerative Therapies Dresden, TU Dresden, 01307 Dresden, Germany.

[17]Biotechnology Center, TU Dresden, 01307 Dresden, Germany.

[18]Centre for Integrative Genomics, University of Lausanne, 1015 Lausanne, Switzerland.

[19]Lilly Research Laboratories, Eli Lilly, 46285-0001 Indianapolis, IN, USA.

[20]CNRS-UMR8199, Lille Pasteur Institute, Lille 59000, France; Lille University, Lille 59000, France; European Genomic Institute for Diabetes (EGID), Lille 59000, France.

[21]Medical Research Council (MRC) Clinical Sciences Centre, Imperial College London, London, UK.

Confidential

*Corresponding authors: michele.solimena@tu-dresden.de; anke.schulte@sanofi.com; mark.ibberson@sib.swiss; piero.marchetti@med.unipi.it

Pages: 42

Title: 153 characters; Abstract: 366 words; Text (main text): 6,567 words

Figures: 6; Tables: 2

Supplementary Figures: 7; Supplementary Tables: 8

Running title: Gene signature of T2D islets

Confidential

Abstract

Objective:

Pancreatic islet beta cell failure causes human type 2 diabetes (T2D). To identify gene expression changes in T2D islets the IMIDIA consortium (www.imidia.org) established a comprehensive, unique multicenter biobank of human islets and pancreas tissues from organ donors (OD) and partially pancreatectomized patients (PPP).

Methods:

Pancreatic islets were isolated either by enzymatic digestion from 103 OD, including 84 non-diabetic (ND) and 19 T2D subjects, or by laser capture microdissection (LCM) from surgical specimens of 103 metabolically phenotyped partially pancreatectomized patients (PPP), including 32 ND, 36 with T2D, 15 with impaired glucose tolerance (IGT) and 20 with 20 with recent onset diabetes (<1 year), conceivably secondary to the pancreatic disorder leading to surgery (T3cD). The islet transcriptome was assessed on Affymetrix microarrays. Bioinformatics tools were used to i) compare the islet transcriptome of T2D vs. ND OD and PPP as well as vs IGT and T3cD within the PPP group; ii) identify transcription factors driving gene co-expression modules correlated with insulin secretion in vitro and glucose tolerance in vivo. Selected genes of interest were validated for expression and function in beta cells.

Results:

Comparative transcriptomic analysis identified 19 genes differentially expressed (fdr ≤0.05, fold change ≥1.5) in T2D islets vs. ND islets from both OD and PPP. Nine out of these 19 dysregulated genes were not previously reported to be differentially expressed in T2D islets. Among the signature genes are *TMEM37*, which we show to inhibit Ca2+-influx in beta cells and insulin secretion and *Arg2,* also shown to influence insulin secretion. Systems biology

Confidential

approaches identified *HNF1A*, *PDX1* and *REST as* drivers of gene co-expression modules correlated with impaired insulin secretion *ex vivo* or glucose tolerance *in vivo*, and enriched in 14/19 differentially expressed genes of T2D islets. None of these genes was significantly dysregulated in islets of IGT or T3cD PPP.

Conclusions:

These studies enabled the stringent definition of a novel transcriptomic signature of T2D islets, regardless of islet source and isolation procedure. Lack of this signature in islets from PPP with IGT or T3cD indicates differences possibly due to peculiarities of these hyperglycemic conditions and/or a role for duration and severity of hyperglycemia. Alternatively, these transcriptomic changes capture but may not precede beta cell failure.

Confidential

Introduction

Impaired beta cell function and viability are the ultimate and possibly primary causes of type 2 diabetes (T2D) (Halban et al, 2014; Kahn, 2003; Mehran et al, 2012; Mehran et al, 2012). These deficits have been ascribed to various, non-mutually exclusive mechanisms, such as glucolipotoxicity secondary to insulin resistance and inflammation, leading to oxidative and ER stress and apoptosis. Microscopy studies of post-mortem pancreata from non-diabetic (ND) and T2D subjects (Marselli et al, 2014; Rahier et al, 2008) as well as acute diabetes reversal following bariatric surgery (Mingrone et al, 2012; Schauer et al, 2012) partial pancreatectomy (Ehehalt et al, 2015) or severe caloric restriction have challenged the notion that beta cell death is the major cause of T2D onset. Instead, insufficient insulin secretion in T2D has been attributed to beta cell dysfunction due to several different mechanisms, possibly including de-differentiation (Cinti et al, 2016; Dor & Glaser, 2013; Marchetti & Ferrannini, 2015; Talchai et al, 2012).

Early comparative studies in islets from ≤7 ND and ≤6 T2D organ donors (OD) reported the downregulation ($p<0.01$) in T2D islets of the transcriptional regulators *HNF4A* and *ARNT* (Gunton et al, 2005), genes involved in regulated exocytosis and mitochondrial function (MacDonald et al, 2009; Ostenson et al, 2006) as well as islet structure and function (Bugliani et al, 2013). Groop and collaborators correlated the transcriptome of 54 ND and 9 T2D OD islets cultured for 1-9 days with *ex vivo* insulin secretion and clinical features, including HbA1c (Taneera et al, 2012). A more recent study by the same group compared the RNA sequencing profile of islets from 51 ND, 12 T2D as well as 15 subjects with impaired glucose tolerance (IGT, i.e. 6%≤ HbA1c <6.5%) (Fadista et al, 2014). Collectively, these studies found several

genes to be differentially expressed in T2D islets, including some related to insulin secretion and/or HbA1c (Fadista et al, 2014; Taneera et al, 2012) beta cell apoptosis (Taneera et al, 2015), or cell cycle and proliferation (Andersson et al, 2012; Taneera et al, 2013). Furthermore, they also reported the upregulation of *SFRP4* in T2D islets, which might link islet inflammation to beta cell dysfunction (Mahdi et al, 2012).

More recently, RNA-seq studies have been published using single human pancreatic cells, obtained from islets isolated from ND and T2D OD by enzymatic digestion (Xin et al, 2016) or dissociation and FACS distribution (Segerstolpe et al, 2016). The comparison of beta cells isolated from ND (respectively from 12 and 6) or T2D (respectively from 6 and 4) ODs revealed 48 (Xin et al, 2016) or 75 (Segerstolpe et al, 2016) transcripts as being differentially expressed between control and diseased samples. Interestingly, only one gene (*FXYD2)* was regulated in both studies, albeit in opposite directions. Therefore, the comparisons of transcriptomic features of single beta cells from ND and T2D ODs have so far been inconsistent. In addition, each of these studies on single beta cells identified 7 regulated transcripts (non overlapping between the two studies) which have been reported already to be regulated by comparing beta cells yielded with laser capture microdissection (LCM) from 10 ND and 10 T2D ODs (Marselli et al, 2010).

While the above mentioned studies provided insights into the molecular phenotype of T2D vs. ND islets and of single islet cell types, the diversities in the relative limited number of studied cases, in islet and cell handling, in platforms and analytic procedures could account for the different results reported in each study. Furthermore, all transcriptomic data were obtained from

Confidential

islets of ODs isolated enzymatically followed by *in vitro* culture; only in one instance beta cells yielded by LCM from frozen tissue sections were used (Marselli et al, 2010).

To identify gene robust expression changes in T2D islets independently of recruitment center and isolation procedure (enzymatic digestion vs. LCM), the IMIDIA consortium (www.imidia.org) has established a large multicenter biobank of human islets from OD and PPP. This innovative enabled us to define a novel transcriptomic signature of T2D islets as well as to evaluate its presence in islets of PPP subjects with glucose intolerance or T3cD.

.

Confidential

Results

The IMIDIA cohorts. We collected pancreatic specimens from two distinct cohorts (Figure 1a and Supplementary Table 1). One cohort consisted of 243 OD, including 204 ND and 39 T2D OD. T2D was diagnosed based on the subject's clinical history, treatment with anti-diabetic drugs, and the lack of multiple autoantibodies directed against GAD65. The second cohort included 201 PPP who underwent partial pancreatectomy for pancreatic diseases. Among PPP 70 were ND (fasting glycaemia <7.0 mmol/l; HbA1c ≤6.5%, glycaemia at 2 h after presurgical oral glucose tolerance test [OGTT] <7.8 mmol/l), 54 had T2D (fasting glycaemia ≥7.0 mmol/l; HbA1c >6.5%, history of diabetes for >1 year), 30 had impaired glucose tolerance (IGT) (fasting glycaemia <7.0 mmol/l; HbA1c ≤6.5%, OGTT at 2 h of ≥7.8 to <11.1 mmol/l), and 46 had diabetes, likely due to the associated pancreatic disorder leading to surgery, also termed type 3c diabetes (T3cD) (Ewald et al, 2012). A diagnosis of T3cD was made if pathological glucose tolerance (fasting glycaemia ≥7.0 mmol/l, HbA1c >6.5% and/or pre-surgical OGTT at 2 h ≥11.1 mmol/l) was first detected <1 year before the symptoms, which led to surgery. Finally, one PPP on insulin treatment had T1D based on the presence of multiple autoantibodies against islet autoantigens (GAD65, IA-2/ICA512). Pathology examination of the resected tissue did not reveal insulitis in any PPP. Notably, the mean age, BMI, and duration of T2D in the OD and PPP cohorts were similar, although males were slightly more frequent in the PPP cohort (Supplementary Table 1). When the function of islets prepared from OD was studied, stimulation of T2D islets with glucose or glyburide, but not with arginine, elicited a reduced insulin secretion [expressed as insulin stimulation index (ISI)] capacity compared to islets from ND OD

(Supplementary Fig. 1), supporting and complementing previous findings (Deng et al, 2004; Rosengren et al, 2012).

Islets for RNA extraction were isolated from pancreatic specimens of 141 OD (115 ND and 26 T2D) and 117 PPP (37 ND, 16 IGT, 41 T2D, 23 T3D) by enzymatic digestion or LCM, respectively. Following filter selection (details in Supplementary Information) RNA from 103 OD (84 ND and 19 T2D) and 103 PPP (32 ND, 36 T2D, 15 IGT and 20 T3cD) were used for transcriptomic profiling (Table 1). Blood fructosamine, a biomarker for glycaemia in the days preceding intensive care unit admission, was greater in T2D OD (222±72 µmol/l, n=11) than in ND OD (180±45 µmol/l, n=46, p=0.018). ND and T2D PPP did not differ regarding the prevalence of chronic pancreatitis, or benign/malignant tumors (Table 1 and Supplementary Fig. 2). Moreover, T2D OD and PPP were comparable for distribution of age (p=0.084), BMI (p=0.450) and duration of diabetes (p=0.709). Likewise, the age (p=0.782) and BMI (p=0.673) distributions of ND OD and PPP were similar.

Differentially expressed genes in T2D islets. In total, 4,438 probe sets of 29,529, corresponding to 2,976 unique genes, were differentially expressed in islets of T2D OD relative to ND OD (FDR ≤0.05). Overall, 608 probe sets corresponding to 444 gene annotations (of which 421 were specifically regulated in OD) showed a change in expression of ≥1.5 fold (Figure 2a and GEO, accession number: GSE76896). Of the top 20 differentially regulated genes, 18 were downregulated, while two were upregulated (Supplementary Table 2). A total of 1,439 of 29,612 probe sets were differentially expressed in T2D PPP islets compared with ND PPP islets (FDR≤0.05), corresponding to 1,039 unique genes. Overall, 208 probe sets corresponding to 136

Confidential

gene annotations (of which 113 were specifically regulated in PPP) showed a change in expression of ≥1.5 fold (Figure 2a and GEO, accession number: GSE76896). Of the top 20 differentially expressed genes, 12 were downregulated in T2D PPP islets, whereas 8 genes were upregulated (Supplementary Table 2). For T2D versus ND comparisons in both OD and PPP, the samples were first carefully filtered to remove any outliers (see Methods and Supplementary Methods). We then performed linear regression analysis with and without correction for different clinical variables to test the effect of potential confounders. From this analysis, age and sex were found to be potential confounders and were corrected for in the statistical analysis. Exocrine and ductal pancreatic markers were comparably low in the OD and PPP islets (see Supplementary Information for details), indicating that transcriptomic changes could not be attributed to differences in the extent of exocrine tissue contamination. Furthermore, islets isolated enzymatically from OD and PPP specimen clustered together by PCA and separately from the cluster of islets isolated by LCM from the same OD and PPP (Figure 1b), suggesting the influence of the isolation procedure (enzymatic for OD and LCM for PPP) rather than differences between OD and PPP.

Confidential

Dysregulated genes common to T2D OD and PPP islets. To identify the most reproducible transcriptomic changes in T2D islets independently from covariates such as the islet retrieval procedure (i.e., enzymatic digestion or LCM), the tissue source (i.e., OD or PPP) and/or the collecting center, we focused on genes that were significantly dysregulated in both samples (Supplementary Table 2). This approach allowed us to identify a restricted pool of 23 genes with FDR ≤0.05 and a fold change of ≥1.5, of which 19 were dysregulated in the same direction in T2D OD and PPP islets (Table 2 and Figure 2a). Fifteen genes were downregulated, including

SLC2A2, *ARG2*, *CHL1*, *PPP1R1A*, *FFAR4*, *TMEM37* (Figure 2b), *G6PC2*, and *CAPN13,* while 4 were upregulated (*KCNH8*, *FAM102B*, *FBXO32* and *CD44*). These 19 genes were correlated to the glucose stimulated insulin secretion index (ISI) of OD islets (Supplementary Fig. 3). Notably, 9 of the dysregulated genes, namely *ANKRD23/39*, *ASCL2*, *HHATL*, *NSG1*, *PCDH20*, *SCTR*, *CD44, FAM102B* and *FBXO32* have not been described in any previous study to be differentially expressed in human T2D islets.

A meta-analysis of a previously published transcriptomic dataset (Mahdi et al, 2012) from which three samples were excluded based on our own Affymetrix quality criteria, revealed dysregulation (FDR ≤0.05) of 114 probe sets, corresponding to 94 unique genes. We searched this dataset for the 19 genes dysregulated in both of our islet cohorts, and found that *CHL1*, *FFAR4* and *SLC2A2* were downregulated with an FDR ≤0.05 and a fold-change of ≥1.5, while *ANKRD23/39*, *ARG2*, *HHATL*, *PPP1R1A,* and *UNC5D* were downregulated with a FDR of ≤0.1 in T2D islets, thus confirming the robust downregulation of *CHL1*, *FFAR4*, and *SLC2A2* in T2D OD islets in a different cohort.

To understand whether our results were influenced by potential contamination of the PPP islet samples with cancer tissue, we used data from a recent published study, which identified the transcriptional profiles of four pancreatic cancer subtypes (Bailey et al, 2016). Comparing the differentially regulated genes from PPP islets to the signatures from each of the four cancer sub-types (as defined by statistical comparison of each subtype with the three others) revealed no enrichment of differentially regulated genes with ADEX, Immunogenic or Progenitor sub-type signatures (Supplementary Table 3). A small but significant enrichment with the squamous

Confidential

signature was found, but this enrichment was also present for OD samples, suggesting that this signature, which contains 2,366 genes (Supplementary Table 3) and is the largest among the four cancer signatures, is more related to islet cells than to the other cancer sub-types. In conclusion, based on available transcriptomics data, we find no evidence of contamination of our PPP islet samples with cancerous tissue.

The availability of islets from PPP with IGT or T3cD (Table 1) allowed us to investigate in these categories the changes in expression profiles of the 19 commonly dysregulated genes in T2D islets according to the extent of hyperglycaemia (Figure 2c). The expression levels of these 19 genes only differed significantly between T2D and ND PPP islets (FDR ≤0.05). Nonetheless, the fold-changes between T3cD and ND PPP islets were in the same direction albeit with smaller differences when compared to the changes between T2D and ND PPP islets. The fold-changes in IGT versus ND PPP islets were very low (≤1.6); only 3/19 genes had absolute fold-changes of >1.2. These diversities between islets from T2D (both OD and PPP), IGT (PPP) and T3cD (PPP) may be due to peculiarities of these conditions and/or different duration and severity of the hyperglycemia.

Validation of the selected genes. Some of the 19 differentially expressed genes detected in T2D OD and PPP islets (*SLC2A2*, *CHL1, PPP1R1A, ARG2*, and *TMEM37)* were previously shown already to be enriched in beta cells and altered in T2D OD islets (Taneera et al, 2012). However, others, including *NSG1* and *UNC5D*, have not previously been associated with T2D. Consistent with recent RNA sequencing data of sorted adult beta cells (n=7, ND) (Blodgett et al, 2015) *in situ* PCR on human pancreas sections confirmed islet expression of the 19 T2D signature genes

(Supplementary Fig. 4 and not shown). As proof of principle, we verified the protein expression and localization of ARG2, PPP1R1A and TMEM37 in human pancreas by immunomicroscopy. ARG2 was detected in a subset of insulin-positive and glucagon-positive cells (Figure 3a and Supplementary Fig. 5). Conversely, PPP1R1A was colocalized with insulin-positive cells, but its expression was weaker in glucagon-positive cells. TMEM37 was colocalized with insulin-positive cells and some glucagon-positive cells. We then compared the expression levels of *ARG2*, *PPP1R1A*, and *TMEM37* in islet alpha and beta cell-enriched fractions from 5 ND and 4 T2D OD by qRT-PCR (Figure 3b). All three genes were enriched in beta cells and downregulated in cells from T2D OD, consistent with our transcriptomic results.

Silencing of either *ARG2* (Supplementary Fig. 6a) or *PPP1R1A* (Supplementary Fig. 6b) in insulinoma INS-1E cells led to reduced ISI (Figures 3c, d), and the opposite was observed by siRNA-mediated downregulation of *TMEM37* in INS-1 832/13 cells (Figure 3e and Supplementary Fig. 6c). This latter finding is consistent with TMEM37 being an inhibitory subunit of voltage-gated calcium channels (Chu et al, 2001). Accordingly, *TMEM37* silencing increased the number of cells in which intracellular Ca^{2+} ($[Ca^{2+}]_i$) concentrations increased in response to glucose stimulation (Supplementary Fig. 6d, e). Additionally, *TMEM37* silencing increased $[Ca^{2+}]_i$ after exposure to high glucose (Figure 3f, Supplementary Fig. 6f). Overexpression of *mTMEM37-V5* (Supplementary Fig. 6g, h) reduced the ISI (Figure 3g) and $[Ca^{2+}]_i$ in basal conditions (Supplementary Fig. 6i) or in response to stimulation with high glucose or potassium (Figure 3h). These data indicate that reduced ARG2 and PPP1R1A expression inhibits insulin secretion while reduced TMEM37 expression enhances it.

Confidential

Enrichment of genes involved in insulin secretion. The differentially expressed probe sets were separated into those showing upregulation or downregulation, and enrichment analyses against gene ontology categories were performed (OD islets: 208 upregulated and 400 downregulated probe sets; PPP islets: 128 upregulated and 80 downregulated probe sets) (Supplementary Table 4). Interestingly, similar biological processes were enriched among the downregulated probe sets in both OD and PPP islets (Supplementary Table 5), particularly genes related to hormone secretion. For OD islets, 28 downregulated probe sets were assigned to insulin secretion (Supplementary Table 6), including 2 signature genes (i.e., *SLC2A2* and *G6PC2*). For PPP islets, the signals were somewhat weaker, with five down regulated probe sets including the same two 2 signature genes assigned to insulin secretion.

Distinct sets of upstream and downstream pathways were predicted for the OD and PPP cohorts. Next, all differentially expressed probe sets were uploaded to IPA (www.ingenuity.com) to identify enriched pathways and to predict downstream processes and upstream regulators. Figure 4 shows the results for OD or PPP islets. Among the enriched pathways, several were previously found to play a role in beta cell function. Two, "Maturity Onset Diabetes of Young (MODY) Signaling" and "Neuropathic Pain Signaling" were the only pathways in common among the top 20 identified in the individual cohorts. Thus, differences at the transcriptional level between the cohorts were confirmed also at the pathway level. Analysis of downstream functions using a literature-based prediction method (Kramer et al, 2014) revealed a decrease in processes controlling cAMP concentrations, neurotransmitter release, and synaptic transmission in OD islets, while pathways related to the quantities of beta cells, islet cells, and neuroendocrine cells were mostly affected in PPP islets (Supplementary Table 7).

The same method was used to identify putatively activated or inhibited upstream regulators of the differentially expressed genes. For OD islets, the highest inhibition scores were found for *ADCYAP1*, *NEUROD1*, *BDNF* and *PAX6* (Supplementary Table 8), supporting the altered differentiation of beta cells during development and/or their function and viability. Significant activation scores were found for *FOXO1* and especially *REST*, two transcriptional regulators, which preclude the differentiation of beta cells and/or their identity retention (Atouf et al, 1997; Talchai et al, 2012). *HNF1A* was the only transcription regulator that was predicted to be significantly inhibited in PPP islets.

Analysis of potential upstream regulators revealed key transcription factors (TFs) involved in beta cell dysfunction in T2D. To obtain a more holistic view of the processes affecting human beta cell function in human islets, we identified the gene co-expression modules and correlated them to patient characteristics and functional traits. Weighted correlation network analysis (WGCNA) (Langfelder & Horvath, 2008) performed on the expression data of ND OD and PPP islets identified 31 OD and 36 PPP gene co-expression modules, with module sizes ranging from 29 to 6,264 genes for OD and from 29 to 1,183 genes for PPP. We selected modules that significantly overlapped between OD and PPP and were correlated with patient or functional traits (Supplementary Information). This retrieved a set of 10 modules for further analysis. These 10 modules were enriched for 14/19 differentially expressed signature genes (p=3.34e−05); only *CAPN13*, *FFAR4*, *NSG1*, *FAM102B*, and *KCNH8* were absent from the selected modules.

Co-expressed genes included in each module may share the same transcriptional control. To investigate how these modules might be regulated, we identified putative TFs that could control

genes within these modules in a concerted fashion and that potentially affect beta cell function (workflow in Figure 5a) by using two complementary approaches. The first approach used a literature-based prediction method (Kramer et al, 2014) while the second focused on the enrichment of predicted transcription factor binding sites (TFBS) in the promoter sequences of the module genes (Kwon et al, 2012). The results of these approaches were used to generate two networks, one for each analysis, describing predicted upstream TF interactions with their predicted target genes. The networks were then merged into a single intersection network representing the TF–target gene interactions predicted by both approaches (Figure 5b). The resulting network contained 17 upstream TFs and 29 predicted TF–target gene interactions (Figure 5c). Several of these modules were correlated with insulin and glycaemia: the *blue, skyblue*, and *darkviolet* modules were correlated with the ISI of isolated OD islets while the *lightpink4* module was correlated with glucose concentrations at 2h after an OGTT in PPP (Figure 5c and Supplementary Information). Of note, 3/19 genes that showed robust differential expression in T2D OD and PPP islets (*PPP1R1A*, *SLC2A2*, and *CD44*) were present in this network and were potential targets of *PDX1*. We therefore hypothesized that *PDX1* and other TFs in the network may regulate the differentially expressed genes in T2D. The volcano plots in Figure 5d shows the 17 TFs in OD and PPP islets. *REST*, *FOXA1*, and *SP1* were upregulated and *HLF* was downregulated in OD islets. Meanwhile, *PDX1*, *HNF1A*, and *HLF* were downregulated in PPP islets. *HNF1A* tended to be downregulated in OD islets (Figure 5d). These TFs, other than HLF, are known regulators of beta cell differentiation and function.

Validation of upstream regulators. Among the TFs identified above, *PDX1*, *HNF1A*, and *HLF* were chosen for further analyses. RT-PCR assays of human islet alpha and beta cell-enriched

fractions confirmed that the beta cell expression of *PDX1* was reduced in T2D islets (Figure 6a). This analysis also revealed a trend for reduced expression of *HNF1A* in T2D beta cells (Figure 6b). Although *HLF* was enriched in beta cells, its expression was not related to the diabetic state (Figure 6c). Therefore, its role in the regulation of T2D islet signature genes was not investigated. Both *PDX1* and *HNF1A* were detected in the nucleus of EndoC-betaH1 cells (Ravassard et al, 2011) (Figure 6d) and silenced with esiRNA (Figures 6e and Supplementary Fig. 7a, b). Depletion of *HNF1A* led to reduced mRNA levels of *PPP1R1A, SLC2A2,* and *TMEM37* (Figure 6f), although none of these genes have a predicted binding site for *HNF1A* within 5 kb upstream or downstream of its transcription start site (Supplementary Information). Silencing of *PDX1* reduced *SLC2A2* mRNA levels but increased *ANKRD23* and *ARG2* mRNA levels (Supplementary Fig. 6f). Interestingly, all three genes include one or more putative binding sites for *PDX1*. The binding of *HNF1A* and *PDX1* to the promoter of genes predicted to contain sites for their recognition was further investigated by chromatin immunoprecipitation. This assay did not provide evidence for binding of *HNF1A* to the promoters of *UNC5D, FAM102B* and *CD44*, but, with *PDX1* it led to the specific recovery of the promoter regions of *ARG2* and *SLC2A2,* the latter being a well-established *PDX1* target (Supplementary Fig. 6g).

Confidential

Discussion

Rationale and novelty of the methodological approach. Our study presents a novel transcriptomic signature of human T2D islets. The novelty of the signature lies in its origin. Our data were obtained from the rigorous analysis of the so far largest assembly of human islets from ND (116) and T2D (55) subjects. In addition, we exploited two different tissue sources of islet material (OD and PPP) in an effort to circumvent the limitations residing in each of them. Disadvantages of islet cohorts from brain-death or cadaveric OD include limited family and clinical records and potential transcriptomic changes resulting from a) stressful life conditions while in intensive care prior to brain-death, which may increase inflammatory infiltration of the pancreas (In't Veld et al, 2010; Toyama et al, 2003) and expression of ER stress markers (Ebrahimi et al, 2017), or prolonged ischemia prior to pancreas explantation, in the case of cadaveric OD; b) the enzymatic islet isolation procedure *per se* and c) the exposure *in vitro* of ND and T2D islets to the same culture *milieu* for days prior to RNA extraction. However, the large yield of islets and beta cell enriched-fractions from the entire pancreas of OD enables extensive and in parallel molecular, biochemical and functional studies from one isolation batch. In contrast, such approach is unfeasible in the case of islets retrieved by enzymatic digestion from small surgical specimens owing to the smaller yield and poorer quality. However, comprehensive information about the family and clinical history of PPP is available, and the patient's metabolic status can be assessed by an OGTT shortly before surgery. The latter is most valuable to distinguish pre-diabetic from truly normoglycaemic subjects. Immediate cryofixation of the surgical specimens and LCM of islets directly from cryosections limits the risk of artifactual transcriptomic changes. A legitimate concern is that the underlying pancreatic disease

may have an influence on gene expression of the islet cells. In our PPP cohort, the prevalence of pancreatitis and benign or malignant pancreatic tumors was comparable between ND and T2D. Notably, none of these disorders were associated with changes in the islet transcriptome, while the presence of "contaminating" acinar and ductal cell markers was equivalent to that in ND and T2D OD islets. Moreover, the duration of T2D in PPP (10.6 ±8.6 years) and OD (9.9 ±7.4 years) was comparable and previous studies found no association between diabetes and pancreatic cancer among patients with long-standing diabetes (Gullo et al, 1994). Furthermore, principal component analysis revealed that the transcriptomes of islets isolated from the same OD either by enzymatic digestion or by LCM did not cluster, whereas the latter clustered with the transcriptome of PPP islets obtained by LCM and vice versa. We further compared our results to recently published signatures for four pancreatic cancer sub-types (Bailey et al, 2016) and found that genes differentially regulated in T2D in OD and PPP samples showed very similar patterns of enrichment against these signatures (Supplementary Table 3). Taken together, these results demonstrate that the transcriptomic differences between OD and PPP samples are not driven by patient differences, but mainly due to the distinct islet isolation procedures used in each cohort for microarray studies.

The transcriptomics analysis described here was performed at the gene level. Microarray technology rather than RNA-Seq was chosen because at the time we initiated the sample processing the former offered the most robust and cost-effective solution for transcriptomics analysis. Nevertheless, since our current study focused at the gene level, the advantage of using RNA-Seq here would have been limited. In future it could of course be valuable to investigate

this large set of human pre-diabetic and diabetic islets also by RNA-Seq (Soneson et al, 2016), for instance to assess alternative splice variants and the status of non-coding RNA (ncRNA).

In our IGT and T3cD PPP, as in a previous cohort of T2D patients undergoing pancreatectomy for pancreatic cancer (Permert et al, 1994) glucose intolerance was correlated with altered hepatic function and elevated insulin resistance secondary to anatomic compression of the biliary duct by a benign or malignant tumor in the head of the pancreas (Ehehalt et al, 2015). Indeed, equivalent type of tumors in the body and tail of the pancreas were not associated with glucose intolerance, which ameliorated quickly after removing tumors located in the head of the pancreas, as also recently observed by others (Kang et al, 2016). Hence, beta cell dysfunction and hyperglycaemia in IGT and T3cD PPP likely resulted from the burden that insulin resistance poses on beta cells, rather than from a direct effect of the tumor on such cells.

We also paid particular attention to other methodological aspects of the study. For instance, OD islets were cultured for <72 h prior to RNA extraction with the same protocol by all three islet collecting teams, while quality assessments and microarray profiling were conducted by a fourth team. Centralized platforms were used for the measurement of islet autoantibodies, *in situ* PCR, validation of primary antibodies, and most importantly, for integrative systems biology of clinical and laboratory data. The latter efforts were pursued in parallel by two teams using either literature- or sequence-based approaches, and only concordant results were considered further. Although this stringent approach most likely captured only part of the "truth", i.e. may possibly exclude genes, which undergo pathogenic-relevant changes in T2D, it increased our confidence in the outcomes.

Confidential

Novelty and relevance of the biological findings. The comparative analysis of our large OD and PPP islet biobank (n=206) identified 19 genes that were dysregulated in the same direction (15 downregulated and 4 upregulated) in T2D islets at FDR ≤0.05 and fold-change of ≥1.5, independently of the tissue source and the islet isolation protocol (Table 2). None of these genes are in any of the established T2D-associated genetic loci (Franks et al, 2013) although *G6PC2* variants are known to affect fasting blood glucose concentration (O'Brien, 2013; Wessel et al, 2015). The activities of most of these genes in beta cells are suggested based on their associations with islet functional traits and clinical parameters. Some of our results confirm prior work showing the downregulation of *ARG2, CAPN13, CHL1, FFAR4, G6PC2, PPP1R1A, SLC2A2, TMEM37* and *UNC5D* and upregulation of *KCNH8* in T2D islets (Mahdi et al, 2012; Taneera et al, 2015; Taneera et al, 2012). The involvement of *SLC2A2*, *FFAR4*, and *G6PC2* in beta cell function is well established (Hutton & O'Brien, 2009; Thorens, 2015) while that of *CHL1* and *PPP1R1A* was reported more recently (Jiang et al, 2013; Taneera et al, 2015). Using RT-qPCR and/or immunostaining, we showed that *PPP1R1A, ARG2*, and *TMEM37* are enriched in human beta cells and that their modulation affects insulin release. The sequence similarity suggests that *TMEM37* encodes an evolutionarily conserved inhibitory subunit of voltage-gated calcium channels, but its activity has never been validated. We show that its acute depletion in INS-1 832/13 cells increased $[Ca^{2+}]_i$ levels in glucose-stimulated conditions as well as the ISI, while its overexpression exerted opposite effects. Hence, reduced expression of *TMEM37* in T2D islets may represent a compensatory change in the context of the complex remodeling of the beta cell transcriptome upon exposure to prolonged hyperglycaemia.

Nine genes that have not been previously reported to be associated with T2D were significantly dysregulated under our stringent criteria in both OD and PPP cohorts. These genes (*ANKRD23/39*, *ASCL2*, *HHATL*, *NSG1*, *PCDH20*, *SCTR*, *CD44, FAM102B* and *FBXO32*) are described here for the first time to be differentially expressed in T2D islets. For brevity, our considerations will be limited to genes with evidence to support their possible relevance to islets and metabolism. *ANKRD23* is a transcriptional regulator enriched in metabolically active tissues, such as muscle and brown fat (Ikeda et al, 2003). In muscles, it reduces *LKB1* expression, AMPK phosphorylation (Shimoda et al, 2015) and cellular palmitate uptake. Interestingly, in rat models of T2D its expression is upregulated in insulin target tissues (Ikeda et al, 2003). *ASCL2* is a transcription factor implicated in fate determination of neuronal precursor cells, while hedgehog acyltransferase-like *HHATL* may inhibit N-terminal protein palmitoylation. Although barely detectable, their downregulation was correlated with de-differentiation of human islets in culture (Negi et al, 2012). *ASCL2*, *NSG1*, *PCDH20,* and *UNC5D* are enriched in neurons, which are functionally closely related to islet endocrine cells. *NSG1* is implicated in the endosomal trafficking of L1/NgCAM, of which *CHL1* is a paralogue, and of glutamate AMPA and NMDA receptors. A recent study revealed an inhibitory role of *NMDA* receptors on insulin secretion (Marquard et al, 2015). *UNC5D*, like *CHL1*, may regulate neuronal migration and survival (Takemoto et al, 2011) while *PCDH20* may inhibit the canonical Wnt signaling pathway. Finally, *SCTR* is the most potent regulator of pancreatic bicarbonate, electrolyte, and volume secretion. Although early research indicated that secretin stimulates insulin release in humans (Lerner & Porte, 1970) the role of this hormone and its receptor in the context of beta cell function remains unclear.

Several other novel genes were upregulated in T2D islets, including *CD44, FAM102B*, and *FBXO32*. *CD44* is involved in cell–cell interactions, cell adhesion, and cell migration, and is associated with islet inflammation in type 1 diabetes (Savinov & Strongin, 2007), adipose tissue inflammation, insulin resistance and hyperglycaemia (Kodama et al, 2015). *FBXO32* is part of the E3-ubiquitin ligase SCF complex involved in phosphorylation-dependent ubiquitination. The ubiquitin-proteasome system is a major intracellular pathway for protein degradation and its alterations are associated with beta cell dysfunction in T2D (Bugliani et al, 2013).

Our results provide several new directions for further study in T2D. In T2D OD islets, 69% (307/444) of the differentially regulated genes were downregulated whereas 62% (84/136) of the differentially regulated genes were upregulated in T2D PPP islets. Upregulation of proinflammatory molecules such as *IL1B, CCL26*, *CCL3*, *CCL8*, *CXCL1*, *CXCL11*, *CXCL12*, *CXL2*, and *CXCR7* in T2D OD islets, but not in T2D PPP islets, likely reflects a "wound" response secondary to enzymatic isolation of islets (Negi et al, 2012). Top genes of interest and of relevance to beta cell function that were exclusively downregulated in T2D OD islets included *GLP1R*, *IAPP*, *PTPRN* and *ERO1LB*. Among the top dysregulated genes in T2D PPP islets, *ALDOB* and *FAIM2* were upregulated and *TMEM27* and *GRIN2D* were downregulated. Interestingly, a distinct aldolase isoform, *ALDOC*, and several glutamate AMPA and NMDA receptor subunits, namely *GRIA2*, *GRIA4*, and *GRIN2A*, were downregulated in T2D OD islets. The convergence on the glutamatergic system may explain why "Neuropathic Pain Signaling" was one of two enriched canonical pathways dysregulated in both islet cohorts, and, interestingly, may be consistent with changes in central nervous system control of insulin secretion in T2D (Stanley et al, 2016). The T2D OD islets were also enriched for genes in the

"Wnt/beta-catenin Signaling" pathway, which may be implicated in the development of neuropathic pain signaling in rodents (Zhang et al, 2013), while *DKK3* and *WNT3*, two genes in the Wnt canonical pathway, were differentially regulated in T2D PPP islets. Although the Wnt signaling-related genes *TCF7L2* and *SFRP4* (Mahdi et al, 2012) were not dysregulated in our cohorts, these observations deserve further consideration.

To further explore the data we used both literature-based and sequence-based approaches to search for upstream TFs that could be key in driving beta cell expression changes in T2D. Specifically we combined literature- and sequence-based TF networks to search for common upstream TFs driving the expression of gene targets. This novel strategy inferred altered activities of *PDX1*, *HNF1A*, and *HLF*, which could represent key regulators in T2D islets. Both *PDX1* and *HNF1A* were downregulated in enriched beta cell fractions from T2D OD, with evidence that *PDX1* targets *ARG2*. Convergence of the literature-based network with the module and sequence-based network on downregulation of *HNF1A*, which lies upstream of *PDX1*, and upregulation of *REST* provides strong evidence supporting de-differentiation of beta cells in T2D. However, this conclusion is tempered by the lack of evidence for upregulation of any of the so-called "disallowed" genes in beta cells (Pullen et al, 2010; Quintens et al, 2008) as expected to occur in the context of clear de-differentiation. However, more sensitive approaches including RNA-Seq may be required to detect changes in these weakly expressed genes.

Our results represent a snapshot of islet gene expression changes occurring in T2D from the largest collection of islet samples so far reported. We describe a gene expression signature derived from the combined analysis of two different but complementary sample cohorts. By

including both cohorts in our analysis and applying stringent, albeit arbitrary, criteria for differential gene expression, our aim was to select the current best targets for subsequent studies in T2D islets. We focused on several genes for validation of our approach based on evidence that these were, both from our study and other recent publications, *bona fide* targets of interest for T2D. However, these validated genes, and the signature from which they were selected, likely represent only the tip of the iceberg in terms of potential targets and biological hypotheses arising from such an analysis. In recent years several groups have published findings derived from analysis of islets from organ donors (Andersson et al, 2012; Bugliani et al, 2013; Fadista et al, 2014; Gunton et al, 2005; MacDonald et al, 2009; Mahdi et al, 2012; Ostenson et al, 2006; Taneera et al, 2015; Taneera et al, 2013; Taneera et al, 2012). Since all reported studies, as well as our own, are each likely to capture only part of the "truth" it would certainly be valuable in the future to integrate all of the available human islet transcriptomic datasets to strengthen robustness. The results presented here by combining data from OD and PPP samples demonstrates that such an analysis, although technically challenging, is feasible, and necessary to define a relevant set of target genes for human T2D.

Finally, an intriguing finding of our study is that although the 19 signature genes in T3cD PPP islets tended to be dysregulated in the same directions to the changes in T2D OD and PPP islets, none of them showed significant expression changes. The differences were even less evident with IGT PPP islets. While these findings must be validated in larger cohorts of IGT and T3cD subjects, one of their implications is that the diverse transcriptomic changes in T2D, IGT and T3cD islets may reflect pathophysiological peculiarities of these conditions and/or may be affected by the duration and severity of the hyperglycemia. Another possibility is that these

Confidential

transcriptomic changes correlate with beta failure but may not precede it. Therefore, the islet gene expression changes preceding beta cell failure remain elusive.

In conclusion, the present study provides a stringent definition of the transcriptomic signature of a large series of T2D islets, regardless of islet source and isolation procedure. The identification of dysregulated genes, some of them not reported previously, the description of downstream and upstream regulators and the identification of key transcription factors involved in beta cell dysfunction, as reported in this study, contribute to the understanding of the complex molecular scenario of type 2 diabetic islet cells.

Confidential

Materials and Methods

Islet procurement and RNA extraction. Pancreata not suitable for transplantation were obtained in Pisa from 161 ND and 39 T2D heart-beating OD under approval of the local ethics committees. Isolated islets were prepared by enzymatic digestion and density gradient purification (Del Guerra et al, 2005; Marselli et al, 2014). RNA was purified 2–3 days after islet isolation with the Arcturus PicoPure Isolation kit. Forty-three additional human islet preparations, all from ND OD were acquired by Eli Lilly from Prodo Laboratories Inc. (Irvine, CA, USA). Pancreatic surgical specimens were obtained in Dresden from 201 partially pancreatectomized patients (PPP) after the patient provided informed consent and under approval of the local ethics committee. Islets from snap-frozen surgical specimens of 117 PPP, including 37 ND, 41 T2D, 16 IGT, and 23 T3cD subjects were directly retrieved from tissue cryosections by LCM and RNA was purified using the Arcturus PicoPure Isolation kit as previously described (Sturm et al, 2013). The methods used to prepare human islet beta and alpha cell-enriched fractions were previously reported (Parnaud et al, 2008) and validated (Bugliani et al, 2013; Kirkpatrick et al, 2010).

Insulin secretion from OD islets. Islet insulin release was assessed as previously described (Del Guerra et al, 2005; Marselli et al, 2014).

RNA quality control and Affymetrix hybridization. The concentration and purity of islet RNA were assessed using a NanoDrop 2000c spectrophotometer (Thermo Scientific, Wilmington, DE) and quality was evaluated with an Agilent 2100 Bioanalyzer system and the Agilent RNA 6000

Pico Kit (Agilent Technologies, Santa Clara, CA). Hybridization of biotin-labeled cDNA to Affymetrix HG_U133Plus2.0 GeneChip microarrays was carried out at ATLAS Biolabs GmbH (Berlin, Germany).

Normalization and statistical analysis of microarray data. Transcriptomic data were summarized and normalized using Robust Multichip Analysis (RMA) on Array Studio software (Omicsoft Corp., Cary, NC). Batch correction of microarray data was performed using the R/Bioconductor package *ComBat* as previously described (Johnson et al, 2007). Correction for the covariates age and gender, and the statistical analysis were performed using the linear modeling features of the R/Bioconductor package Limma (Ritchie et al, 2015). All data are MIAME compliant, and the raw data have been deposited in a MIAME database (GEO, accession number: GSE76896).

Pathway analysis of differentially expressed genes. Putatively active pathways, including the downstream processes and upstream regulators were determined using IPA (Ingenuity® Systems, Redwood City, CA).

Gene co-expression network analysis. WGCNA was performed on genes expressed in islets of 84 ND OD and 32 ND PPP. Normalized expression data were first batch-corrected using *ComBat* (Johnson et al, 2007) and corrected for age and gender effects by linear regression using *LmFit* in the *limma* package in R (Gentleman et al, 2004). Both datasets were filtered by calculating a covariance matrix and removing the 25% least covariant genes. Co-expression networks were constructed by calculating adjacency matrices for each dataset using a soft-threshold power of 7 and Spearman correlation using pairwise complete observations. A topological overlap matrix (TOM) was calculated for each adjacent matrix, converted to the

distance, and clustered by hierarchical clustering using average linkage clustering. Modules were identified using a dynamic tree cut with a cut height of 0.995 and a minimum module size of 20 with a hybrid method. Module *eigengenes* were calculated and similar modules were merged together using a module *eigengene* distance of 0.15 as the threshold. These modules were then correlated to clinical and functional traits, and were used to generate the upstream TF networks.

Additional information on experimental procedures is given in the Supplementary Information (link).

Author contributions

FE, DR, MK, MD, RG, KP, JM, GB, DS, H-DS and JW were responsible for clinical activities concerning PPP and isolated islets from surgical specimens. PM, LM, MB, MSu, FS, UB, FF, CBW and KB were responsible for collection of clinical data and islets from OD. AMS, BM-P, DM and MvB were responsible for transcriptomic analyses of islet samples and their bioinformatic analysis together with MI, IX, FB, RL, EP, AM-M and LW. ML, AD and EN contributed to transcriptomic studies. LM, HM, K-PK, JP, MB, AJ, AF, CW, AF, CBW, RS, BM-P, SL and GR validated genes of interest and contributed to the interpretation of the corresponding data. EB measured antibodies for T1D autoantigens. MS, AMS, PM, PF and MI designed the study with contributions from PMe, SL and BT. MS, AMS, MI and PM coordinated the project and wrote the manuscript with contributions from MvB, LM, DR, HM, K-PK, GR and PF.

Confidential

Acknowledgments

We dedicate this work to Alain Ktorza, an excellent scientist and friend who left us. We thank Werner Kramer, Peter Hecht, Veikko Koivisto, and all of the members of the IMIDIA consortium for their support and advice. We thank Hella Hartmann and Britta Schroth-Diez in the light microscopy facilities of the BIOTEC/CRTD at TU Dresden and of the MPI-CBG for their support. We thank Frank Josef Möller for his editorial support. The work was supported by the Innovative Medicines Initiative Joint Undertaking (grant no. 155005) for IMIDIA, which received financial contributions from the European Union's Seventh Framework Program (FP7/2007-2013); companies belonging to the European Federation of Pharmaceutical Industries and Associations; the German Center for Diabetes Research (DZD e.V.), which is supported by the German Ministry for Education and Research (to MS); the Italian Ministry of Education and Research (Prin 2010-2011) (to PM); the Wellcome Trust (Advanced Investigator Award WT098424AIA); the Medical Research Council (Programme MR/J0003042/1); and the Royal Society (Wolfson Research Merit Award to GAR). AMS, BM-P, DM and MvB are employees of Sanofi-Aventis; KB is an employee of Lilly; EN is an employee of F. Hoffmann-La Roche. Authors do not have conflicts of interest

For Peer Review

References

Andersson SA, Olsson AH, Esguerra JL, Heimann E, Ladenvall C, Edlund A, Salehi A, Taneera J, Degerman E, Groop L et al (2012) Reduced insulin secretion correlates with decreased expression of exocytotic genes in pancreatic islets from patients with type 2 diabetes. Mol Cell Endocrinol 364**:** 36-45

Atouf F, Czernichow P, Scharfmann R (1997) Expression of neuronal traits in pancreatic beta cells. Implication of neuron-restrictive silencing factor/repressor element silencing transcription factor, a neuron-restrictive silencer. J Biol Chem 272**:** 1929-1934

Bailey P, Chang DK, Nones K, Johns AL, Patch AM, Gingras MC, Miller DK, Christ AN, Bruxner TJ, Quinn MC et al (2016) Genomic analyses identify molecular subtypes of pancreatic cancer. Nature 531**:** 47-52

Blodgett DM, Nowosielska A, Afik S, Pechhold S, Cura AJ, Kennedy NJ, Kim S, Kucukural A, Davis RJ, Kent SC et al (2015) Novel Observations From Next-Generation RNA Sequencing of Highly Purified Human Adult and Fetal Islet Cell Subsets. Diabetes 64**:** 3172-3181

Bugliani M, Liechti R, Cheon H, Suleiman M, Marselli L, Kirkpatrick C, Filipponi F, Boggi U, Xenarios I, Syed F et al (2013) Microarray analysis of isolated human islet transcriptome in type 2 diabetes and the role of the ubiquitin-proteasome system in pancreatic beta cell dysfunction. Mol Cell Endocrinol 367**:** 1-10

Cinti F, Bouchi R, Kim-Muller JY, Ohmura Y, Sandoval PR, Masini M1, Marselli L, Suleiman M, Ratner LE, Marchetti P, Accili D. Evidence of β-Cell Dedifferentiation in Human Type 2 Diabetes. J Clin Endocrinol Metab. 2016 Mar;101(3):1044-54.

Chu PJ, Robertson HM, Best PM (2001) Calcium channel gamma subunits provide insights into the evolution of this gene family. Gene 280**:** 37-48

Del Guerra S, Lupi R, Marselli L, Masini M, Bugliani M, Sbrana S, Torri S, Pollera M, Boggi U, Mosca F et al (2005) Functional and molecular defects of pancreatic islets in human type 2 diabetes. Diabetes 54**:** 727-735

Deng S, Vatamaniuk M, Huang X, Doliba N, Lian MM, Frank A, Velidedeoglu E, Desai NM, Koeberlein B, Wolf B et al (2004) Structural and functional abnormalities in the islets isolated from type 2 diabetic subjects. Diabetes 53**:** 624-632

Dor Y, Glaser B (2013) beta-cell dedifferentiation and type 2 diabetes. N Engl J Med 368**:** 572-573

Ebrahimi A, Jung MH, Dreyfuss JM, Pan H, Sgroi D, Bonner-Weir S, Weir GC (2017) Evidence of stress in β cells obtained with laser capture microdissection from pancreases of brain dead donors. Islets 9:19-29.

Confidential

Ehehalt F, Sturm D, Rosler M, Distler M, Weitz J, Kersting S, Ludwig B, Schwanebeck U, Saeger HD, Solimena M et al (2015) Blood Glucose Homeostasis in the Course of Partial Pancreatectomy--Evidence for Surgically Reversible Diabetes Induced by Cholestasis. PLoS One 10**:** e0134140

Ewald N, Kaufmann C, Raspe A, Kloer HU, Bretzel RG, Hardt PD (2012) Prevalence of diabetes mellitus secondary to pancreatic diseases (type 3c). Diabetes Metab Res Rev 28**:** 338-342

Fadista J, Vikman P, Laakso EO, Mollet IG, Esguerra JL, Taneera J, Storm P, Osmark P, Ladenvall C, Prasad RB et al (2014) Global genomic and transcriptomic analysis of human pancreatic islets reveals novel genes influencing glucose metabolism. Proc Natl Acad Sci U S A 111**:** 13924-13929

Franks PW, Pearson E, Florez JC (2013) Gene-environment and gene-treatment interactions in type 2 diabetes: progress, pitfalls, and prospects. Diabetes Care 36**:** 1413-1421

Gentleman RC, Carey VJ, Bates DM, Bolstad B, Dettling M, Dudoit S, Ellis B, Gautier L, Ge Y, Gentry J et al (2004) Bioconductor: open software development for computational biology and bioinformatics. Genome Biol 5**:** R80

Gullo L, Pezzilli R, Morselli-Labate AM (1994) Diabetes and the risk of pancreatic cancer. N Engl J Med 331**:** 81-84

Gunton JE, Kulkarni RN, Yim S, Okada T, Hawthorne WJ, Tseng YH, Roberson RS, Ricordi C, O'Connell PJ, Gonzalez FJ et al (2005) Loss of ARNT/HIF1beta mediates altered gene expression and pancreatic-islet dysfunction in human type 2 diabetes. Cell 122**:** 337-349

Halban PA, Polonsky KS, Bowden DW, Hawkins MA, Ling C, Mather KJ, Powers AC, Rhodes CJ, Sussel L, Weir GC. β-cell failure in type 2 diabetes: postulated mechanisms and prospects for prevention and treatment. Diabetes Care. 2014 Jun;37(6):1751-8

Hutton JC, O'Brien RM (2009) Glucose-6-phosphatase catalytic subunit gene family. J Biol Chem 284**:** 29241-29245

Ikeda K, Emoto N, Matsuo M, Yokoyama M (2003) Molecular identification and characterization of a novel nuclear protein whose expression is up-regulated in insulin-resistant animals. J Biol Chem 278**:** 3514-3520

In't Veld P, De Munck N, Van Belle K, Buelens N, Ling Z, Weets I, Haentjens P, Pipeleers-Marichal M, Gorus F, Pipeleers D (2010) Beta-cell replication is increased in donor organs from young patients after prolonged life support. Diabetes 59**:** 1702-1708

Jiang L, Brackeva B, Ling Z, Kramer G, Aerts JM, Schuit F, Keymeulen B, Pipeleers D, Gorus F, Martens GA (2013) Potential of protein phosphatase inhibitor 1 as biomarker of pancreatic beta-cell injury in vitro and in vivo. Diabetes 62**:** 2683-2688

Confidential

Johnson WE, Li C, Rabinovic A (2007) Adjusting batch effects in microarray expression data using empirical Bayes methods. Biostatistics 8**:** 118-127

Kahn SE. The relative contributions of insulin resistance and beta-cell dysfunction to the pathophysiology of Type 2 diabetes. Diabetologia. 2003 Jan;46(1):3-19

Kang MJ, Jung HS, Jang JY, Jung W, Chang J, Shin YC, Kim SW (2016) Metabolic effect of pancreatoduodenectomy: Resolution of diabetes mellitus after surgery. Pancreatology 16**:** 272-277

Kirkpatrick CL, Marchetti P, Purrello F, Piro S, Bugliani M, Bosco D, de Koning EJ, Engelse MA, Kerr-Conte J, Pattou F et al (2010) Type 2 diabetes susceptibility gene expression in normal or diabetic sorted human alpha and beta cells: correlations with age or BMI of islet donors. PLoS One 5**:** e11053

Kodama K, Toda K, Morinaga S, Yamada S, Butte AJ (2015) Anti-CD44 antibody treatment lowers hyperglycemia and improves insulin resistance, adipose inflammation, and hepatic steatosis in diet-induced obese mice. Diabetes 64**:** 867-875

Kramer A, Green J, Pollard J, Jr., Tugendreich S (2014) Causal analysis approaches in Ingenuity Pathway Analysis. Bioinformatics 30**:** 523-530

Kwon AT, Arenillas DJ, Worsley Hunt R, Wasserman WW (2012) oPOSSUM-3: advanced analysis of regulatory motif over-representation across genes or ChIP-Seq datasets. G3 (Bethesda) 2**:** 987-1002

Langfelder P, Horvath S (2008) WGCNA: an R package for weighted correlation network analysis. BMC Bioinformatics 9**:** 559

Lerner RL, Porte D, Jr. (1970) Uniphasic insulin responses to secretin stimulation in man. J Clin Invest 49**:** 2276-2280

MacDonald MJ, Longacre MJ, Langberg EC, Tibell A, Kendrick MA, Fukao T, Ostenson CG (2009) Decreased levels of metabolic enzymes in pancreatic islets of patients with type 2 diabetes. Diabetologia 52**:** 1087-1091

Mahdi T, Hanzelmann S, Salehi A, Muhammed SJ, Reinbothe TM, Tang Y, Axelsson AS, Zhou Y, Jing X, Almgren P et al (2012) Secreted frizzled-related protein 4 reduces insulin secretion and is overexpressed in type 2 diabetes. Cell metabolism 16**:** 625-633

Marchetti P, Ferrannini E (2015) β-Cell mass and function in human type 2 diabetes. In International Textbook of Diabetes Mellitus pp 354-370. John Wiley & Sons, Ltd

Confidential

Marquard J, Otter S, Welters A, Stirban A, Fischer A, Eglinger J, Herebian D, Kletke O, Klemen MS, Stozer A et al (2015) Characterization of pancreatic NMDA receptors as possible drug targets for diabetes treatment. Nat Med 21**:** 363-372

Marselli L, Suleiman M, Masini M, Campani D, Bugliani M, Syed F, Martino L, Focosi D, Scatena F, Olimpico F et al (2014) Are we overestimating the loss of beta cells in type 2 diabetes? Diabetologia 57**:** 362-365

Marselli L, Thorne J, Dahiya S, Sgroi DC, Sharma A, Bonner-Weir S, Marchetti P, Weir GC (2010) Gene expression profiles of Beta-cell enriched tissue obtained by laser capture microdissection from subjects with type 2 diabetes. PLoS One 5**:** e11499

Mehran AE, Templeman NM, Brigidi GS, Lim GE, Chu KY, Hu X, Botezelli JD, Asadi A, Hoffman BG, Kieffer TJ et al (2012) Hyperinsulinemia drives diet-induced obesity independently of brain insulin production. Cell metabolism 16**:** 723-737

Mingrone G, Panunzi S, De Gaetano A, Guidone C, Iaconelli A, Leccesi L, Nanni G, Pomp A, Castagneto M, Ghirlanda G et al (2012) Bariatric surgery versus conventional medical therapy for type 2 diabetes. N Engl J Med 366**:** 1577-1585

Negi S, Jetha A, Aikin R, Hasilo C, Sladek R, Paraskevas S (2012) Analysis of beta-cell gene expression reveals inflammatory signaling and evidence of dedifferentiation following human islet isolation and culture. PLoS One 7**:** e30415

O'Brien RM (2013) Moving on from GWAS: functional studies on the G6PC2 gene implicated in the regulation of fasting blood glucose. Curr Diab Rep 13**:** 768-777

Ostenson CG, Gaisano H, Sheu L, Tibell A, Bartfai T (2006) Impaired gene and protein expression of exocytotic soluble N-ethylmaleimide attachment protein receptor complex proteins in pancreatic islets of type 2 diabetic patients. Diabetes 55**:** 435-440

Parnaud G, Bosco D, Berney T, Pattou F, Kerr-Conte J, Donath MY, Bruun C, Mandrup-Poulsen T, Billestrup N, Halban PA (2008) Proliferation of sorted human and rat beta cells. Diabetologia 51**:** 91-100

Permert J, Larsson J, Westermark GT, Herrington MK, Christmanson L, Pour PM, Westermark P, Adrian TE (1994) Islet amyloid polypeptide in patients with pancreatic cancer and diabetes. N Engl J Med 330**:** 313-318

Pullen TJ, Khan AM, Barton G, Butcher SA, Sun G, Rutter GA (2010) Identification of genes selectively disallowed in the pancreatic islet. Islets 2**:** 89-95

Quintens R, Hendrickx N, Lemaire K, Schuit F (2008) Why expression of some genes is disallowed in beta-cells. Biochem Soc Trans 36**:** 300-305

Confidential

Rahier J, Guiot Y, Goebbels RM, Sempoux C, Henquin JC (2008) Pancreatic beta-cell mass in European subjects with type 2 diabetes. Diabetes Obes Metab 10 Suppl 4**:** 32-42

Ravassard P, Hazhouz Y, Pechberty S, Bricout-Neveu E, Armanet M, Czernichow P, Scharfmann R (2011) A genetically engineered human pancreatic beta cell line exhibiting glucose-inducible insulin secretion. J Clin Invest 121**:** 3589-3597

Ritchie ME, Phipson B, Wu D, Hu Y, Law CW, Shi W, Smyth GK (2015) limma powers differential expression analyses for RNA-sequencing and microarray studies. Nucleic Acids Res 43**:** e47

Rosengren AH, Braun M, Mahdi T, Andersson SA, Travers ME, Shigeto M, Zhang E, Almgren P, Ladenvall C, Axelsson AS et al (2012) Reduced insulin exocytosis in human pancreatic beta-cells with gene variants linked to type 2 diabetes. Diabetes 61**:** 1726-1733

Savinov AY, Strongin AY (2007) Defining the roles of T cell membrane proteinase and CD44 in type 1 diabetes. IUBMB Life 59**:** 6-13

Schauer PR, Kashyap SR, Wolski K, Brethauer SA, Kirwan JP, Pothier CE, Thomas S, Abood B, Nissen SE, Bhatt DL (2012) Bariatric surgery versus intensive medical therapy in obese patients with diabetes. N Engl J Med 366**:** 1567-1576

Segerstolpe A, Palasantza A, Eliasson P, Andersson EM, Andreasson AC, Sun X, Picelli S, Sabirsh A, Clausen M, Bjursell MK et al (2016) Single-Cell Transcriptome Profiling of Human Pancreatic Islets in Health and Type 2 Diabetes. Cell metabolism 24**:** 593-607

Shimoda Y, Matsuo K, Kitamura Y, Ono K, Ueyama T, Matoba S, Yamada H, Wu T, Chen J, Emoto N et al (2015) Diabetes-Related Ankyrin Repeat Protein (DARP/Ankrd23) Modifies Glucose Homeostasis by Modulating AMPK Activity in Skeletal Muscle. PLoS One 10**:** e0138624

Soneson C, Matthes KL, Nowicka M, Law CW, Robinson MD (2016) Isoform prefiltering improves performance of count-based methods for analysis of differential transcript usage. Genome Biol 17**:** 12

Stanley SA, Kelly L, Latcha KN, Schmidt SF, Yu X, Nectow AR, Sauer J, Dyke JP, Dordick JS, Friedman JM (2016) Bidirectional electromagnetic control of the hypothalamus regulates feeding and metabolism. Nature 531**:** 647-650

Sturm D, Marselli L, Ehehalt F, Richter D, Distler M, Kersting S, Grutzmann R, Bokvist K, Froguel P, Liechti R et al (2013) Improved protocol for laser microdissection of human pancreatic islets from surgical specimens. J Vis Exp

Takemoto M, Hattori Y, Zhao H, Sato H, Tamada A, Sasaki S, Nakajima K, Yamamoto N (2011) Laminar and areal expression of unc5d and its role in cortical cell survival. Cereb Cortex 21**:** 1925-1934

Confidential

Talchai C, Xuan S, Lin HV, Sussel L, Accili D (2012) Pancreatic beta cell dedifferentiation as a mechanism of diabetic beta cell failure. Cell 150**:** 1223-1234

Taneera J, Fadista J, Ahlqvist E, Atac D, Ottosson-Laakso E, Wollheim CB, Groop L (2015) Identification of novel genes for glucose metabolism based upon expression pattern in human islets and effect on insulin secretion and glycemia. Hum Mol Genet 24**:** 1945-1955

Taneera J, Fadista J, Ahlqvist E, Zhang M, Wierup N, Renstrom E, Groop L (2013) Expression profiling of cell cycle genes in human pancreatic islets with and without type 2 diabetes. Mol Cell Endocrinol 375**:** 35-42

Taneera J, Lang S, Sharma A, Fadista J, Zhou Y, Ahlqvist E, Jonsson A, Lyssenko V, Vikman P, Hansson O et al (2012) A systems genetics approach identifies genes and pathways for type 2 diabetes in human islets. Cell metabolism 16**:** 122-134

Thorens B (2015) GLUT2, glucose sensing and glucose homeostasis. Diabetologia 58**:** 221-232

Toyama H, Takada M, Suzuki Y, Kuroda Y (2003) Activation of macrophage-associated molecules after brain death in islets. Cell transplantation 12**:** 27-32

Wessel J, Chu AY, Willems SM, Wang S, Yaghootkar H, Brody JA, Dauriz M, Hivert MF, Raghavan S, Lipovich L et al (2015) Low-frequency and rare exome chip variants associate with fasting glucose and type 2 diabetes susceptibility. Nat Commun 6**:** 5897

Xin Y, Kim J, Okamoto H, Ni M, Wei Y, Adler C, Murphy AJ, Yancopoulos GD, Lin C, Gromada J (2016) RNA Sequencing of Single Human Islet Cells Reveals Type 2 Diabetes Genes. Cell metabolism 24**:** 608-615

Zhang YK, Huang ZJ, Liu S, Liu YP, Song AA, Song XJ (2013) WNT signaling underlies the pathogenesis of neuropathic pain in rodents. J Clin Invest 123**:** 2268-2286

Confidential

Figure and Table Legends

Figure 1. Transcriptional profiling of islet samples using complementary isolation techniques.

(a). Overview of our approach. Islets from OD and PPP subjects were analysed by Affymetrix profiling to identify differentially expressed (DE) genes. These data were combined with clinical and functional data to identify gene co-expression modules correlated with T2D related traits.

(b). Islet samples prepared from OD and PPP isolated enzymatically or by LCM cluster separately. PCA analysis of OD and PPP islets isolated enzymatically or by LCM using all transcribed genes. Left panel: LCM islet samples (green: PPP; blue: OD) cluster separately from enzymatically isolated islet samples (red: OD; black: PPP) regardless of patient origin. Right panel: Duplicate OD (orange) and PPP (purple) samples isolated either enzymatically or by LCM are highlighted, confirming that clustering is according to the isolation method.

Figure 2. Transcriptomic Analyses Revealed a Common Gene Signature in T2D Islets of OD and PPP.

(a). Venn diagram showing the number of differentially expressed (DE) genes in T2D OD and PPP islets versus ND OD and PPP islets. The numbers include genes mapping to more than one probeset. Twenty-three DE genes overlapped between the two datasets ($p=9.1^{-12}$; hypergeometric test assuming a background of 15,165 expressed genes). Heatmaps indicate the number of upregulated (red) and downregulated (blue) genes in OD and PPP islets.

(b). Box plots for the expression changes of 6/19 DE genes that were dysregulated in the same direction in T2D OD and PPP islets relative to the corresponding ND islets. (c). Fold-changes in

Confidential

the expression of the 19 commonly dysregulated genes in T2D islets from IGT PPP (purple bars), T3cD PPP (grey bars), and T2D PPP (orange bars) versus ND PPP islets.

Figure 3. Functional Validation of the Dysregulated Genes *ARG2*, *PPP1R1A*, and *TMEM37* in Insulin-Producing Cells.

(a). Confocal microscopy of human pancreas tissue sections co-immunostained for insulin and ARG2, PPP1R1A or TMEM37. (b). RT-qPCR analysis of *ARG2*, *PPP1R1A*, and *TMEM37* expression levels in human islet alpha and beta cell-enriched fractions from ND (n=5) and T2D (n=4) OD. (c)–(e). Insulin stimulation index (ISI) of INS-1E cells (c and d) or INS-1 832/13 (e) cells after silencing of *ARG2* (c), *PPP1R1A* (d), or *TMEM37* (e) expression with siRNA versus cells treated with a control (siCtrl) siRNA oligonucleotide. (f). Ca^{2+} concentrations in INS-1 832/13 cells after silencing of *TMEM37* (red trace) versus cells treated with a control (siCtrl) siRNA oligonucleotide (black trace). The curves show the mean ± standard error of the mean (SEM) Fura-2 AM ratios for 11 (n=351 $siGLO^{+}$, siCtrl-treated cells) and 12 (n=480 $siGLO^{+}$, siTMEM37-treated cells) coverslips. Changes in glucose and KCl concentrations are indicated. The inset shows the mean + SEM cumulative Ca^{2+} changes in response to glucose (**$p<0.01$, Mann–Whitney *U* test). (g). ISI of INS-1 832/13 cells transfected with m*TMEM37-V5* or the empty *pcDNA3.1* vector (Ctrl). (h). Ca^{2+} concentrations in $eGFP^{+}$ INS-1 832/13 cells co-transfected with m*TMEM37-V5* (red trace) and $eGFP^{+}$ INS-1 832/13 cells co-transfected with the empty *pcDNA3.1* vector (Ctrl) (black trace). The curves shown the mean ± SEM Fura Red ratios (R) for 10 (n=332 $eGFP^{+}$, m*TMEM37-V5* co-transfected cells) and 12 (n=419 $eGFP^{+}$, *pcDNA3.1* co-transfected cells) coverslips. The glucose concentration was increased from 3 to 15 mmol/l, and 20 mmol/l KCl was added at the indicated times. The Inset shows mean + SEM of the peak

Ca^{2+} amplitudes in response to high glucose and KCl stimulation (*p<0.05, unpaired two-tailed *t* test).

Figure 4. Genes Regulated in T2D OD and PPP Islets are Enriched for Beta Cell Function-Related Pathways.

The significance of pathway enrichment is shown as the *–log enrichment p-value* for significant DE genes (*Limma* empirical Bayes adjusted p≤0.05, absolute fold-change ≤1.5 for OD and ≤1.2 for PPP) in OD (left) and PPP (right) islets. Black bars represent enriched pathways involved in beta cell function. The analysis was performed using *Ingenuity Pathway Analysis* software.

Confidential

Figure 5. Systems Biology Analysis Predicted the Key Transcription Factors (TFs) Regulated in T2D.

(a). Workflow used to identify upstream TFs. (b). Top panel: Schematic showing how literature and sequence-based networks were combined to generate an intersection network. TFs are represented by inverted triangles and genes are represented by squares. Evidence for TF-gene targets are shown by arrows (literature red, sequence-based green). Intersection Network (orange) shows TF target gene interactions present in both literature and sequence-based networks (bottom panel). Hive plots of the three networks showing edges between upstream TFs, target genes, and gene co-expression modules (bottom panel). Modules are shown as colored nodes on the vertical axes. TFs are represented on the left axes and their predicted target genes on the right axes. Edges are coloured according to the gene co-expression module of the source node. Nodes are ordered along the axes by increasing degree from the center outwards. (c). Network representation of the Intersection Network shown in (b). Gene co-expression modules

are represented as large coloured nodes in the corresponding module color. *skyblue*, *blue*, and *darkviolet* modules are correlated with the ISI of OD islets (solid boxes), while *lightpink4* module correlates with glucose concentrations at 2-h after an OGTT in PPP islets (dashed boxes). Yellow nodes indicate potential upstream TFs for each module. Blue or orange nodes indicate putative target genes (TFs in orange). Network edges were predicted by both literature and sequence motif-based approaches. For visualization, the network was filtered to remove all gene nodes except for TFs with only one edge. (d). Volcano plots of DE TFs in T2D OD (left) and PPP (right) islets. Significantly differentially regulated TFs (limma empirical Bayes adjusted (BH) $p \leq 0.05$, fold-change ≥ 1.2) are shown as red (upregulated) or blue (downregulated) dots, while potentially differentially regulated TFs with lower fold-changes (FDR$\leq$0.05; no fold change cutoff) are shown as black dots. Upregulated and downregulated TFs are also indicated on the right side of each plot.

Confidential

Figure 6. Validation of PDX1, HNF1A, and HLF as Transcription Factors (TFs) Located Upstream of the T2D Islet Signature Genes.

(a)–(c). RT-qPCR of *PDX1* (a), *HNF1A* (b), and *HLF* (c) expression levels in alpha and beta cell-enriched fractions from human ND (n=5) and T2D (n=4) OD islets. (d). Co-immunostaining for insulin (green) and *PDX1* or *HNF1A* (red) in human EndoC-betaH1 cells. Nuclei are counterstained with DAPI (blue). (e). Immunoblots for *PDX1, HNF1A* or gamma-tubulin in EndoC-betaH1 cells treated with esiRNA for *PDX1*, *HNF1A* or with a control esiRNA. (f). RT-qPCR of the 19 T2D islet signature genes in EndoC-betaH1 cells treated with esiRNA for *PDX1* or *HNF1A* or with a control esiRNA (ANOVA; *p<0.05, **p<0.01, and ***p<0.001) (n=4, except for *ANKRD39,* which was measured three times). (g). Enrichment of T2D islet signature

genes with predicted binding sites for *PDX1* by chromatin immunoprecipitation with anti-PDX1 antibody or control IgG followed by RT-qPCR with primers flanking the predicted binding site. The values in (g) are from three independent chromatin immunoprecipitations that were pooled and analysed by qPCR. Star in (a) are for comparison between ND and T2D and hash signs in (b) and (c) are for comparison between alpha and beta cells.

Confidential

Confidential

Table 1

	Gender [F/M]	Age [years]	BMI [kg/m²]	Diabetes duration [years]	Glycemia in ICU [mmol/l]	Fasting glucose [mmol/l]	HbA1c [%]	Glycemia after OGTT at 2 hours [mmol/l]	Histopathology		
									Chronic pancreatitis	Benign tumor	Malign tumor
Main clinical information of OD (n= 103)											
ND 84 (81.6%)	46/38	60±16	25.8±4.2 (n=83)	–	8.0±1.8 (n=59)	–	–	–	–	–	–
T2D 19 (18.4%)	6/13	72±7**	26.5±3.6 (n=19)	9.9 ±7.4 (n=16)	11.7±4.3** (n=19)	–	–	–	–	–	–
Main clinical information of PPP (n= 103)											
ND 32 (31.0%)	16/16	60 ± 14	24.9 ± 3.4	–	–	5.3 ± 0.6 (n=27)	5.6 ± 0.6 (n=31)	6.1 ± 1.3 (n=27)	6 (18.7%)	8 (25.0%)	18 (56.3%)
T2D 36 (35.0%)	13/23	66 ± 12	25.8 ± 5.0	10.6 ±8.6	–	8.0 ± 2.7*** (n=30)	7.5 ± 1.4*** (n=34)	–	7 (19.4%)	6 (16.7%)	23 (63.9%)
IGT 15 (14.6%)	6/9	63 ± 13	25.7 ± 3.5	–	–	5.3 ± 0.4 (n=15)	5.8 ± 0.3 (n=15)	9.2± 0.8*** (n=15)	2 (13.3%)	5 (33.3%)	8 (53.3%)
T3cD 20 (19.4%)	6/14	66 ± 9	26.0 ± 3.9	0.02 ±0.1	–	6.7 ± 1.7** (n=20)	6.4± 0.9** (n=20)	12.0± 1.4*** (n=12)	4 (20.0%)	1 (5.0%)	15 (75.0%)

Table 1. Clinical Characteristics of the OD and PPP Cohorts Included in this Study. BMI, body mass index; ICU, intensive care unit; IGT, impaired glucose tolerant subjects; OD, organ donors; OGTT, oral glucose tolerance test; ND, non-diabetic subjects; PPP, partially pancreatectomized patients; T2D, type 2 diabetic subjects; T3cD, type 3c diabetic subjects. Except for gender, the values are means ± standard deviation (two-tailed t-test; *p<0.05, **p<0.01, and ***p<0.001) versus ND. T2D patients were treated as follows: 16 OD and 13 PPP with anti-oral diabetic agents, 1 OD and 17 PPP with insulin, 1 OD and 4 PPP with anti-oral diabetic agents and insulin, 1 PPP with anti-oral diabetic agents, insulin and liraglutide, and 1 OD and 1 PPP with diet only.

Confidential

Table 2

			Islet OD			LCM Islets PPP		
Entrez ID	**Symbol**	**Gene name**	**Probe ID**	**Ratio**	**adj.P.Val.**	**Probe ID**	**Ratio**	**adj.P.Val.**
51239 / 200539	ANKRD23 / 39	ankyrin repeat domain 23 / 39	229052_at	0.585	1.14E-02	1553366_s_at	0.600	1.80E-03
384	ARG2	arginase 2	203946_s_at	0.605	3.28E-04	203946_s_at	0.463	1.47E-09
430	ASCL2	achaete-scute complex homolog 2	229215_at	0.540	2.52E-03	229215_at	0.463	1.74E-08
92291	CAPN13	calpain 13	229499_at	0.535	2.52E-03	229499_at	0.614	4.66E-03
10752	CHL1	cell adhesion molecule with homology to L1CAM	204591_at	0.411	1.61E-03	204591_at	0.446	1.56E-05
338557	FFAR4	free fatty acid receptor 4	240856_at	0.604	1.10E-02	240856_at	0.566	1.79E-03
57818	G6PC2	glucose-6-phosphatase, catalytic, 2	221453_at	0.616	3.43E-02	221453_at	0.643	2.77E-02
57467	HHATL	hedgehog acyltransferase-like	223572_at	0.388	1.09E-04	223572_at	0.415	4.44E-04
27065	NSG1	neuron specific gene family member 1	209569_x_at	0.624	2.41E-02	209569_x_at	0.610	8.59E-04
64881	PCDH20	protocadherin 20	232054_at	0.628	2.98E-02	232054_at	0.612	4.02E-02
5502	PPP1R1A	protein phosphatase 1, regulatory subunit 1A	235129_at	0.419	3.07E-04	235129_at	0.475	5.54E-06
6344	SCTR	secretin receptor	1565737_at	0.531	4.68E-04	1565737_at	0.495	8.30E-04
6514	SLC2A2	solute carrier family 2 , member 2	206535_at	0.273	1.65E-04	206535_at	0.362	1.74E-08
140738	TMEM37	transmembrane protein 37	1554485_s_at	0.654	3.90E-03	227190_at	0.504	3.84E-09
137970	UNC5D	unc-5 homolog D	231325_at	0.535	1.29E-02	231325_at	0.589	1.20E-02
960	CD44	CD44 molecule	217523_at	1.561	2.30E-02	1557905_s_at	1.681	1.84E-02
284611	FAM102B	family with sequence similarity 102, member B	226568_at	1.538	9.05E-03	226568_at	1.636	2.15E-02
114907	FBXO32	F-box protein 32	232729_at	1.716	1.51E-03	225328_at	1.505	7.66E-03
131096	KCNH8	potassium voltage-gated channel, subfamily H, member 8	1552742_at	1.529	1.09E-02	1552742_at	1.644	1.74E-02
1600	DAB1	Dab, reelin signal transducer, homolog 1 (Drosophila)	228329_at	0.616	3.90E-02	228329_at	1.551	4.59E-02
2596	GAP43	growth associated protein 43	204471_at	0.611	1.94E-02	204471_at	1.880	2.33E-02
5166	PDK4	pyruvate dehydrogenase kinase, isozyme 4	1562321_at	0.537	8.37E-03	1562321_at	2.120	4.06E-02

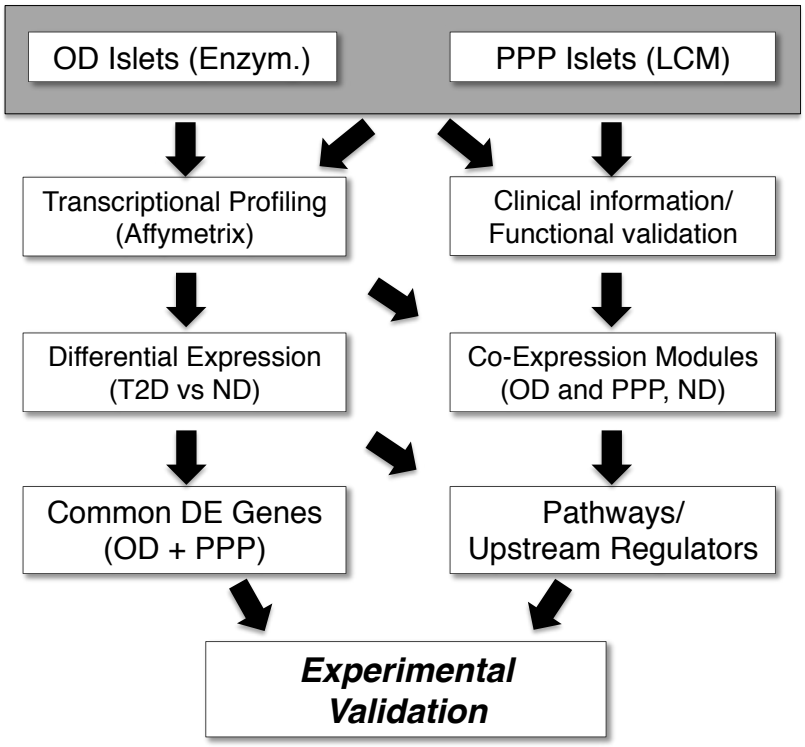
Confidential

6004	RGS16	regulator of G-protein signaling 16	209324_s_at	0.663	2.23E-02	209324_s_at	1.687	3.80E-02

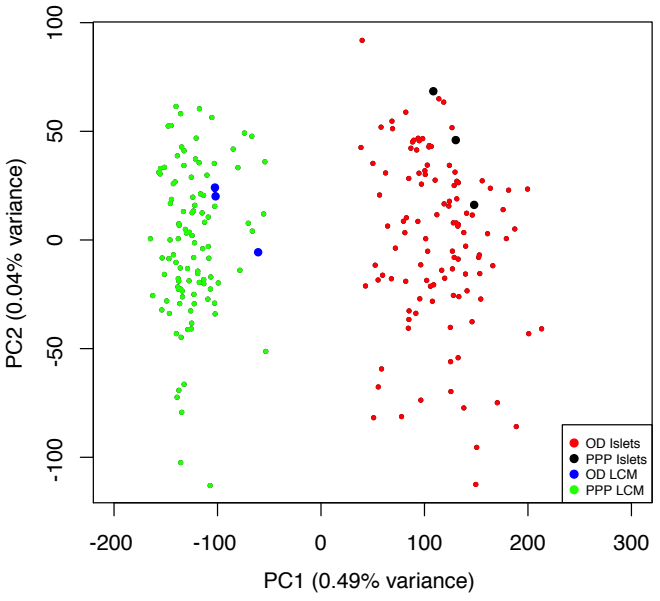
Table 2. Genes Showing Differential Regulation in T2D OD and PPP Islets (Adjusted p≤0.05, Absolute Fold-Change ≤1.5). OD, organ donors; PPP, partially pancreatectomized patients; probe ID, probe set ID; adj. p., adjusted p-value after correcting for multiple hypothesis tests using the Benjamini–Hochberg method. Genes 1–15 are downregulated (blue) in OD and PPP; genes 16–19 are upregulated (orange) in OD and PPP; and genes 20–23 are downregulated (blue) in OD and upregulated (orange) in PPP.

Confidential

a


OD Islets (Enzym.)
PPP Islets (LCM)
Transcriptional Profiling (Affymetrix)
Clinical information/ Functional validation
Differential Expression (T2D vs ND)
Co-Expression Modules (OD and PPP, ND)
Common DE Genes (OD + PPP)
Pathways/ Upstream Regulators
Experimental Validation

b


PC2 (0.04% variance)
PC1 (0.49% variance)
OD Islets
PPP Islets
OD LCM
PPP LCM

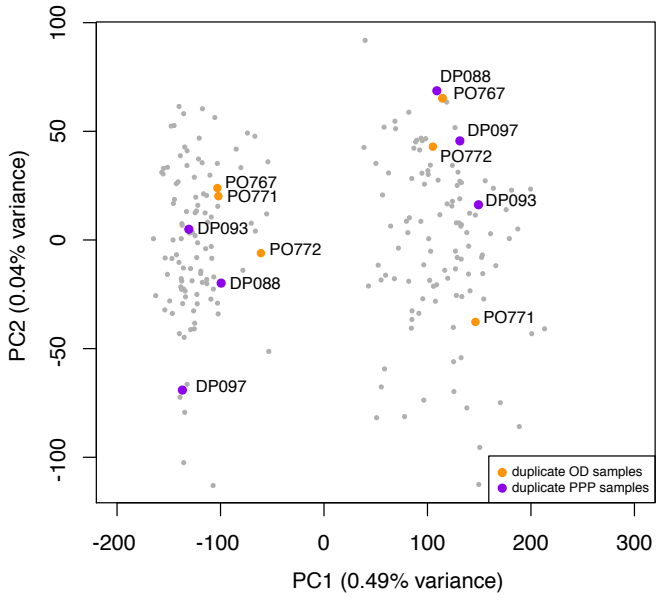

PC2 (0.04% variance)
PC1 (0.49% variance)
DP088
PO767
DP097
PO772
PO767
PO771
DP093
DP093
PO772
DP088
PO771
DP097
duplicate OD samples
duplicate PPP samples

Figure 2

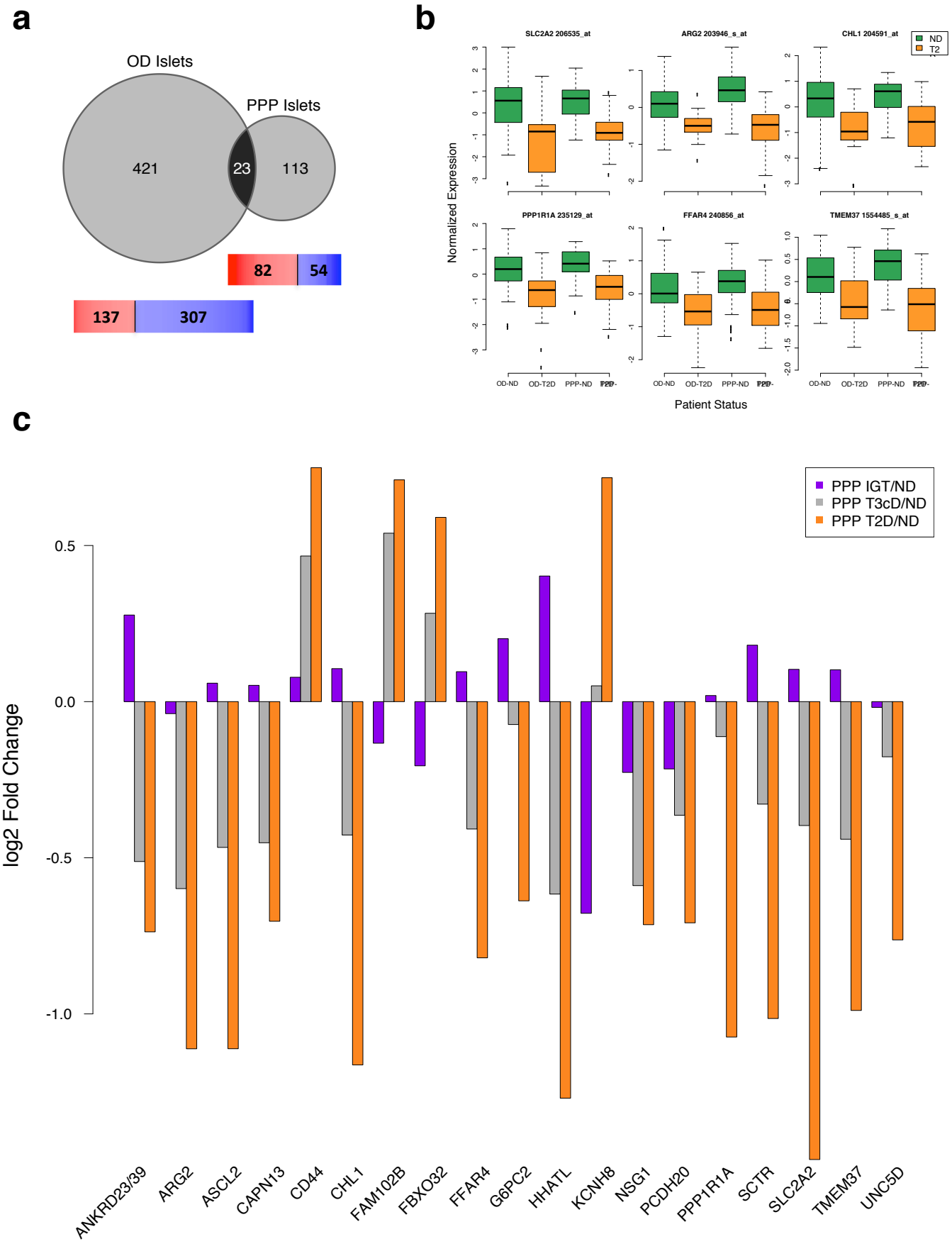

a
OD Islets
PPP Islets
421
23
113
82
54
137
307
b
SLC2A2 206535_at
ARG2 203946_s_at
CHL1 204591_at
PPP1R1A 235129_at
FFAR4 240856_at
TMEM37 1554485_s_at
ND
T2
Normalized Expression
OD-ND
OD-T2D
PPP-ND
Patient Status
c
PPP IGT/ND
PPP T3cD/ND
PPP T2D/ND
log2 Fold Change
0.5
0.0
-0.5
-1.0
ANKRD23/39
ARG2
ASCL2
CAPN13
CD44
CHL1
FAM102B
FBXO32
FFAR4
G6PC2
HHATL
KCNH8
NSG1
PCDH20
PPP1R1A
SCTR
SLC2A2
TMEM37
UNC5D

Figure 3

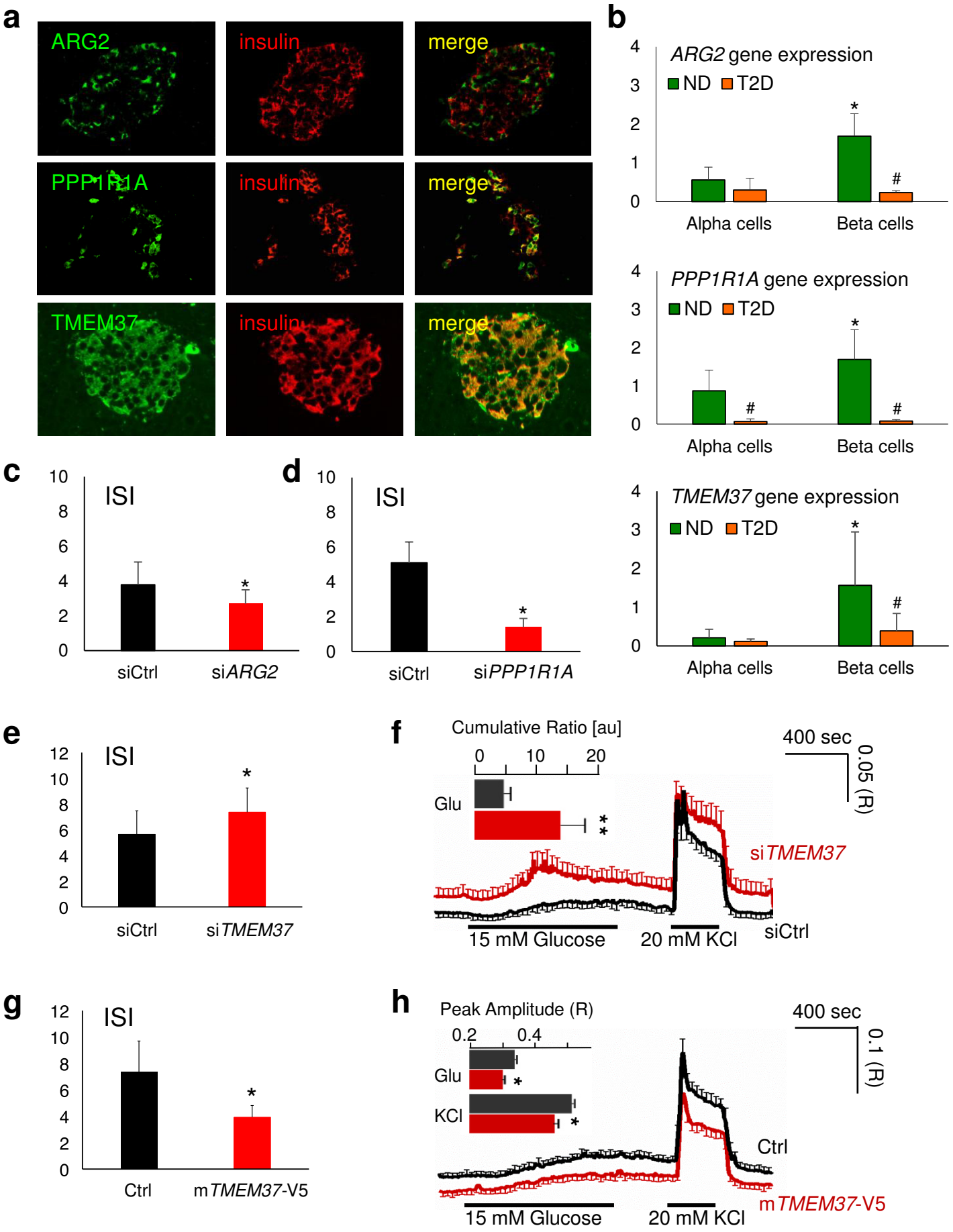
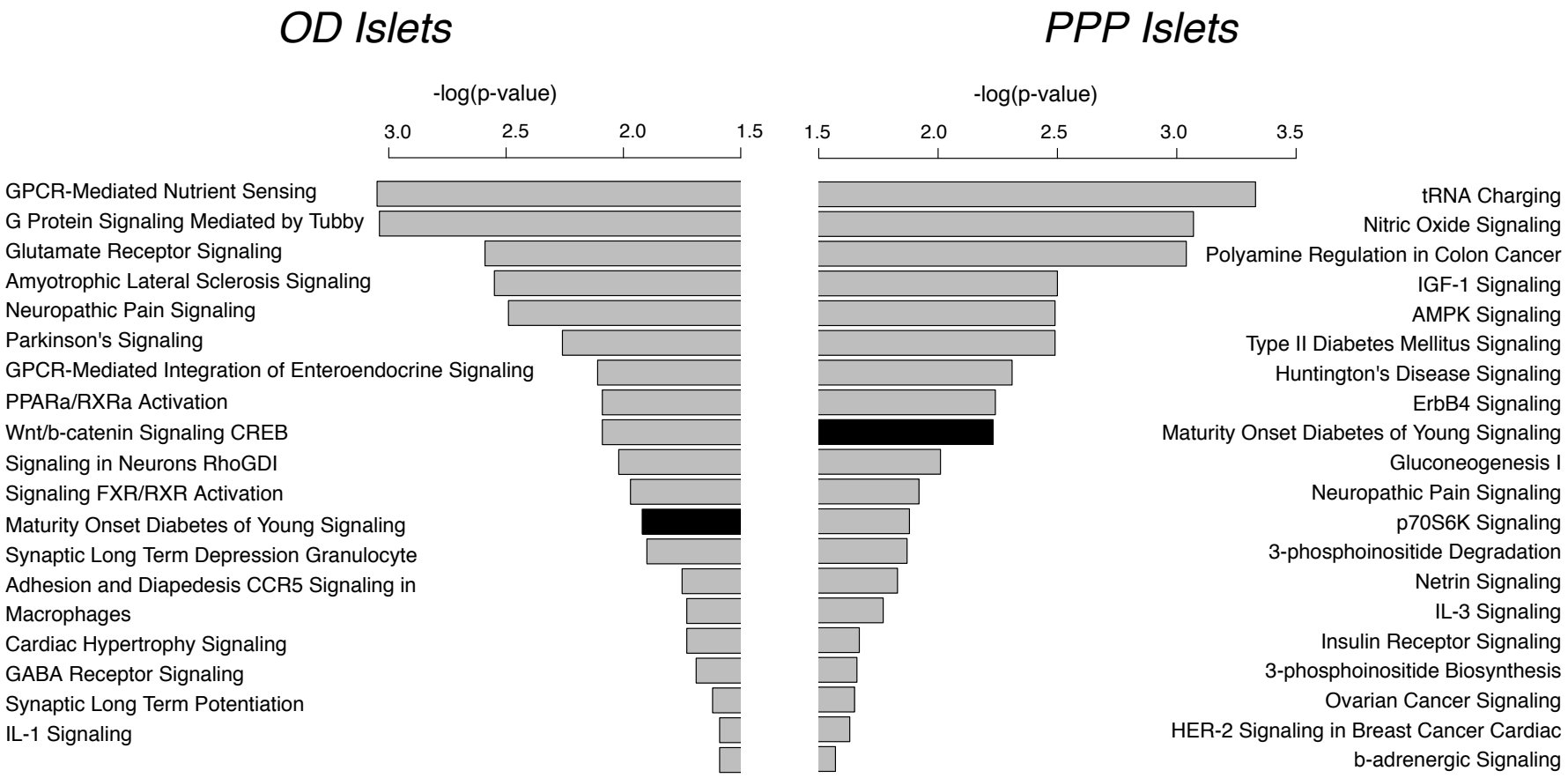
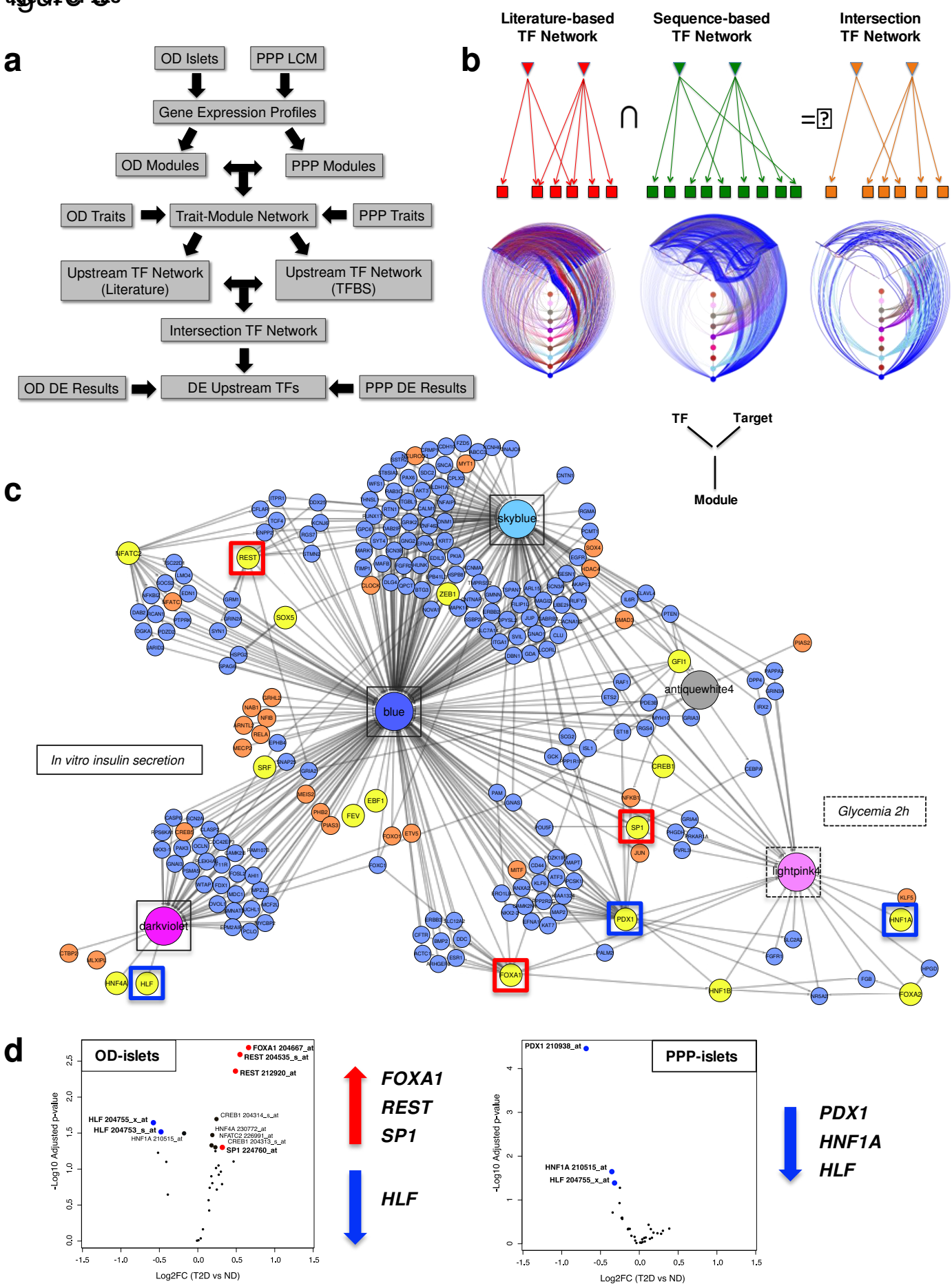
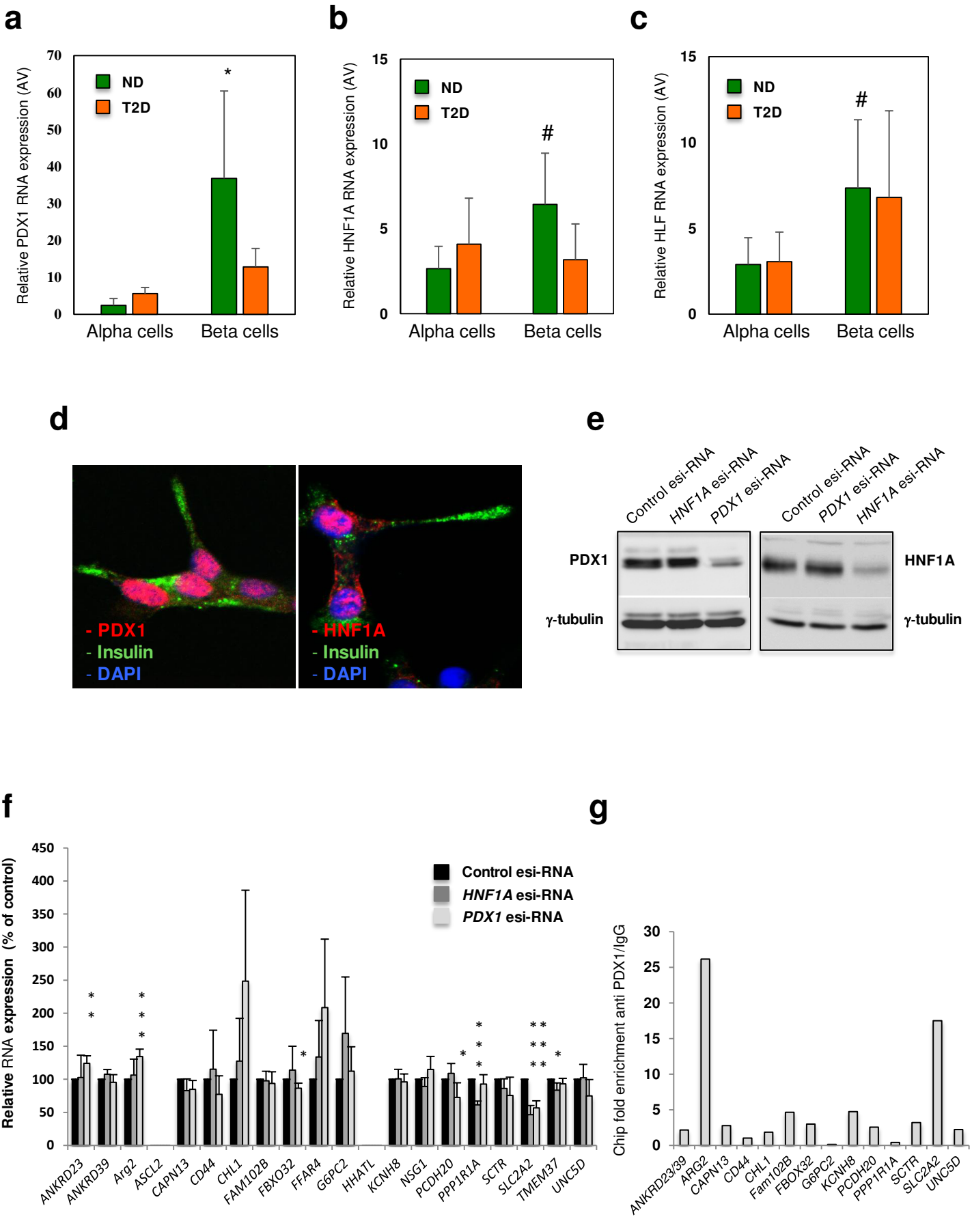

a
ARG2
insulin
merge
PPP1R1A
insulin
merge
TMEM37
insulin
merge
b
ARG2 gene expression
ND T2D
Alpha cells
Beta cells
PPP1R1A gene expression
ND T2D
Alpha cells
Beta cells
TMEM37 gene expression
ND T2D
Alpha cells
Beta cells
c
ISI
siCtrl
siARG2
d
ISI
siCtrl
siPPP1R1A
e
ISI
siCtrl
siTMEM37
f
Cumulative Ratio [au]
Glu
15 mM Glucose
20 mM KCl
siTMEM37
siCtrl
400 sec
0.05 (R)
g
ISI
Ctrl
mTMEM37-V5
h
Peak Amplitude (R)
Glu
KCl
15 mM Glucose
20 mM KCl
Ctrl
mTMEM37-V5
400 sec
0.1 (R)

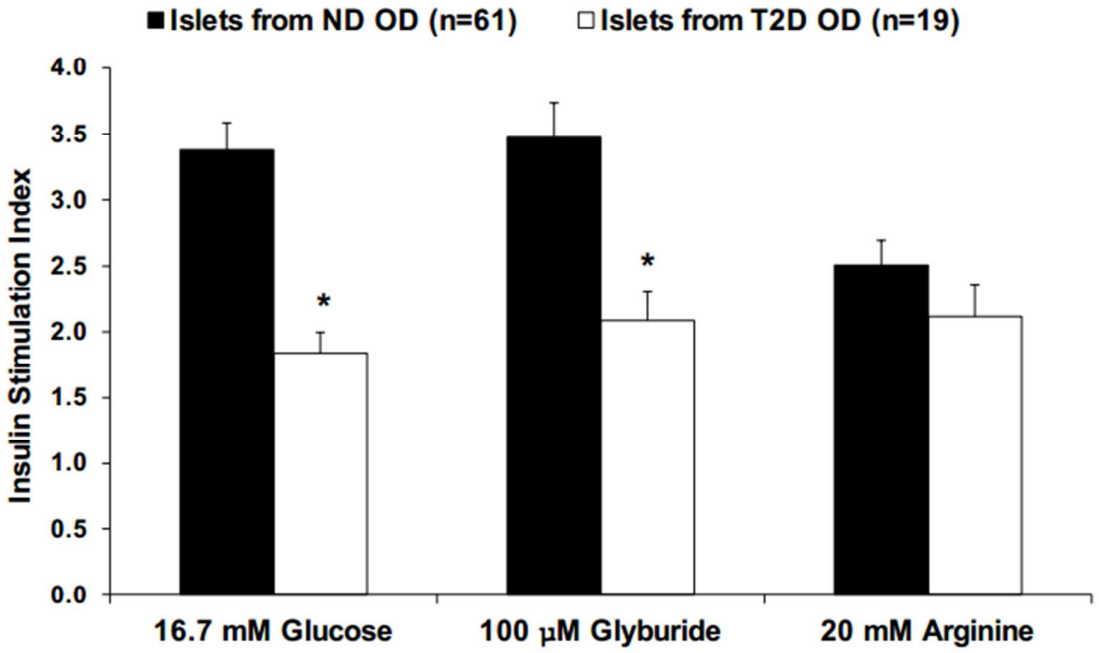
Figure 4


OD Islets
-log(p-value)
3.0
2.5
2.0
1.5
GPCR-Mediated Nutrient Sensing
G Protein Signaling Mediated by Tubby
Glutamate Receptor Signaling
Amyotrophic Lateral Sclerosis Signaling
Neuropathic Pain Signaling
Parkinson's Signaling
GPCR-Mediated Integration of Enteroendocrine Signaling
PPARa/RXRa Activation
Wnt/b-catenin Signaling CREB
Signaling in Neurons RhoGDI
Signaling FXR/RXR Activation
Maturity Onset Diabetes of Young Signaling
Synaptic Long Term Depression Granulocyte
Adhesion and Diapedesis CCR5 Signaling in Macrophages
Cardiac Hypertrophy Signaling
GABA Receptor Signaling
Synaptic Long Term Potentiation
IL-1 Signaling
PPP Islets
-log(p-value)
1.5
2.0
2.5
3.0
3.5
tRNA Charging
Nitric Oxide Signaling
Polyamine Regulation in Colon Cancer
IGF-1 Signaling
AMPK Signaling
Type II Diabetes Mellitus Signaling
Huntington's Disease Signaling
ErbB4 Signaling
Maturity Onset Diabetes of Young Signaling
Gluconeogenesis I
Neuropathic Pain Signaling
p70S6K Signaling
3-phosphoinositide Degradation
Netrin Signaling
IL-3 Signaling
Insulin Receptor Signaling
3-phosphoinositide Biosynthesis
Ovarian Cancer Signaling
HER-2 Signaling in Breast Cancer Cardiac
b-adrenergic Signaling


a
OD Islets
PPP LCM
Gene Expression Profiles
OD Modules
PPP Modules
OD Traits
Trait-Module Network
PPP Traits
Upstream TF Network (Literature)
Upstream TF Network (TFBS)
Intersection TF Network
OD DE Results
DE Upstream TFs
PPP DE Results
b
Literature-based TF Network
Sequence-based TF Network
Intersection TF Network
c
TF
Target
Module
skyblue
blue
darkviolet
antiquewhite4
lightpink4
In vitro insulin secretion
Glycemia 2h
d
OD-islets
FOXA1 204667_at
REST 204535_s_at
REST 212920_at
HLF 204755_x_at
HLF 204753_s_at
HNF1A 210515_at
CREB1 204314_s_at
HNF4A 230772_at
NFATC2 226991_at
CREB1 204373_s_at
SP1 224760_at
-Log10 Adjusted p-value
Log2FC (T2D vs ND)
FOXA1
REST
SP1
HLF
PPP-islets
PDX1 210938_at
HNF1A 210515_at
HLF 204755_x_at
-Log10 Adjusted p-value
Log2FC (T2D vs ND)
PDX1
HNF1A
HLF

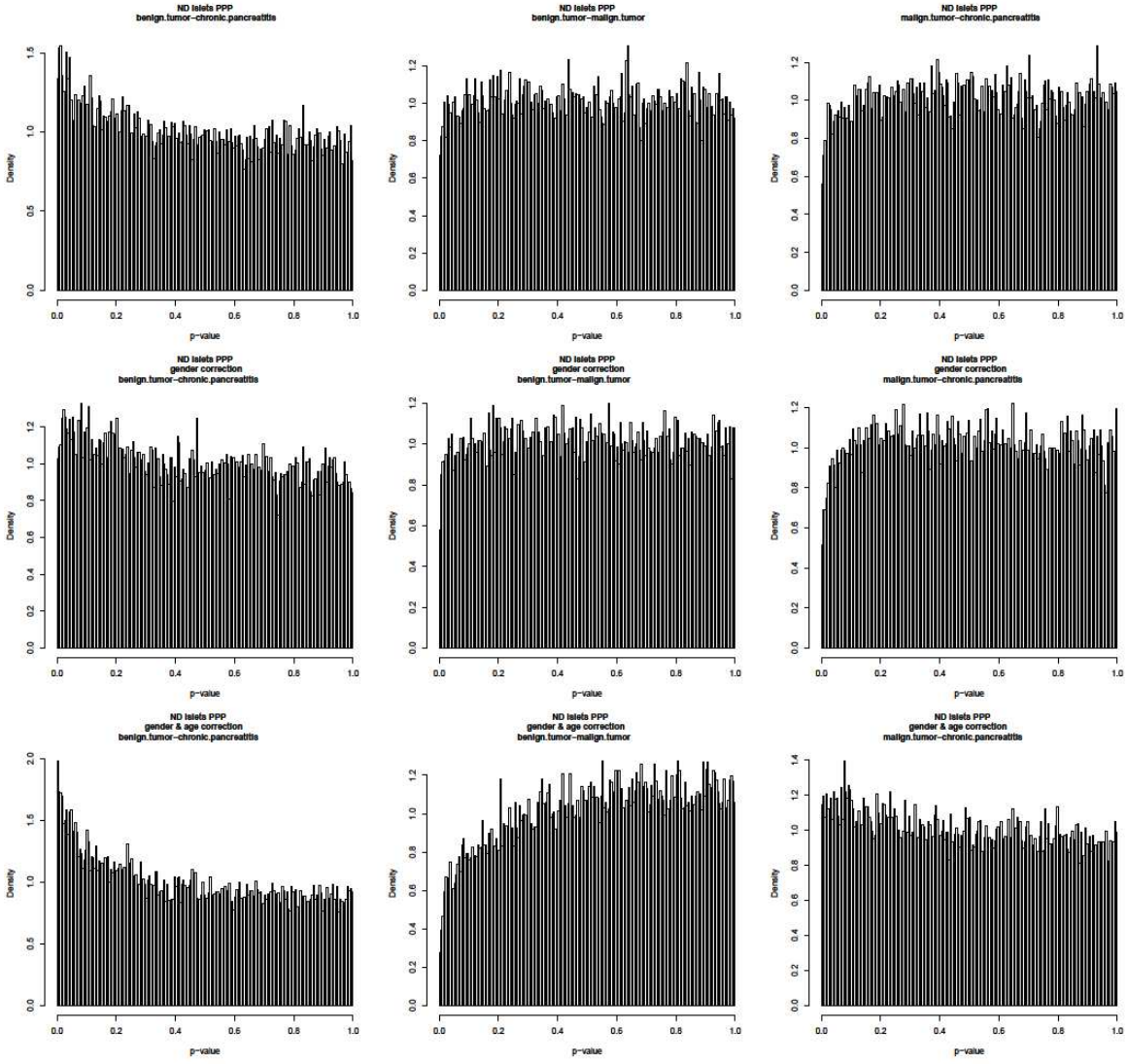

a
Relative PDX1 RNA expression (AV)
ND
T2D
*
Alpha cells
Beta cells
b
Relative HNF1A RNA expression (AV)
#
c
Relative HLF RNA expression (AV)
d
- PDX1
- Insulin
- DAPI
- HNF1A
e
Control esi-RNA
HNF1A esi-RNA
PDX1 esi-RNA
PDX1
γ-tubulin
HNF1A
f
Relative RNA expression (% of control)
Control esi-RNA
HNF1A esi-RNA
PDX1 esi-RNA
ANKRD23
ANKRD39
Arg2
ASCL2
CAPN13
CD44
CHL1
FAM102B
FBXO32
FFAR4
G6PC2
HHATL
KCNH8
NSG1
PCDH20
PPP1R1A
SCTR
SLC2A2
TMEM37
UNC5D
g
Chip fold enrichment anti PDX1/IgG
ANKRD23/39
ARG2
CAPN13
CD44
CHL1
Fam102B
FBOX32
G6PC2
KCNH8
PCDH20
PPP1R1A
SCTR
SLC2A2
UNC5D

Supplementary Figure 1



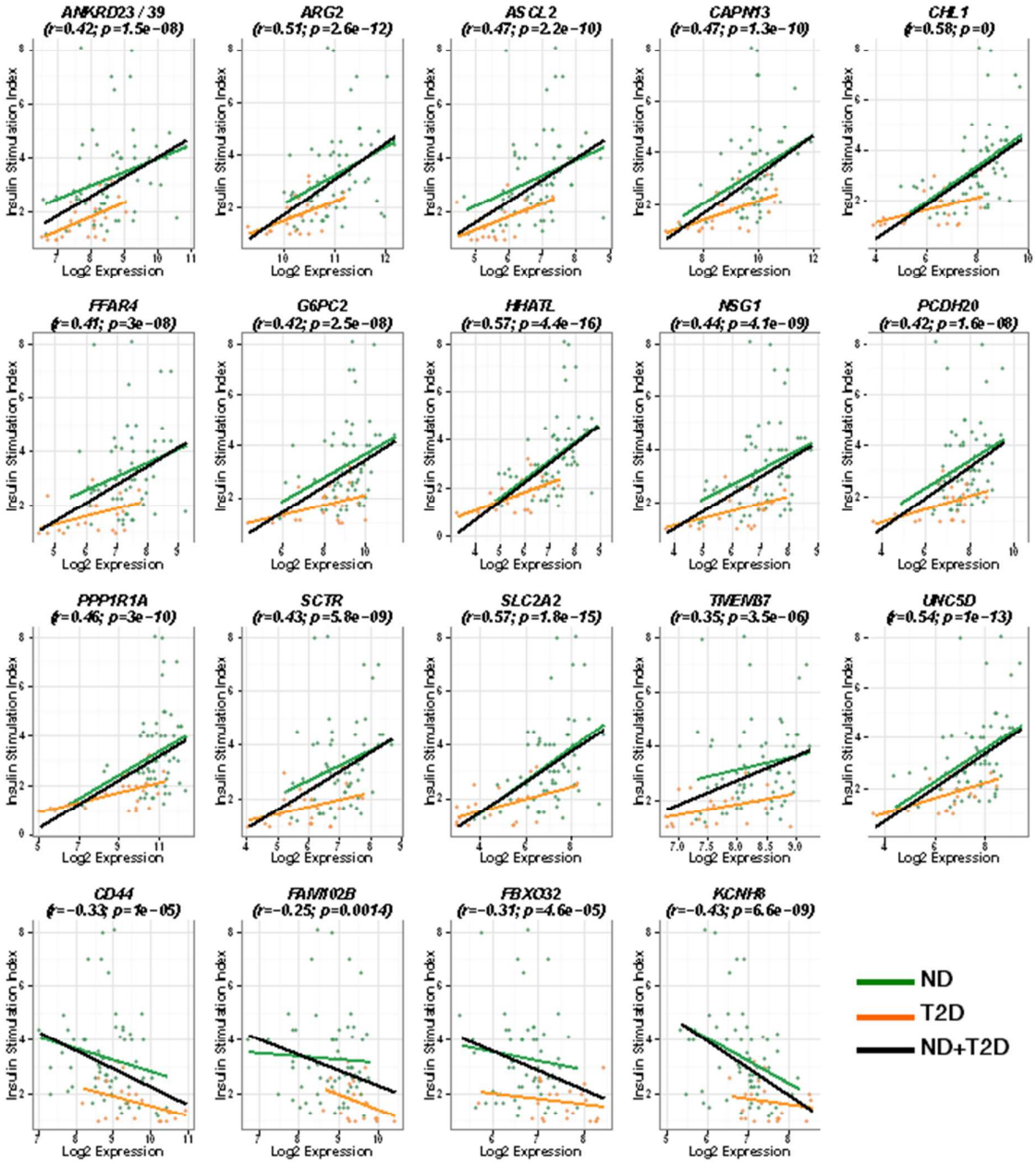
Supplementary Figure 1. Related to Table 1. T2D OD islets secrete less insulin in response to glucose or glyburide. Hand-picked islets of ND and T2D OD were exposed to 3.3 mmol/l glucose for 45 min to assess basal insulin release (µU/islet/min, mean±SE) and then challenged with 16.7 mmol/l glucose, 3.3 mmol/l glucose plus 100 µmol/l glyburide, or 3.3 mmol/l glucose plus 20 mmol/l arginine. Basal insulin release was 0.032±0.002 and 0.031±0.001 for T2D and ND OD islets, respectively (p=0.77 by the two-tailed Student's t-test). Insulin secretion in response to 16.7 mmol/l glucose (0.062±0.009 vs 0.118±0.012, p=0.01) and glyburide (0.067±0.008 vs 0.110±0.009, p=0.01), but not to arginine (0.068±0.008 vs 0.075±0.006, p=0.47), was lower in T2D islets. Accordingly, the insulin stimulation index (stimulated over basal insulin release, ISI) was lower in T2D islets after stimulation with glucose or glyburide (*p<0.01 by the two-tailed Student's t-test).

Supplementary Figure 2



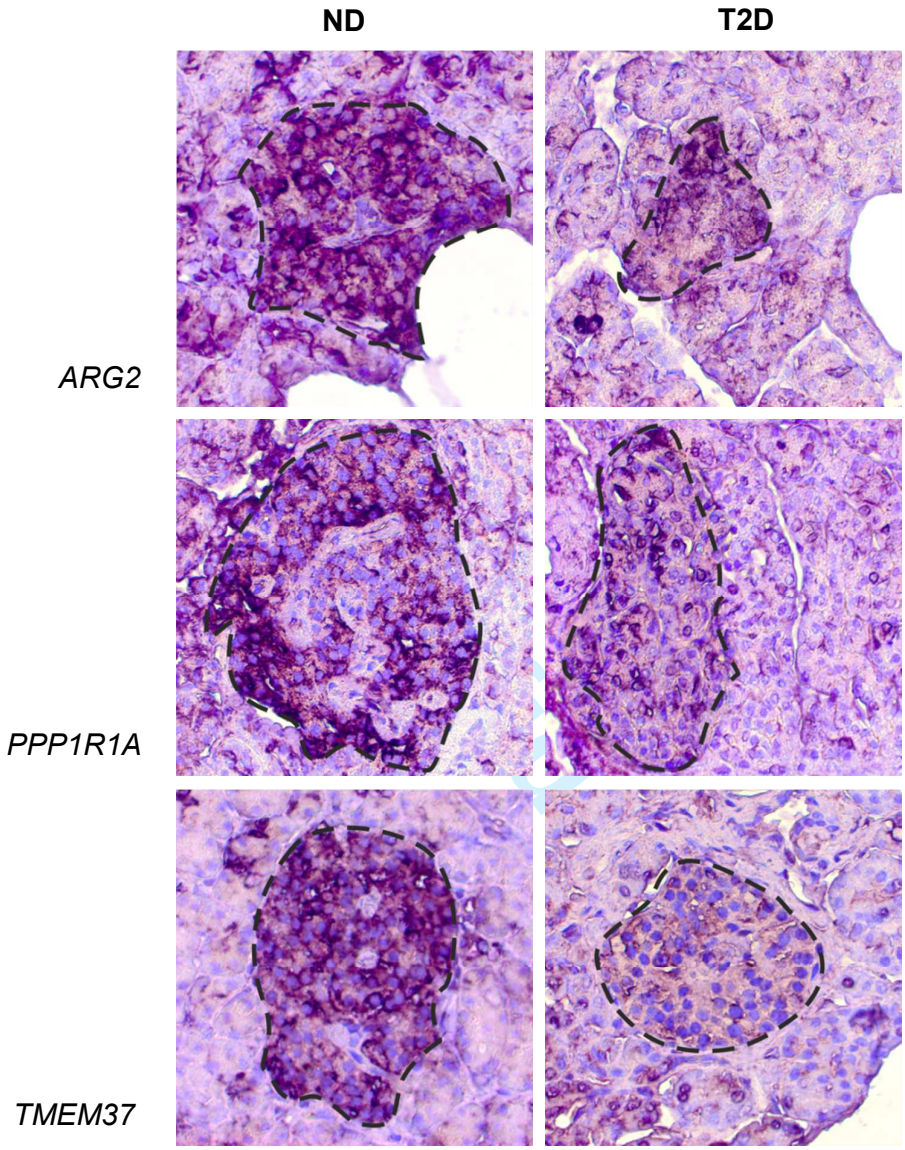
Supplementary Figure 2. Related to Figure 2 and Table 1. Linear regression for pancreatic disease in islets from ND PPP. Islets were obtained by LCM. Linear regression was performed without and with adjustment of the covariance for age and gender. Most p-value distributions follow a nearly uniform distribution, showing only a mild enrichment of low p-values. Linear regression for benign tumor versus chronic pancreatitis with gender and age correction shows the highest enrichment of low p-values (60 probe sets with $p \leq 0.001$ and 0 probe sets with an FDR of ≤ 0.05).

Supplementary Figure 3



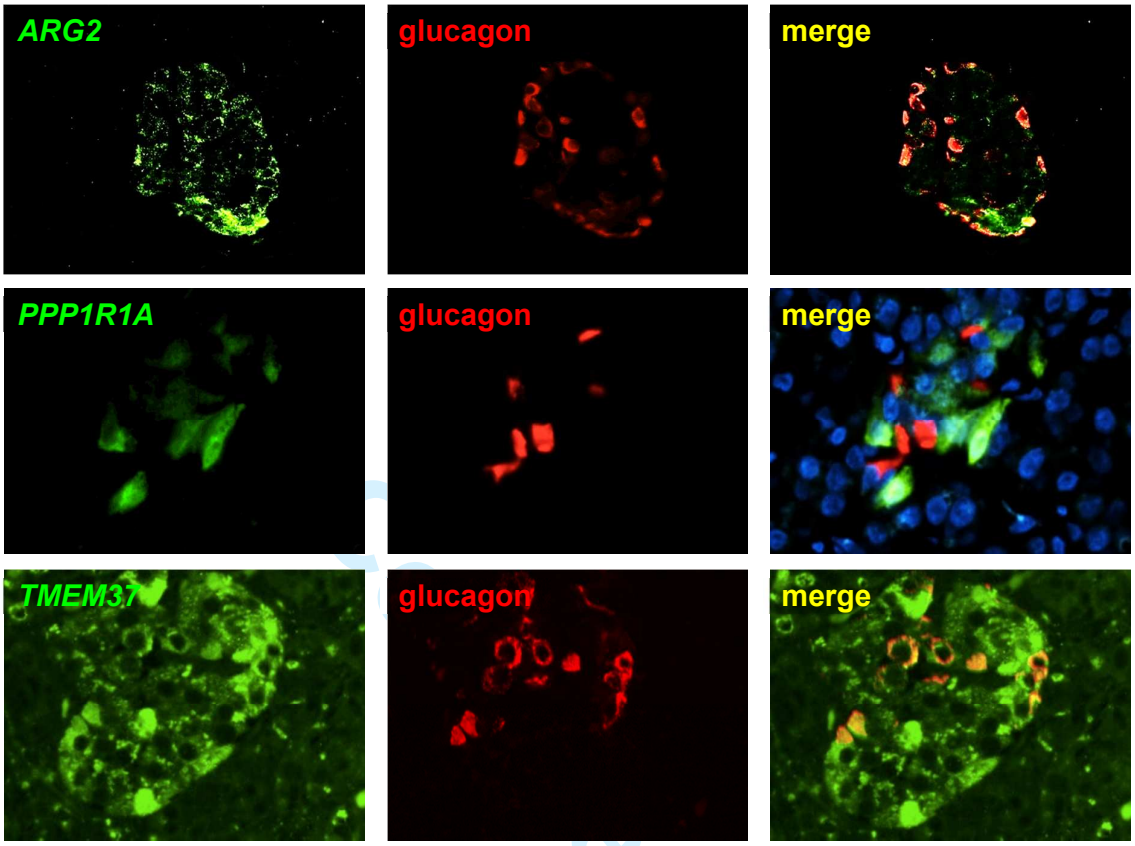
Supplementary Figure 3. Related to Figure 2. Scatterplots of log2-normalized expression values of the 19 T2D islet signature genes against the ISI of islets from OD. The scatterplots show ND samples (green markers/regression line) and T2D samples (orange markers/regression line) separately. A regression line for the ND and T2D samples combined is colored black. Pearson's correlation coefficients (*r*) and the corresponding p-values are indicated at the top of each plot.

Supplementary Figure 4



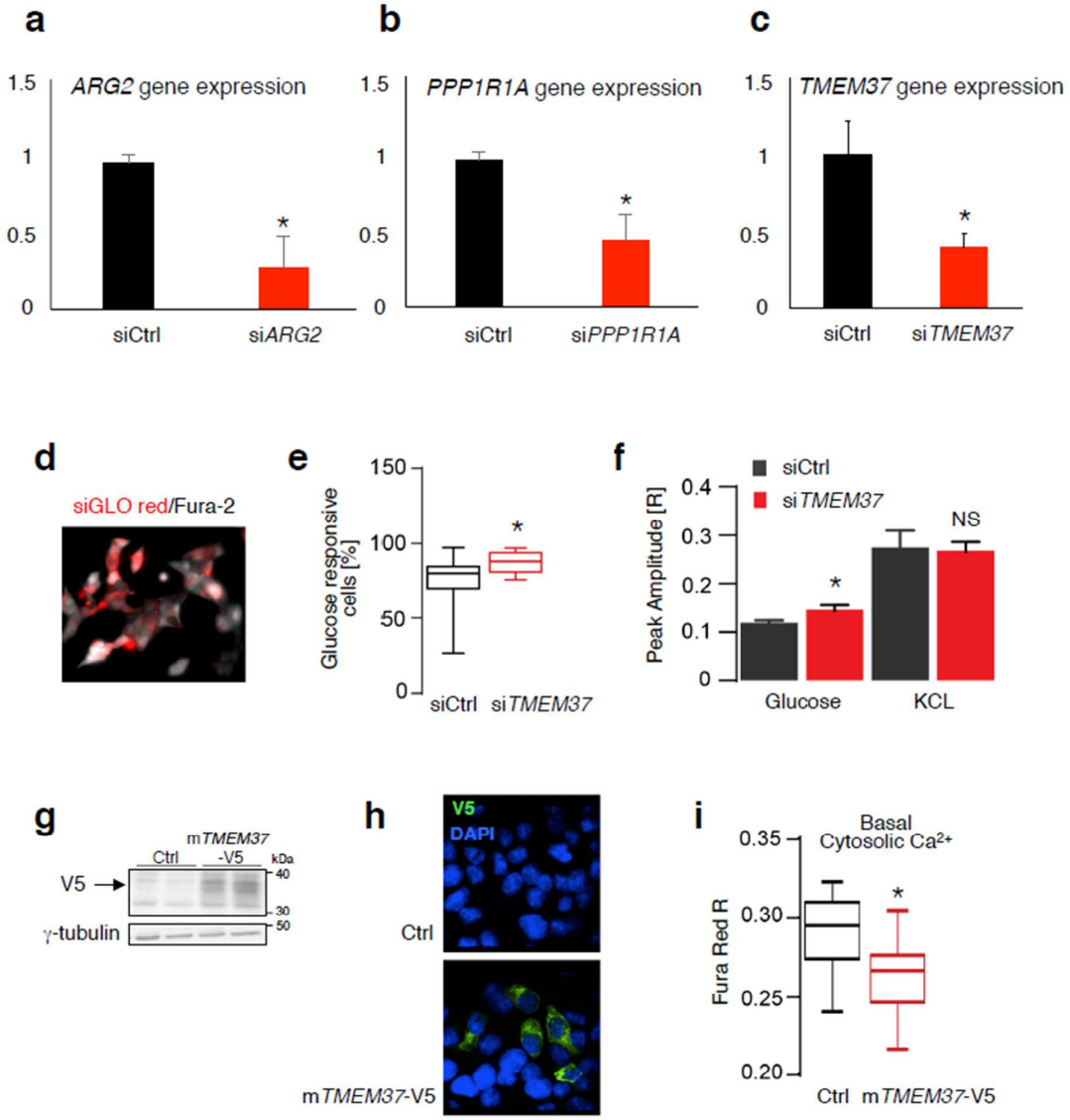
Supplementary Figure 4. Related to Figure 3 and Table 2. *In situ* RT-PCR for *ARG2*, *PPP1R1A*, and *TMEM37* expression in ND pancreatic sections. The dashed black lines indicate the margins of the islets. The images are representative of 80 islets analysed in each group.

Supplementary Figure 5



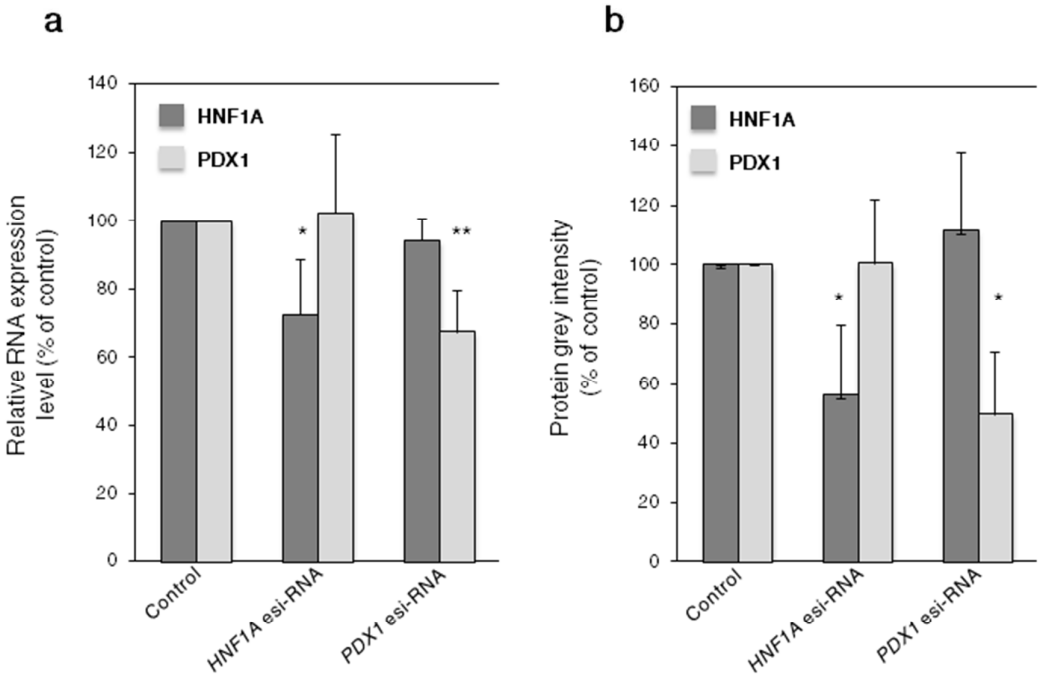
Supplementary Figure 5. Related to Figure 3 and Table 2. Confocal microscopy of human pancreas sections for *ARG2*, *PPP1R1A*, and *TMEM37* in addition to glucagon. The immunostaining was performed on pancreatic tissue that were fixed in paraformaldehyde and embedded in paraffin.

Supplementary Figure 6



Supplementary Figure 6. Related to Figure 3. Functional validation of ARG2, PPP1R1A, and TMEM37 in insulin-producing cells. (a)-(c). Silencing of *ARG2* (a), *PPP1R1A* (b), and *TMEM37* (c) in INS-1E (a) and (b) and INS-1 832/13 cells (c) was confirmed by RT-qPCR. Expression levels were normalized to those of *beta-actin* mRNA. (d). Image of INS-1 832/13 cells transfected with siGLO^{+} (red) and loaded with Fura-2 AM (grey). (e). Boxplot showing the median (line), 25th and 75th percentiles (box), and minimum–maximum (whiskers) percentage of *siTMEM37*- or siCrtl-treated INS-1 832/13 cells with changes in cytosolic Ca^{2+} concentrations in response to glucose. (f). Peak Ca^{2+} amplitudes in *siTMEM37*- or siCrtl-treated INS-1 832/13 cells in response to high glucose or high KCl (NS, p>0.05, *p<0.05, **p<0.01, Mann–Whitney *U* test). (g). Immunoblots for V5 and gamma-tubulin in *TMEM37-V5*-transfected and control INS-1 832/13 cells. (h). Immunostaining for V5 (green) in *TMEM37-V5*-transfected and control INS-1 832/13 cells. Nuclei were counterstained with DAPI (blue). (i). Boxplot showing the median (line), 25th and 75th percentiles (box), and minimum–maximum (whiskers) basal cytosolic Ca^{2+} concentrations in 332 siCrtl-treated (n=10 coverslips) and 419 *siTMEM37*-treated (n=12 coverslips) INS-1 832/13 cells (*p<0.05, unpaired two-tailed t-test).

Supplementary Figure 7



Supplementary Figure 7. Related to Figure 6. Efficiency of *PDX1* and *HNF1A* esiRNA-induced silencing in EndoC-betaH1 cells. (a). RT-qPCR. (b). Immunoblotting (Student's t-test, *p<0.05, **p<0.01).

Confidential

Supplementary Table 1

	Gender [F/M]	Age [years]	BMI [kg/m²]	Diabetes duration [years]	Glycemia [mmol/l] in ICU	Fasting glucose [mmol/l]	HbA1c [%]	Glycemia after OGTT at 2 hours [mmol/l]	Histopathology		
									Chronic pancreatitis	Benign tumor	Malign tumor
Main clinical information of OD (n=243)											
ND 204 (84.0%)	108/96	61±17	25.6±3.8 (n=196)	–	8.5±2.2 (n=178)	–	–	–	–	–	–
T2D 39 (16.0%)	12/27	73±8	26.2±3.7 (n=39)	10.4±6.9 (n=32)	11.8±3.7 (n=37)	–	–	–	–	–	–
Main clinical information of PPP (n=201)											
ND 70 (34.8%)	35/35	61±13	24.5±4.0	–	–	5.3±0.6 (n=60)	5.5±0.5 (n=69)	5.9±1.3 (n=53)	11 (16%)	22 (31%)	37 (53%)
T2D 54 (26.9%)	20/34	65±13*	25.6±5.3	10.7±8.9	–	8.2±2.4*** (n=47)	7.4±1.2*** (n=52)	–	14 (26%)	6 (11%)	34 (63%)
IGT 30 (14.9%)	13/17	63±12	26.1±4.1	–	–	5.5±0.6 (n=30)	5.6±0.4 (n=30)	9.3±0.8*** (n=30)	4 (13%)	10 (33%)	16 (54%)
T3cD 46 (22.9%)	18/28	67±10**	25.9±4.2	0.05±0.1	–	7.3±4.3** (n=44)	6.6±1.4*** (n=46)	12.8±2.7*** (n=23)	9 (19%)	5 (11%)	32 (70%)
T1D 1 (0.5%)	0/1	53	26.9	6.0	–	7.6	7.8	–	–	–	1 (100%)

Supplementary Table 1. Related to Figure 1. Main clinical information on the global IMIDIA cohorts of organ donors (OD) and partially pancreatectomized patients (PPP). BMI: body mass index; ICU: intensive care unit; OGTT: oral glucose tolerance test; ND: non-diabetic subjects; T2D: type 2 diabetic subjects, IGT: impaired glucose tolerant subjects; T3cD: type 3c diabetic subjects; T1D: type 1 diabetic subjects. Except for gender, the values are means ± standard deviation (two-tailed t-test; *p<0.05, **p<0.01, and ***p<0.001) versus ND.

Confidential

Supplementary Table 2

OD islets						
Entrez ID	**Symbol**	**Gene name**	**Probe ID**	**Ratio**	**P.Value**	**adj.P.Val.**
10058	ABCB6	ATP-binding cassette, sub-family B (MDR/TAP), member 6	203192_at	0.645	3.44E-12	1.020E-07
57467	HHATL	hedgehog acyltransferase-like	223572_at	0.388	1.86E-08	1.098E-04
6514	SLC2A2	solute carrier family 2 (facilitated glucose transporter), member 2	206535_at	0.273	3.93E-08	1.657E-04
8544	PIR	pirin (iron-binding nuclear protein)	207469_s_at	0.586	1.00E-07	3.073E-04
5502	PPP1R1A	protein phosphatase 1, regulatory (inhibitor) subunit 1A	235129_at	0.419	1.25E-07	3.073E-04
384	ARG2	arginase 2	203946_s_at	0.605	2.47E-07	3.286E-04
56605	ERO1LB	ERO1-like beta (S. cerevisiae)	220012_at	0.554	3.08E-07	3.627E-04
64130	LIN7B	lin-7 homolog B (C. elegans)	219760_at	0.589	4.08E-07	4.155E-04
7057	THBS1	thrombospondin 1	201110_s_at	1.761	4.59E-07	4.515E-04
3375	IAPP	islet amyloid polypeptide	207062_at	0.580	6.12E-07	5.312E-04
79623	GALNT14	UDP-N-acetyl-alpha-D-galactosamine:polypeptide N-acetylgalactosaminyltransferase 14 (GalNAc-T14)	219271_at	0.493	1.08E-06	7.407E-04
773 /// 100507353	CACNA1A /// LOC100507353	calcium channel, voltage-dependent, P/Q type, alpha 1A subunit /// uncharacterized LOC100507353	1558945_s_at	0.469	1.39E-06	7.641E-04
486 /// 100533181	FXYD2 /// FXYD6-FXYD2	FXYD domain containing ion transport regulator 2 /// FXYD6-FXYD2 readthrough	207434_s_at	0.594	1.54E-06	7.641E-04
2740	GLP1R	glucagon-like peptide 1 receptor	208400_at	0.526	1.38E-06	7.641E-04
89765	RSPH1	radial spoke head 1 homolog (Chlamydomonas)	230093_at	0.654	1.55E-06	7.641E-04
4093	SMAD9	SMAD family member 9	227719_at	0.554	1.58E-06	7.641E-04
84623	KIRREL3	kin of IRRE like 3 (Drosophila)	240402_at	0.445	2.14E-06	8.332E-04
3428	IFI16	interferon, gamma-inducible protein 16	208965_s_at	1.525	2.26E-06	8.663E-04
5798	PTPRN	protein tyrosine phosphatase, receptor type, N	204945_at	0.548	2.73E-06	9.673E-04
309	ANXA6	annexin A6	200982_s_at	0.654	3.02E-06	1.002E-03

Confidential

PPP islets						
Entrez ID	**Symbol**	**Gene name**	**Probe ID**	**Ratio**	**P.Value**	**adj.P.Val.**
26577	PCOLCE2	procollagen C-endopeptidase enhancer 2	219295_s_at	6.519	1.23E-15	3.65E-11
392617	ELFN1	extracellular leucine-rich repeat and fibronectin type III domain containing 1	229581_at	4.391	7.10E-15	1.05E-10
229	ALDOB	aldolase B, fructose-bisphosphate	204705_x_at	4.588	1.85E-13	1.24E-09
384	ARG2	arginase 2	203946_s_at	0.463	2.98E-13	1.47E-09
140738	TMEM37	transmembrane protein 37	227190_at	0.504	9.09E-13	3.84E-09
430	ASCL2	achaete-scute complex homolog 2 (Drosophila)	229215_at	0.463	5.97E-12	1.74E-08
145270	PRIMA1	proline rich membrane anchor 1	230087_at	4.975	7.65E-12	1.74E-08
6514	SLC2A2	solute carrier family 2 (facilitated glucose transporter), member 2	206535_at	0.362	7.52E-12	1.74E-08
27122	DKK3	dickkopf WNT signaling pathway inhibitor 3	221127_s_at	2.335	1.35E-11	2.86E-08
23017	FAIM2	Fas apoptotic inhibitory molecule 2	203619_s_at	3.826	1.47E-11	2.91E-08
151647	FAM19A4	family with sequence similarity 19 (chemokine (C-C motif)-like), member A4	242348_at	0.379	1.47E-10	2.41E-07
5172	SLC26A4	solute carrier family 26, member 4	206529_x_at	3.379	2.11E-10	3.29E-07
57393	TMEM27	transmembrane protein 27	223784_at	0.572	4.25E-10	6.29E-07
2906	GRIN2D	glutamate receptor, ionotropic, N-methyl D-aspartate 2D	229883_at	0.423	1.03E-09	1.32E-06
203111	C8orf47	chromosome 8 open reading frame 47	1552389_at	0.554	3.61E-09	3.58E-06
5502	PPP1R1A	protein phosphatase 1, regulatory (inhibitor) subunit 1A	235129_at	0.475	5.80E-09	5.54E-06
192668	CYS1	cystin 1	228739_at	0.395	6.92E-09	6.29E-06
170691	ADAMTS17	ADAM metallopeptidase with thrombospondin type 1 motif, 17	1552727_s_at	3.053	1.68E-08	1.42E-05
10752	CHL1	cell adhesion molecule with homology to L1CAM (close homolog of L1)	204591_at	0.446	1.95E-08	1.56E-05
83876	MRO	maestro	231358_at	0.432	2.08E-08	1.62E-05

Supplementary Table 2. Related to Figure 2 and Table 2. Top 20 regulated genes (absolute fold-change of ≥1.5) in islets of T2D OD versus islets of ND OD and in islets of T2D PPP versus islets of ND PPP. Adj.p, adjusted p-value after correcting for multiple hypothesis tests using the Benjamini-Hochberg method. ND, non-diabetic subjects; OD, organ donors; PPP, partially pancreatectomized patients; T2D, type 2 diabetic subjects; probe ID=probe set ID.

Confidential

Supplementary Table 3

See Excel-sheet '*Supplementary Table 3'* attached/implemented.



Supplementary Table 3.xlsx

Supplementary Table 3. Bailey Comparison. Related to Figure 2 and Tables 1 and 2. Differential expression analysis results for ADEX, Immunogenic, Progenitor and Squamous pancreatic cancer subtypes were downloaded from Bailey et al., 2016 supplementary information. The comparisons of each of the four sub-types against the other three subtypes were used to define a specific gene expression signature for each sub-type, which were then compared to the differential expression results from PPP and OD samples (T2D vs ND). Only genes with a fold change $\geq$1.5 and adjusted p-value $\leq$0.05 were considered to be differentially expressed for each comparison. The number of up- or down-regulated genes, as well as the total number of DE genes in OD and PPP T2D vs ND that overlap with each signature is shown. Significance of overlap between PPP or OD T2D vs ND comparisons and each of the pancreatic cancer sub-type signatures was calculated using the hypergeometric distribution with the background as the total number of expressed genes in the OD or PPP samples. The genes overlapping between OD/PPP and the tumor signatures are also shown.

Confidential

Supplementary Table 4

See Excel-sheet '*Supplementary Table 4'* attached/ implemented.



Supplementary Table 4.xlsx

Supplementary Table 4. Related to Figure 2 and Table 2. Differentially Regulated Genes in Islets from OD and PPP. Adj.p, adjusted p-value after correcting for multiple hypothesis tests using the Benjamini–Hochberg method; OD, organ donors; PPP, partially pancreatectomized patients; probe ID, probe set ID; reg. OD, regulated in organ donors; reg. PPP, regulated in partially pancreatectomized patients.

Confidential

Confidential

Supplementary Table 5

Top 20 GOs for T2D vs. ND down-regulated probe sets in OD islets				
GOBPID	**Term**	**P-value**	**Count**	**Size**
GO:0007267	cell-cell signaling	4.091E-25	69	771
GO:0023061	signal release	6.532E-24	44	308
GO:0030072	peptide hormone secretion	4.371E-19	31	185
GO:0046879	hormone secretion	7.427E-19	33	218
GO:0009914	hormone transport	1.143E-18	33	221
GO:0002790	peptide secretion	1.147E-18	31	191
GO:0051046	regulation of secretion	4.334E-18	44	430
GO:0010817	regulation of hormone levels	5.722E-18	38	318
GO:1903530	regulation of secretion by cell	8.089E-18	42	397
GO:0030073	insulin secretion	1.504E-17	28	164
GO:0007268	synaptic transmission	2.265E-17	44	449
GO:0015833	peptide transport	3.849E-17	32	231
GO:0046883	regulation of hormone secretion	1.626E-16	28	179
GO:0042886	amide transport	1.742E-16	32	243
GO:0090276	regulation of peptide hormone secretion	1.844E-16	26	151
GO:0002791	regulation of peptide secretion	3.588E-16	26	155
GO:0050796	regulation of insulin secretion	2.644E-15	24	139
GO:0097479	synaptic vesicle localization	5.884E-15	21	104
GO:0032940	secretion by cell	7.003E-15	49	642
GO:0071705	nitrogen compound transport	1.701E-14	44	537
Top 20 GOs for T2D vs. ND down-regulated probe sets in PPP islets				
GOBPID	**Term**	**P-value**	**Count**	**Size**
GO:0043583	ear development	1.498E-05	6	139
GO:0010817	regulation of hormone levels	2.255E-05	8	311
GO:0046879	hormone secretion	1.669E-04	6	214
GO:0009914	hormone transport	1.800E-04	6	217
GO:0048729	tissue morphogenesis	1.897E-04	8	421
GO:0050796	regulation of insulin secretion	2.362E-04	5	145
GO:0035295	tube development	3.170E-04	8	454
GO:0090276	regulation of peptide hormone secretion	3.217E-04	5	155
GO:0002009	morphogenesis of an epithelium	3.259E-04	7	343
GO:0009790	embryo development	3.325E-04	10	714
GO:0002791	regulation of peptide secretion	3.619E-04	5	159
GO:0050708	regulation of protein secretion	4.291E-04	6	255
GO:0009887	organ morphogenesis	4.650E-04	9	608
GO:0030073	insulin secretion	4.788E-04	5	169
GO:0046883	regulation of hormone secretion	5.614E-04	5	175
GO:0044707	single-multicellular organism process	5.759E-04	27	4085
GO:0010721	negative regulation of cell development	7.050E-04	5	184
GO:0048562	embryonic organ morphogenesis	7.403E-04	5	186
GO:0090087	regulation of peptide transport	7.403E-04	5	186
GO:0030072	peptide hormone secretion	7.585E-04	5	187

Supplementary Table 5. Related to Figure 4. The top 20 enriched biological process Gene Ontologies for the downregulated probe sets in T2D islets from OD and PPP. OD, organ donors; PPP, partially pancreatectomized patients; T2D, type 2 diabetic subjects.

Confidential

Supplementary Table 6

T2D vs. ND down-regulated genes in OD islets assigned to "insulin secretion" GO			
Probe ID	**Symbol**	**Ratio**	**Adj.P.Val**
210246_s_at	ABCC8	0.509	1.223E-03
1552519_at	ACVR1C	0.649	4.461E-02
209869_at	ADRA2A	0.646	2.229E-02
1558944_at	CACNA1A	0.528	1.037E-03
1558945_s_at	CACNA1A	0.469	7.641E-04
204811_s_at	CACNA2D2	0.626	3.070E-03
223500_at	CPLX1	0.635	1.003E-02
205630_at	CRH	0.463	8.142E-03
1561507_at	FFAR1	0.579	7.271E-03
221453_at	G6PC2	0.616	3.440E-02
231291_at	GIPR	0.664	1.557E-02
208400_at	GLP1R	0.526	7.641E-04
208401_s_at	GLP1R	0.602	1.002E-03
217057_s_at	GNAS	0.528	7.948E-03
229380_at	ILDR2	0.573	2.654E-03
206762_at	KCNA5	0.655	3.043E-02
216096_s_at	NRXN1	0.632	7.760E-03
205825_at	PCSK1	0.644	7.105E-03
1554789_a_at	PDE8B	0.566	6.236E-03
204945_at	PTPRN	0.548	9.673E-04
219140_s_at	RBP4	0.577	5.728E-03
222049_s_at	RBP4	0.564	6.530E-03
1552673_at	RFX6	0.620	8.586E-03
229823_at	RIMS2	0.657	1.458E-02
206535_at	SLC2A2	0.273	1.657E-04
1552985_at	SLC30A8	0.654	3.325E-02
202508_s_at	SNAP25	0.634	1.026E-02
204729_s_at	STX1A	0.549	2.029E-03
202260_s_at	STXBP1	0.658	1.559E-03
240236_at	STXBP5L	0.583	5.083E-03
232025_at	SYT7	0.629	2.233E-03
T2D vs. ND down-regulated genes in PPP islets assigned to "insulin secretion" GO			
Probe ID	**Symbol**	**Ratio**	**Adj.P.Val**
221453_at	G6PC2	0.643	2.773E-02
210938_at	PDX1	0.631	6.419E-05
209992_at	PFKFB2	0.644	2.833E-02
206535_at	SLC2A2	0.362	1.743E-08
223784_at	TMEM27	0.572	6.288E-07

Supplementary Table 6. Related to Figure 4. Downregulated genes assigned to the insulin secretion Gene Ontology (GO: 0030073) for islets from T2D OD and T2D PPP. OD, organ donors; PPP, partially pancreatectomized patients: T2D, type 2 diabetic subjects.

Confidential

Supplementary Table 7

Ingenuity downstream functions for T2D vs ND regulated probe sets in OD islets				
Diseases or Functions Annotation	**Predicted Activation State**	**Activation z-score**	**P-value**	**Gene number**
coordination	Decreased	-3.225	2.03E-05	18
size of body	Decreased	-3.220	3.35E-06	52
transport of metal ion	Decreased	-2.822	2.98E-07	26
long-term potentiation	Decreased	-2.796	5.30E-04	17
transport of metal	Decreased	-2.703	5.86E-09	30
transport of monovalent inorganic cation	Decreased	-2.646	1.79E-04	16
conditioning	Decreased	-2.407	1.51E-05	18
concentration of cyclic AMP	Decreased	-2.380	1.09E-06	19
release of neurotransmitter	Decreased	-2.325	2.80E-12	24
transport of cation	Decreased	-2.313	1.53E-05	27
neoplasia of epithelial tissue	Decreased	-2.296	2.91E-04	329
rearing	Decreased	-2.282	4.09E-05	11
growth of neurites	Decreased	-2.211	7.15E-07	35
outgrowth of neurites	Decreased	-2.207	1.89E-06	31
quantity of vesicles	Decreased	-2.170	5.37E-04	9
accumulation of cyclic AMP	Decreased	-2.115	2.16E-04	13
differentiation of tumor cell lines	Decreased	-2.105	1.61E-03	22
outgrowth of cells	Decreased	-2.078	3.20E-06	32
heart septal defect	Decreased	-2.033	1.88E-03	9
synaptic transmission	Decreased	-2.018	1.83E-08	31
neonatal death	Increased	2.121	4.50E-07	34
hyperesthesia	Increased	2.157	1.66E-03	9
ataxia	Increased	2.161	1.03E-03	17
organismal death	Increased	2.246	1.30E-06	116
seizure disorder	Increased	2.361	2.63E-09	40
seizures	Increased	2.361	1.53E-08	35
Movement Disorders	Increased	2.545	2.32E-07	65
proliferation of tumor cell lines	Increased	2.760	3.50E-04	69
hyperactive behavior	Increased	2.920	3.82E-06	15

Ingenuity downstream functions for T2D vs ND regulated probe sets in PPP islets				
Diseases or Functions Annotation	**Predicted Activation State**	**Activation z-score**	**P-value**	**Gene number**
quantity of beta islet cells	Decreased	-2.805	1.43E-04	8
quantity of secretory structure	Decreased	-2.503	2.27E-02	12
cell survival	Decreased	-2.460	1.07E-02	84
quantity of islet cells	Decreased	-2.447	1.06E-03	9
quantity of apud cells	Decreased	-2.442	1.63E-04	9
Clathrin mediated endocytosis	Decreased	-2.407	2.11E-02	6
cell viability	Decreased	-2.340	1.66E-02	77
quantity of neuroendocrine cells	Decreased	-2.299	8.50E-04	11
size of brain	Decreased	-2.164	2.57E-02	12
quantity of protein in blood	Decreased	-2.076	4.95E-04	40
phagocytosis of phagocytes	Increased	2.011	1.15E-02	11
phagocytosis of myeloid cells	Increased	2.154	4.86E-03	12

phagocytosis of neutrophils	Increased	2.190	6.38E-03	6
quantity of carbohydrate	Increased	2.342	7.61E-03	36
seizure disorder	Increased	2.433	2.69E-03	35
organismal death	Increased	2.453	1.45E-03	146

Supplementary Table 7. Related to Figures 2 and 4. Downstream functions predicted to be significantly increased or decreased among the differentially regulated probe sets in islets from T2D OD and T2D PPP. OD, organ donors; PPP, partially pancreatectomized patients; T2D, type 2 diabetic subjects.

Confidential

Supplementary Table 8

Ingenuity upstream regulators of T2D vs ND regulated probe sets in OD islets					
Upstream regulator	**Log ratio**	**Molecule type**	**Predicted activation state**	**Activation z-score**	**P-value**
TNF	0.515	cytokine	Activated	4.078	1.49E-05
REST	0.559	transcription regulator	Activated	3.395	2.92E-18
IL1B	0.817	cytokine	Activated	3.031	7.95E-08
STAT1	0.086	transcription regulator	Activated	2.630	2.24E-02
IL1A	0.486	cytokine	Activated	2.595	5.67E-03
IFI16	0.613	transcription regulator	Activated	2.412	5.81E-03
AR	-0.215	ligand-dependent nuclear receptor	Activated	2.377	2.33E-02
FOXO1	0.111	transcription regulator	Activated	2.270	6.61E-03
TLR3	0.446	transmembrane receptor	Activated	2.206	4.90E-02
PRKCD	-0.096	kinase	Activated	2.166	3.78E-02
MAP3K8	0.292	kinase	Activated	2.159	1.12E-02
IKBKB	0.079	kinase	Activated	2.126	8.36E-04
CTNNB1	0.106	transcription regulator	Activated	2.064	6.04E-04
NTRK2	-0.136	kinase	Inhibited	-2.000	3.60E-02
TAB1	-0.089	enzyme	Inhibited	-2.000	3.24E-03
PAX6	-0.596	transcription regulator	Inhibited	-2.070	2.30E-04
BDNF	0.027	growth factor	Inhibited	-2.166	2.37E-07
NEUROD1	-0.545	transcription regulator	Inhibited	-2.619	1.10E-05
ADCYAP1	-0.811	other	Inhibited	-2.720	1.34E-02
Ingenuity upstream regulators of T2D vs ND regulated probe sets in PPP islets					
Upstream regulator	**Log ratio**	**Molecule type**	**Predicted activation state**	**Activation z-score**	**P-value**
RICTOR	0.130	other	Activated	2.848	1.40E-02
SRC	-0.052	kinase	Inhibited	-2.156	2.13E-03
HNF1A	-0.328	transcription regulator	Inhibited	-2.573	8.81E-04

Supplementary Table 8. Related to Figure 2 and Figure 5. Upstream regulators predicted to be significantly activated or inhibited among the differentially regulated probe sets in islets from OD and PPP. OD, organ donors; PPP, partially pancreatectomized patients.

Supplementary Methods

Islet procurement from OD. Pancreata not suitable for transplantation were obtained in Pisa from 161 ND and 39 T2D heart-beating OD under approval from the local ethics committees. The donor's full clinical history and major laboratory parameters, such blood glucose during the intensive care unit stay and fructosamine, were collected to assess the presence of diabetes. Well-preserved islets were isolated from the pancreata of 153 ND and 34 T2D OD, and were cultured for 2±1 days before being hand-picked and processed for further analyses. Forty-three human islet preparations, all from ND OD, were acquired by Eli Lilly from Prodo Laboratories Inc. (Irvine, CA). Isolated islets were prepared by enzymatic digestion and were shipped to Lilly after recovery for 1–2 days in culture.

Insulin secretion from OD islets. Islet insulin release was assessed as previously described (Marselli et al, 2014). After isolation, the islets were cultured for 2–3 days before groups of 15 islets of comparable size were hand-picked and incubated at 37°C for 45 min in Krebs–Ringer bicarbonate solution (KRB), 0.5% albumin, pH 7.4, and 3.3 mmol/l glucose. Then, the medium was completely removed, assayed for basal insulin secretion, and replaced with KRB containing either 16.7 mmol/l glucose, 3.3 mmol/l glucose plus 100 μmol/l glyburide, or 3.3 mmol/l glucose plus 20 mmol/l arginine. After incubation for 45 min, the medium was removed and insulin levels were measured to assess stimulated insulin release. Insulin secretion was also expressed as insulin stimulation index (ISI) – the ratio of stimulated to basal insulin secretion.

Extraction of RNA from islets isolated enzymatically from OD pancreata. Using previously described methods, at 2–3 days after isolation, groups of 100–120 islets from 125 OD at Univ. Pisa were hand-picked, rinsed in sterile PBS (Sigma-Aldrich) and centrifuged at 3,000 × *g* for 5 min. The supernatant was disposed and 100 μl of extraction buffer (PicoPure RNA Isolation Kit; Life Technologies, Foster City, CA) was added. Samples were incubated at 42°C for 30 min, centrifuged at 3,000 × *g* for 2 min, and the supernatant was collected and stored at −80°C until RNA isolation. RNA isolation was performed according to the manufacturer's protocol. Briefly, 100 μl of 70% ethanol were added to the cell extract, the mixture was added to the purification columns, washed, and subjected to DNase treatment by incubation with 40 μl of DNase I solution (RNase-Free DNase Set; Qiagen GmbH, Hilden, Germany) for 15 min. Two additional washes were performed and RNA was eluted in 30 μl of elution buffer. The RNA concentration and purity were evaluated using a NanoDrop 2000c spectrophotometer (Thermo Scientific, Wilmington, DE) and RNA quality was evaluated using the Agilent 2100 Bioanalyzer system and the Agilent RNA 6000 Pico Kit (Agilent Technologies, Santa Clara, CA). The same procedure was applied at Lilly, Indianapolis for RNA extraction from islets of 39 OD. The mean yield of total RNA from 100–200 islets from ND and T2D at Univ. Pisa was 913±340 ng (RNA Integrity Number, RIN: 8.1±0.5) and 1016±329 ng (RIN: 8.3±0.4), respectively. In the case of islets processed at Lilly in Indianapolis, the mean yield of total RNA from 5,000 islet equivalents was 7.13±6.61 μg with a RIN of 8.0±0.5.

Islet procurement from PPP. Pancreatic tissues and blood samples were collected from patients undergoing partial pancreatectomy in the Department of Surgery, University Hospital of TU Dresden. Patients age <18 years were excluded. The local ethics committee approved the study and all of the patients provided written informal consent. Information collected immediately before surgery included: individual and family medical history, BMI, standard clinical parameters, HbA1c concentrations, and fasting glucose and insulin concentrations. ND subjects with fasting glycemia <7.0 mmol/l underwent an OGTT to measure glucose, insulin, proinsulin and C-peptide at 0, 60 at 120 min after a glucose load within a few days before surgery. Fasting

potassium and magnesium concentrations were measured to exclude false-positive results. All patients were screened for autoantibodies against insulin, GAD65, ZnT8, and IA-2/ICA512, as previously described (Bonifacio, 2015).

Extraction of RNA from islets isolated enyzmatically or by LCM from PPP surgical specimens. Pancreatic islets within resected pancreas specimens were isolated in Dresden by LCM with a Zeiss Palm MicroBeam system in the light microscopy facilities of the BIOTEC/CRTD at TU Dresden and MPI-CBG. In the case of three PPP islets were also isolated in parallel from small surgical specimens as previously described (Botticher et al, 2011), except for the use of MTF as protease blend (Roche, Penzberg, Germany). Total RNA extraction was performed as previously described (Sturm et al, 2013). Information about average islet yield, RNA quantity and RIN is provided in the table below.

	Mean n° of LCM islets/patient	Mean LCM islet volume [µm³]/patient	Range islet RNA/patient [ng]	RIN
ND 32	42±15	29,673,810±11,210,130	4.9-207.8	6.6±0.7
T2D 36	47±14	32,597,030±11,405,690	5.9-784.0	6.0±0.8
IGT 15	39±13	25,991,280±6,031,880	4.8-335.0	6.3±0.7
T3cD 20	45±11	28,103,890±6,420,620	7.5-163.3	6.4±0.7
Total 103	44±14	29,854,390±10,048,130	4.8-784.0	6.3±0.8

Confidential

RNA quality assessment, processing, and transcriptomic profiling. Total RNA of islets from OD and PPP was quantified with the NanoDrop 2000 Spectrophotometer (Thermo Scientific). RNA quality was assessed using the Agilent 2100 Bioanalyzer and the Agilent RNA 6000 Pico kit (Agilent Technologies) and further processed for Affymetrix if a RIN value of >4.1 was measured. For cDNA preparation, 10–25 ng of total RNA was amplified using the Ovation RNA Amplification System V2 and was subsequently labeled with Biotin using the Encore™ Biotin Module according to the manufacturer's instructions (NuGEN Technologies, San Carlos, CA). The length distribution of the amplified cDNA products were determined using an Agilent 2100 Bioanalyzer (Agilent Technologies). Hybridization of biotin-labeled cDNA to Affymetrix HG_U133Plus2.0 GeneChip microarrays was performed at ATLAS Biolabs GmbH (Berlin, Germany). Briefly, 3.75 µg of cDNA per sample were hybridized to the genechips for 16 – 18 h at 45°C in a rotating hybridization oven at 60 rpm (Hybridization Oven 640; Affymetrix). The array was subsequently washed and stained with a fluidics station (GeneChip® Fluidics Station 450; Affymetrix) according to the EukGe_WSv4_450 fluidics protocol for eukaryotic 3'-expression arrays. Arrays were scanned using GeneChip Scanner 3000 7G (Affymetrix) and primary data analysis was performed with Affymetrix software GeneChip Operating System (GCOS) v1.4.

Normalization and statistical analysis of microarray data. The transcriptomics data were summarized and normalized by Robust Multichip Analysis (RMA) on Array Studio software (Omicsoft Corp., Cary, NC). Batch correction of microarray data was performed using the R/Bioconductor package ComBat (Johnson et al, 2007). Elimination of technical outlier samples was performed at two steps of the transcriptomics analysis (Figure 5a). Briefly, before batch correction and statistical analysis, the array data were filtered to detect genes showing significant expression. The criterion for expression was an intensity value >75% for ≥25% of the samples in that group. Subsequently, islet samples from OD with no previous history of diabetes but with high blood fructosamine (>285 µmol/l) or glucose (>11.1 mmol/l) were excluded from the analysis to avoid the impact of confounding factors, such hyperglycemia caused by the patient's stressful clinical situation. Islet samples from ND and T2D OD with insulin expression levels below one standard deviation from the within-group mean were also eliminated. Covariate correction for age and gender, as well as the statistical analyses, were performed using the linear modeling features of the R/Bioconductor package Limma (Ritchie et al, 2015). In comparisons between T2D OD and ND OD islets, significant differences were defined as a change in expression of ≥1.5 after correction for multiple hypothesis testing using the Benjamini–Hochberg method ($p \leq 0.05$). Principal component analysis was performed using the R package prcomp. The analysis of all islet sample types and of a single sample type (islets from OD or PPP) was based on the intensities of the probe sets after batch correction. Contamination of islet samples with exocrine pancreatic tissue was determined using selected markers of exocrine and ductal cells, as indicated in the table below.

Annotation				Log intensities			
Probe ID	Entrez ID	Symbol	Gene Name	OD-ND	OD-T2D	PPP-ND	PPP-T2D
209301_at	760	CA2	carbonic anhydrase II	8.709	8.913	7.326	7.649
206208_at	762	CA4	carbonic anhydrase IV	6.102	6.006	6.385	6.403
205043_at	1080	CFTR	cystic fibrosis transmembrane conductance regulator (ATP-binding cassette sub-family C, member 7)	11.702	12.016	9.516	9.943
206297_at	11330	CTRC	chymotrypsin C (caldecrin)	12.545	12.543	12.575	12.442
220275_at	50624	CUZD1	CUB and zona pellucida-like domains 1	12.655	12.828	11.526	11.734
214324_at	2813	GP2	glycoprotein 2 (zymogen granule membrane)	11.657	11.741	12.346	12.220
200697_at	3098	HK1	hexokinase 1	9.022	9.183	6.543	6.773

Confidential

202934_at	3099	HK2	hexokinase 2	9.339	9.560	5.850	6.483
201650_at	3880	KRT19	keratin 19	12.606	12.749	8.176	8.488
208949_s_at	3958	LGALS3	lectin, galactoside-binding, soluble, 3	12.036	12.156	8.908	9.590
213693_s_at	4582	MUC1	mucin 1, cell surface associated	12.672	12.846	9.655	10.023
217109_at	4585	MUC4	mucin 4, cell surface associated	6.160	6.820	absent	absent
205912_at	5406	PNLIP	pancreatic lipase	13.594	13.533	13.440	13.197
206694_at	5407	PNLIPRP1	pancreatic lipase-related protein 1	12.107	12.239	11.687	11.512
205869_at	5644	PRSS1	protease, serine, 1 (trypsin 1)	12.915	12.929	12.585	12.346
211429_s_at	5265	SERPINA 1	serpin peptidase inhibitor, clade A (alpha-1 antiproteinase, antitrypsin), member 1	13.354	13.360	13.006	13.287
202936_s_at	6662	SOX9	SRY (sex determining region Y)-box 9	11.118	11.786	9.042	9.062
209875_s_at	6696	SPP1	secreted phosphoprotein 1	12.732	13.023	9.627	10.759

Access to raw microarray data. All data are MIAME compliant, and the raw data have been deposited in a MIAME database (GEO, accession number: GSE76896).

Preparation of human islet beta and alpha cell-enriched fractions. The methods used to prepare the human islet beta and alpha cell-enriched fractions were previously described (Parnaud et al, 2008) and validated (Bugliani et al, 2013; Kirkpatrick et al, 2010)[8, 9]. Briefly, human islets were dissociated into single-cell suspensions by incubation with constant agitation for 3 min at 37°C in 0.05% trypsin-EDTA (Thermo Fisher Scientific Inc.) supplemented with 3 mg/ml DNAse I (Roche, Basel, Switzerland), followed by pipetting vigorously to complete the dissociation. Labeling and sorting of the alpha and beta cell fractions was performed by Newport Green labeling (Lukowiak et al, 2001) followed by FACS, as previously described (Kirkpatrick et al, 2010).

cDNA vectors. The open reading frames for human *ARG2* (BCA001350), *PPP1R1A* (NM_006741), and *TMEM37* (XM_005263597, NM_019432) were cloned into pcDNA3.1neo_DEST. Human *TMEM37* was also cloned into pcDNA3.1neo_3cMYC_DEST, while mouse *Tmem37* (NM_019432) was inserted into pcDNA3.1D/V5-His-Topo according to

the manufacturer's instructions (Thermo Fisher Scientific Inc.). The forward and reverse primers were as follows:

Genes	Accession n° [NCBI]	Species	Forward Primer	Reverse Primer
ARG2	BC001350.1	human	5′-ATGTCCCTAAGGGGCAGCC-3′	3′-GTTCGTGCACACTCTTAAATC-5′
PPP1R1A	NM_006741	human	5′-ATGGAGCAAGACAACAGCCC-3′	3′-CCCTCGGTTGAGCCAGACT-5′
TMEM37	XM_005263597	human	5′-ATGACCCGACCTGACTGTTC-3`	3′-GTGGGTAGGGACCCTTACT-5′
TMEM37	NM_019432	mouse	5′-CACCATGACGGCCATCGGCGCGCAG-3`	3′-′TATCAGAGAAGTCCCATCATAAC-5′

Cell culture and transfection. CHO cells grown on SuperFrost Plus slides were transiently transfected with cDNA vectors using Lipofectamine according to the manufacturer's instructions (Thermo Fisher Scientific Inc.). Cells were fixed for 24 h after transfection with formalin for 30 min and then used for validation of anti-ARG2, anti-PPP1R1A or anti-TMEM37 antibodies for immunocytochemistry using the Ventana XT staining system (Roche). Cell transfection was verified in parallel by immunocytochemical detection of overexpressed GFP. Silencing of *PDX1* and *HNF-1A* in EndoC-betaH1 cells (Ravassard et al, 2011) was achieved using 50 pmol of esiRNA (Eupheria, Dresden, Germany) with Dharmafect4 as the transfection reagent (GE Dharmacon, Lafayette, CO).

INS-1E and INS-1 832/13 cells were cultured in a humidified atmosphere containing 5% CO_2 in complete RPMI 1640 medium (Thermo Fisher Scientific Inc.) supplemented with 10% heat-inactivated fetal bovine serum, 1 mmol/l sodium pyruvate, 50 µmol/l 2-mercaptoethanol, 2 mmol/l glutamine, 10 mmol/l HEPES, 100 U/ml penicillin, and 100 µg/ml streptomycin. Silencing of *PPP1R1A* and *ARG2* in INS-1E cells and *TMEM37* in INS-1 832/13 cells was achieved by transfection with the respective siRNAs and Lipofectamine 3000 diluted in Opti-MEM. After incubation overnight, the cells were cultured in RPMI medium for 24 h. For cytoplasmic Ca^{2+} imaging experiments, INS-1 832/13 cells were co-transfected with the fluorescent transfection marker siGLO RISC-Free siRNA to identify siRNA-transfected cells. For overexpression of *TMEM37-V5*, INS-1 832/13 cells were transfected with the corresponding pcDNA3.1 vector using Lipofectamine 2000. Four days after transfection, cells were harvested for immunoblotting and immunocytochemistry. For Ca^{2+} imaging analysis, *TMEM37-V5* INS-1 832/13 cells were identified by co-transfection with pEGFP-C1 (Takara Bio Inc., Kusatsu, Japan).

RT-qPCR. Total RNA was extracted from human dispersed, FACS-sorted islet cells, rat INS-1E and INS-1 832/13 cells, and human EndoC-betaH1 cells using RNAeasy kits according to the manufacturer's instructions (Qiagen) and then reverse-transcribed using Superscript Reverse

Transcriptase II (Thermo Fisher Scientific Inc.). RT-qPCR was performed using GoTaq qPCR Master Mix (Promega, Madison, WI). The mRNA levels of the genes of interest in human islet dispersed cells were quantified and normalized to β-actin in a VIIA7 system (Applied Biosystems). The gene expression levels in INS-1 832/13 cells, EndoC-betaH1 cells and human islets were normalized to β-actin expression. The forward and reverse primers purchased from commercial suppliers are indicated in the table below.

Genes	Accession n° [NCBI]	Forward Primer	Reverse Primer
ACTB	NM_001101	5'-CATCGAGCACGGCATCGTCAC-3'	5'-CAGCACAGCCTGGATAGCAACG-3'
ANKRD23	NM_144994	5'-GTTGGTAAGTGGAGAAAGAGTTG-3'	5'-TCTTTGAACCAAGTTTTCCAAGTC-3'
ANKRD39	NM_016466	5'-ACGCTGGAGGAGATGGACTTC-3'	5'-CTTATGCAGACTGGTCATGCC-3'
ARG2	NM_001172	5'-CCTCCTGAACATTTTATTTTAAAG-3'	5'-GGATTGACTTCAACAAGATCCAG-3'
ASCL2	NM_005170	5'-TGCGCTGCAGCCGGCGGCGGCG-3'	5'-CGTGCGGCACGTGCTGCCGCAGCG-3'
CAPN13	NM_144575	5'-CTGGTGGACCTCACAGGAGG-3'	5'-CATCCAAAACTCGCCATCTTCC-3'
CD44	NM_000610	5'-CATGGACAAGTTTTGGTGGCAC-3'	5'-CCTTCTATGAACCCATACCTGC-3'
CHL1	NM_006614	5'-GTACATTAGTTAAAGTTACCTGGTC-3'	5'-GTGGCAGTGTCTTTATCAACTTTG-3'
FAM102B	NM_001010883	5'-TTTGCTGGATCAGGAAATACCAC-3'	5'-CTTTGCTGAAAGATCTGCTATTCC-3'
FBXO32	NM_058229	5'-TACAACTGAACATCATGCAGAGG-3'	5'-TACATCTTCTTCCAATCCAGCTG-3'
FFAR4	NM_181745	5'-	5'-

Confidential

		AGCCTGGAGCGCATGGTGTG-3’	GAGTAACTGATCACAATGACCAG-3’
G6PC2	NM_021176	5’-TTTTATGTCCAATGTTGGAGACC-3’	5’-TGGCCAGATGGACTTCCTGG-3’
HHATL	NM_020707	5’-GTGGTCTGTTCTTAACTGCTTC-3’	5’-GGAAGCCTGTAAGTATCAGGC-3’
HNF1A	NM_000545	5’-CACCAGAAAGCCGTGGTGGAG-3’	5’-GGAACAGGATCTGCTGGGATG-3’
KCNH8	NM_144633	5’-AATTCAAAGGAGAAATTATGTTCTAC-3’	5’-GTCTCCGGGCTGAGTCAAAGTG-3’
NSG1	NM_014392	5’-TCACCGAGAGGTTTAAGGTCTC-3’	5’-TCCCGGGCACTGGAGTCTTG-3’
PCDH20	NM_022843	5’-TTTTCCTTAGACAGTGTCACAGG-3’	5’-GGACTGTTGTCATTTTTATCCAAC-3’
PDX1	NM_000209	5’-CAAAGCTCACGCGTGGAAAGG-3’	5’-GATGTGTCTCTCGGTCAAGTTC-3’
PPP1R1A	NM_006741	5’-CAATGTCTCCACGGCAACGGAAG-3’	5’-CTGTGTCTGGGATCCCAGGTG-3’
SCTR	NM_001980	5’-CAACTACATCCACATGCACCTG-3’	5’-AATGGCTGGAGAACCCCATCC-3’
SLC2A2	NM_000340	5’-TTCTGTCCAGAAAGCCCCAG-3’	5’-GCCCTGCCTTCTCCACAAG-3’
TMEM37	NM_183240	5’-TCCTTCATCCGGACCCTCATCATC-3’	5’-GAGGAAGGAGGCAGTGAATTC-3’
UNC5D	NM_080872	5’-CTTTTGTGAGGGAATGTCAGTG-3’	5’-TTGGGGTTTTATTTCATGAAGAGG-3’

Confidential

In situ RT-PCR. Pancreatic sections from 10 ND and 10 age-matched T2D OD and from 10 ND and 10 age-matched T2D PPP were placed on three-chamber slides. Briefly, after dewaxing and different pre-incubation steps, reverse transcription was performed with oligo-dT primers (Invitrogen), M-MLV reverse transcriptase (0.5 U/µl) (Invitrogen), and RNasin (Promega) for 1 h at 37°C in a humidified chamber. After inactivation of the reverse transcriptase, 15 µl of PCR reaction mix containing 5% digoxigenin (DIG)-11-dUTP, the mRNA-specific primers and selfseal-reagent (BioRad) was applied to each chamber of the slide. The slides were sealed with coverslips and were placed into a PTC-200 DNA Engine thermal cycler with a slide block (BioRad, Munich, Germany) for *in situ* RT-PCR, as previously described (Jorns et al, 2014; Jorns et al, 2005). Amplification for 12 (*ARG2, ASCL2*, *CHL1 (CHL1iso-1*; *CHL1iso-2*, *CHL1-iso3)*, *FAM102B*, *FFAR4A*, *HHATL*, *KCNH8*, *PPP1R1A*, *SCTR*, *SCL2A*, *TMEM37* and *UNC5D)* out the 19 signature genes of T2D islets was performed according to the following protocol: initial denaturation at 95°C for 3 min, followed by 35–40 cycles with a denaturation step at 95°C for 45 sec, annealing at 57°C for 45 sec and extension at 72°C for 45 sec, followed by a final extension for 10 min at 72°C. Primers are indicated in the table below.

Genes	Accession n° [NCBI]	Forward Primer	Reverse Primer
ARG2	NM_001172	5'-TGGTTAGCAGAGCTGTGTCAGA-3'	5'-TTGGTCTTTGTCTCTTGCCAAT-3'
ASCL2	NM_005170	5'-GGTGAACTTGGGCTTCCAG-3'	5'-CCCTAACCAGCTGGAGAAGTC-3'
CHL1-iso1	NM_006614	5'-ATCTCCACTCAAGGCTGGTTT-3'	5'-TCCATTGCTTTCAACAGATCC-3'
CHL1-iso2	NM_001253387	5'-TGGTCAACAGTTCCAAAGGAC-3'	5'-CTGGGCTTTGATGGAGTTGTA-3'
CHL1-iso3	NM_001253388	5'-TCCATCGAACAATTCAGGAAC-3'	5'-TCATTGCGACTGTCCTTTTCT-3'
FAM102B	NM_001010883	5'-TACAAGCAAACTGTGTTCGCTG-3'	5'-TTCTAGAATGTCCACAGGCACC-3'
FFAR4	NM_181745.3	5'-AGGAAATTTCGATTTGCACACT-3'	5'-TCTTGCTTGAAGTTCTGGATCA-3'
HHATL	NM_020707	5'-TGATGTGGTTCACCTCCTTTC-3'	5'-CTTGAGCAGGTCAGCTAAGGA-3'

Confidential

KCNH8	NM_144633	5'-GCCTATATTGCCGCTCTGTACT-3'	5'-CGGAGCACAGAAAGAGGTTTTG-3'
PPP1R1A	NM_006741	5'-TGACCAGTCATCCCCAGAGATA-3'	5'-GGAATCCAGTGGTGGTATATGG-3'
SCTR	NM_002980	5'-GGAAGGCCTCTACCTTCACAC-3'	5'-ACGATGTAGTGGATGCCAAAG-3'
SLC2A2	NM_000340	5'-GATCAATGCACCTCAACAGG-3'	5'-CCAATTTTGAAAACCCCATC-3'
TMEM37	NM_183240	5'-CGGTCCTTCTTTGAATCCTTC-3'	5'-ATTAGGGTGAAGCCGATGAGT-3'
UNC5D	NM_080872.2	5'-AGGGAATGTCAGTGCAGAAAAT-3'	5'-ACCTGTCAATGCAGAAGAGTCA-3'

After a blocking step, the incorporated DIG-labeled nucleotides were detected by incubation with ABC-AP goat IgG and a goat anti-digoxigenin antibody (Enzo Life Sciences, Lörrach, Germany) (1:500) at room temperature for 1 h. Slides were developed with nitroblue tetrazolium chloride/5-bromo-4-chloro-3-indolyl phosphate toluidine salt for 1 h at room temperature and counterstained with hematoxylin.

Immunoblotting. The protein concentration of each extract was determined using the BCA assay (Thermo Fisher Scientific Inc.). Extracted proteins (20 μg/lane) were separated on 12% SDS-PAGE and transferred onto polyvinylidene difluoride membranes (GE Healthcare Europe, Little Chalfont, UK). Membranes were probed with mouse monoclonal anti-V5 (Thermo Fisher Scientific Inc.), mouse monoclonal anti-gamma-tubulin (Sigma-Aldrich), rabbit polyclonal anti-PDX1 (Merck Millipore, Billerica, MA), and rabbit polyclonal anti-HNF1A (Abcam, Cambridge, UK).

Immunomicroscopy. Human pancreatic samples from OD were taken before islet isolation, fixed in 4% paraformaldehyde and embedded in paraffin, essentially as previously described (Marselli et al, 2013; Marselli et al, 2014). Surgical pancreatic specimens were immediately fixed after collection with 4% paraformaldehyde in PBS and embedded in paraffin. For cryosections, small tissue fragments were embedded in TissueTek, snap frozen, and stored at −80°C. Formalin-fixed, paraffin-embedded tissue sections (2–3-mm-thick) were stained with the following validated primary antibodies: guinea pig polyclonal anti-insulin (1:1,000), rabbit monoclonal anti-PPP1R1A (ab40877; 1:200), and rabbit polyclonal anti-TMEM37 (ab111287; 1:30) (all Abcam); mouse monoclonal anti-glucagon (1:3,000), and rabbit polyclonal anti-ARG2 (1:25) (both Sigma-Aldrich). After adding fluorochrome-conjugated secondary antibodies, the sections were imaged using a Leica 1DM5500B microscope (Leica, Wetzlar,

Germany) or a Scanscope FL instrument (Roche) to image the TMEM37 staining profile. EndoC-betaH1 cells grown on coverslips were fixed with 4% paraformaldehyde and immunostained with the following primary antibodies: mouse monoclonal anti-insulin (Sigma-Aldrich), guinea pig polyclonal anti-PDX1 (Abcam), and rabbit polyclonal anti-HNF1A (Bethyl Laboratories, Montgomery, TX). Nuclei were counterstained with DAPI (Sigma Aldrich), and coverslips were mounted with Mowiol (Calbiochem/EMD Millipore, Darmstadt, Germany). Images of 0.5-µm-thick optical sections were acquired at room temperature with an inverted confocal microscope (Zeiss Axiovert 200M) equipped with a Plan-Apochromat ×63 oil objective (numerical aperture 1.4), a Zeiss LSM510 scan head with photomultiplier tubes, and analyzed using Zeiss LSM 510 AIM software version 4 (Zeiss, Göttingen, Germany).

Ca^{2+} imaging. INS-1 832/13 cells were grown on glass coverslips. The wide-field imaging system consisted of an Olympus IX70 multi-parameter fluorescence microscope, monochromator, and objective lens (×40/1.35NA oil UApo/340; Olympus). All imaging experiments were performed at 37°C in a heated perfusion chamber using pre-bubbled imaging solution (in mmol/l: 140 NaCl, 3.6 KCl, 0.5 NaH_2PO_4, 0.5 $MgSO_4$, 1.5 $CaCl_2$, 10 HEPES and 2 $NaHCO_3$, pH 7.4). The basal and loading solution contained 3 mmol/l glucose, essentially as previously described (Ravier & Rutter, 2010). In imaging solution containing 20 mmol/l KCl, NaCl was reduced to 123.6 mmol/l (3 mmol/l glucose). Cytoplasmic (intracellular) free Ca^{2+} levels ($[Ca^{2+}]_i$) were recorded using ratiometric Ca^{2+}-sensitive dyes. Cells were loaded for 40 min at 37°C with either 4 µmol/l Fura Red or 4 µmol/l Fura-2 AM in imaging solution containing 0.004% Pluronic (Thermo Fisher Scientific Inc.). After loading, the cells were washed in basal solution for ≥20 min to allow de-esterification of the dyes. Images were acquired using Micromanager software at a rate of 1 frame/3 sec. Cells were excited at 420 and 480 nm for Fura Red loaded cells and at 340 and 380 nm for Fura-2 AM loaded cells. The emitted light was passed through an ET525/50 filter equipped with a T495lpxr dichroic mirror for Fura-2 AM or an ET630/75 filter equipped with a T585lpxr dichroic mirror for Fura Red (Chroma, Bellows Falls, VT). Cells with responses of ≥3 standard deviations higher than the averaged baseline to both KCl and glucose stimuli and with an increase of ≥10% after an increase to 15 mmol/l glucose were considered responsive and were included in the analysis. The basal cytosolic Ca^{2+} concentration was calculated as the mean of the ratios measured over the first 150 sec. The maximal fluorescent intensity value was taken as the peak amplitude. To calculate the cumulative fluorescence, curves were first smoothed using a fast Fourier transform filter and the baseline was subtracted. Then, the area under the curve was derived via integration.

Gene ontology overrepresentation analysis of differentially expressed genes. The Bioconductor package GOstats (Falcon & Gentleman, 2007) was used to test for the association between the biological process gene ontology terms and the lists of differentially expressed genes in islets of OD and PPP. For differentially expressed genes, a FDR threshold of 0.05 and an absolute fold-change threshold of 1.5 were used. A significance threshold of $p \leq 0.05$ and a minimum number of three genes per term were used in the gene ontology-based over-representation analyses.

Pathway, and downstream and upstream analysis of differentially expressed genes. Putatively active pathways, downstream processes, and upstream regulators were determined by IPA (Ingenuity® Systems). A FDR threshold of 0.05 and an absolute fold-change threshold of 1.5 were used to identify differentially expressed genes in OD islets. The absolute fold-change threshold was relaxed to 1.2 to identify differentially expressed genes in PPP islets. The enriched canonical pathway analyses were performed with a p-value threshold of 0.05. Only pathways containing at least three regulated genes were considered. An absolute z-score

threshold of 2 and a p-value threshold of 0.05 were applied to predict increased/decreased downstream processes and activated/inhibited upstream regulators (Kramer et al, 2014).

Prediction of binding sites for HNF1A and PDX1 in T2D islet signature genes. T2D islet signature genes were searched for the inclusion of putative binding sites for HNF1A and PDX1 within 5 Kb upstream and downstream of their respective transcription start site using oPOSSUM 3.0.

Gene symbol	ENTREZ ID	HNF1A	PDX1
ANKRD23/39	51239/200539		1
ARG2	384		5
ASCL2	430		
CAPN13	92291		13
CHL1	10752		39
FFAR4	338557		
G6PC2	E57818		15
HHATL	57467		1
NSG1/D4S234E	27065		
PCDH20	64881		2
PPP1R1A	5502		3
SCTR	6344		1
SLC2A2	6514		5
TMEM37	140738		
UNC5D	137970	1	33
CD44	960	2	19
FAM102B	284611	1	2
FBXO32	114907		19
KCNH8	131096		15

Chromatin immunoprecipitation $2x10^7$ EndoC-betaH1 cells grown in T75 flasks were cross-linked with 10 ml of 1% formaldehyde for 30 min and then quenched with 1.25 ml 1M Glycine for 10 min. Cells were resuspended in nuclear lysis buffer and sonicated with 20 pulses of 20 sec each with breaks of 20 sec between each sonication cycle to achieve fragments ranging in

Confidential

size between 2,000-200 bp. The sonicated cells were diluted 10 fold, centrifuged for 10 min at 13,000 x g. Rabbit polyclonal anti-PDX1 (Merck Millipore, Billerica, MA) and anti-HNF1A (Abcam) antibodies and control rabbit IgG (Dianova, Hamburg, Germany) were used at 10 µg/ml for ChIP analysis. Purified DNA was analyzed by RT PCR (Aria Mx cycler, Agilent Technologies) using 1µl of DNA as template in 20 µl reaction carried out in triplicate. Primer concentration was 100 nM and their sequences are indicated in the table below.

Genes	Ensemble ID	Forward Primer	Reverse Primer
ANKRD23/39	ENSG00000163126/ ENSG00000213337	5'-CAGCTGGATAGCAGGTCCCG-3'	5'-TCCTCCTGCAACACAGCCCA-3'
ARG2	ENSG00000081181	5'-CCAGCGCTCCCGTTATTCAGG-3'	5'-AATCTTCACGCCCGGCTGATG-3'
CAPN13	ENSG00000162949	5'-CTGTGGGCTCAGTGCAAGCACTG-3'	5'-GGGAAGATCACGAGAATCCTC-3'
CD44	ENSG00000026508	5'-CAGGTTCGGTCCGCCATCCT-3'	5'-CCCAGGCTGCGTGCCACCAA-3'
CHL1	ENSG00000134121	5'-CGAGGCTGTAAGGTCAATCTC-3'	5'-GCAAGTCCTCTTTGTTGG-3'
FAM102B	ENSG00000162636	5'-GGGCAACAGAGTAAGACTCTG -3'	5'-GCCTCAGTTGAATAGACCACCA-3'
FBXO32	ENSG00000156804	5'-ACCGCCAGTCCTGCCCGAGG-3'	5'-AGCATCCGCCCCGGGTGGCA-3'
G6PC2	NSG00000152254	5'-TTCAGCAGAGGAGGGCTGGT-3'	5'-AAGTGCTCTGATTCCCACCG-3'
KCNH8	ENSG00000183960	5'-ACGGAGAGGGAACAAAGGGG-3'	5'-GCTGAGCCTCCCGGTCTCCA-3'
PCDH20	ENSG00000197991	5'-GGGGCTGTACATGGAGTTCA-3'	5'-GGGGCTGAGGTTTACCACTTC-3'
PPP1R1A	ENSG00000135447	5'-AACCTTAACCCCGT	5'-AGCTGTCCACTACG

Confidential

		CGTGGCT-3’	ACGGCT-3’
SCTR	ENSG00000080293	5’-CGTCAGATCCAGCAGTGAGT-3’	5’-GGCACCCAGCATTCCTGTTG-3’
SLC2A2	ENSG00000163581	5’-TGCTGATACCAGCCGTCTGA-3’	5’-GTTCTAGGGTGCATGCCGCT-3’
UNC5D	ENSG00000156687	5’-ACGTGGAGCGGCCTCTGGCT-3’	5’-GCCAATGAGCCGGGCTGGGG-3’

Identification of gene co-expression modules from OD-Islet and PPP-LCM samples. Module generation was performed using Weighted Correlation Network Analysis (WGCNA) (Langfelder & Horvath, 2008). With WGCNA, weighted correlations are calculated between genes based on the gene’s expression in the different samples; a weighted correlation is a correlation raised to a certain power (called the soft thresholding power). In WGCNA, the weighted correlations are used to create a specific type of network (a topological overlap network). This network is based on network topology rather than direct correlations between genes: genes are strongly linked together in this network if they share many correlated neighbours with each other. This topological overlap network is then analysed to identify network modules of genes that are strongly linked together.

Identifying network modules from the gene expression in this way focuses on groups of genes that are predicted to be functionally related based only on the gene expression data.
WGCNA was performed on genes from 84 OD-Islet and 32 PP-LCM samples from non-diabetics (ND). ND samples were chosen so that the gene-gene correlations would not be driven by differences between T2D and ND sample groups and would rather reflect putative functional links between genes. Normalized expression data was first batch corrected using *ComBat* (Johnson et al, 2007) and corrected for age and gender effects by linear regression using *LmFit* from the limma package in R (Gentleman et al, 2004). Both sets of data were then filtered by calculating a co-variance matrix and removing the 25% least co-variant genes. Co-expression networks were constructed by calculating adjacency matrices for each data set using a soft-thresholding power of 7 and Spearman correlation using pairwise complete observations. A topological overlap matrix (TOM) was then calculated from each adjacency matrix, converted to distances, and clustered by hierarchical clustering using average linkage clustering. Modules were identified by dynamic tree cut with a cut height of 0.995 with a minimum module size=20, using the hybrid method. Module *eigengenes* were calculated and similar modules were merged together using a module *eigengene* distance of 0.15 as the threshold.

Generation of a trait module network linking OD-Islet with PPP-LCM modules. Since one of the main goals of our study was to investigate T2D-related genes in two different sample collections, we measured similarities at the level of the gene co-expression modules. To do this we compared each OD-Islet with each PPP-LCM module pairwise and calculated the significance of enrichment using a one-sided Fisher’s exact test. Figure *OD-Islet modules*

Confidential

(Set1) comparison to PPP-Islet modules (Set2) is a heatmap showing the pairwise module overlaps. In the figure, red indicates that a pair of modules has a significant number of overlapping genes. From the figure it is clear that a number of modules significantly overlap between the two sample types.

We next correlated the *eigengenes* (the first principal components) of the modules to clinical and functional traits specific to each sample type using Spearman correlation (pairwise complete observations) and calculated corresponding p-values for the correlations using the *cor.test* function in R. The traits that were correlated to the module *eigengenes* are shown in the table '*Clinical and functional traits used for the module correlations'* below.

Clinical and functional traits used for the module correlations

Trait	Sample type
Gender (M/F)	OD+PPP
Age (years)	OD+PPP
Height (cm)	OD+PPP
Weight (kg)	OD+PPP
BMI (kg/m^2)	OD+PPP
Diabetes status (T2D, T3D, IGT, ND)	OD+PPP
Mean glycemia (ICU) (mmol/l)	OD
Fructosamine (µmol/l)	OD
Glucose-induced insulin stimulation index (ISI)	OD
Glibenclamide-induced insulin stimulation index	OD
Arginine-stimulated insulin secretion index	OD
Basal insulin secretion at 3.3mm glucose (µU/islet/minute)	OD
Glucose stimulated insulin secretion at 16.7mm glucose (µU/islet/minute)	OD
Glibenclamide stimulated insulin secretion at 100mm glibenclamide (µU/islet/minute)	OD
Arginine stimulated insulin secretion at 100mm arginine (µU/islet/minute)	OD
Oral glucose tolerance (AUC)	PPP
Blood sugar IV OGTT 0h (mmol/l)	PPP
Blood sugar IV OGTT 1h (mmol/l)	PPP
Blood sugar IV OGTT 2h (mmol/l)	PPP
Hba1c (%)	PPP
HOMA1 IR Index	PPP
HOMA1 B Index	PPP
HOMA1 S Index	PPP
Fasting insulin IP (pmol/l)	PPP
Fasting glucose IP (mmol/l)	PPP
Fasting insulin IS (nmol/l)	PPP
Insulin IS 1h (nmol/l)	PPP
Insulin IS 2h (nmol/l)	PPP
Fasting C peptide IS (nmol/l)	PPP
C peptide IS 1h (nmol/l)	PPP
C peptide IS 2h (nmol/l)	PPP
Fasting pro-insulin IS (pmol/l)	PPP

Confidential

Pro-insulin IS 1h (pmol/l)	PPP
Pro-insulin IS 2h (pmol/l)	PPP
K IS (mmol/l)	PPP
Mg IS (mmol/l)	PPP
C peptide IS 1h / Fasting C peptide (ratio)	PPP
Insulin IS 1h / Fasting Insulin IS (ratio)	PPP
Pro-insulin IS 1h / Fasting pro-insulin IS (ratio)	PPP

We identified the modules that were most correlated with the traits by applying a p-value (unadjusted) cutoff of p ≤0.05. These module-trait correlations were then plotted as separate heatmaps for OD and PPP modules (Figures below).

The module-module overlaps and the module-trait correlations were combined together into a module-trait network, where modules and traits were represented as nodes and module-module enrichment scores (-log10 p-value) and module-trait correlations represented the edges. The network was constructed by creating an edge between two modules if the p-value (adjusted) for enrichment was ≤0.05, or between a module and a trait if the module-trait correlation was considered as significant (unadjusted p-value ≤0.05). The largest connected component in this network comprised a set of 10 modules (4 from OD Islets and 6 from PPP Islets) that were connected to each other either because the modules were significantly overlapping, or because the modules were correlated to the same traits within the OD and PPP datasets (Figure *OD-Islet modules (Set1) comparison to PPP-Islet modules (Set2)*). These modules were used as a starting point for further analysis (below).

Significance of gene co-expression modules. We tested the significance of the co-expression modules by performing a bootstrap test as follows. For each selected module of size *N*, we randomly sampled *N* probe sets from the expression data 1000X and calculated the intramodular connectivity (Langfelder & Horvath, 2008) (the connectivity of nodes to other nodes within the same module) of the probe sets. To measure the degree of connectivity within the modules compared to the background, we calculated a Z score as:

$$Z = \frac{k - \mu}{\sigma}$$

where k is the intra-modular connectivity and μ and σ are the mean and standard deviation of intramodular connectivity from 1000 randomly sampled modules of size N respectively. Empirical p-values were also calculated as the fraction of background intramodular connectivity scores greater than or equal to the intramodular connectivity for a particular module. All of the background intramodular connectivity scores were below the module intramodular connectivity for the selected modules.

Significance of selected OD and PPP modules. The Z-score is a measure of the number of standard deviations of the intramodular connectivity of probesets within a module above a background model based on 1000 samples of the same size.

Module	Type	Zscore	P-value
blue	OD	80.54	<0.001

Confidential

skyblue	OD	73.89	<0.001
darkviolet	OD	47.22	<0.001
plum1	OD	35.99	<0.001
antiquewhite4	PPP	80.11	<0.001
firebrick	PPP	86.72	<0.001
deeppink2	PPP	68.73	<0.001
lightpink4	PPP	76.46	<0.001
coral3	PPP	23.91	<0.001

The results in the above table show that all of the selected modules have high Zscores, indicating that it is extremely unlikely to find modules of the same size and connectivity by chance from the expression data.

Identification of module hub genes and measuring overlap with signature genes. A hub gene is a highly connected gene within a module that could be influencing a particular trait. Such genes might therefore represent key genes that could have a stronger influence on a trait compared to other genes. Hub genes were selected for each significantly correlated module/trait pair in the module-trait network (Figure '*Module-trait heatmap showing OD and PPP module correlations with functional and clinical traits'*) as those that correlated with the modules *eigengene*, the first principal component of the module (spearman's $|r| \geq 0.6$), and the trait (spearman's $|r| \geq 0.3$). We tested the hub genes for enrichment of the 19 genes differentially regulated in both OD and PPP cohorts using the hypergeometric distribution in R (hyperg function) with the background number of genes equal to the union of the numbers of expressed genes in OD and PPP cohorts (N=15716). The total number of module hub genes was 4285. We found 15 of the 19 signature genes were hub genes in these modules and this is statistically significant (hypergeometric p-value=3.34e-05). These signature 'hub' genes are: ARG2, CHL1, PPP1R1A, CD44, HHATL, ANKRD23/39, ASCL2, UNC5D, PCDH20, FBXO32, SCTR, G6PC2, TMEM37 and SLC2A2. Four of the signature genes CAPN13, FFAR4, NSG1 and FAM102B were not module 'hub' genes.

Generation of a Sequence-based Transcription Factor network. We reasoned that the hub genes could also be targets for transcription factors (TFs) affecting a particular trait, since these genes are both highly connected to other module genes and are also correlated to glycemia-related traits. In order to identify possible TFs upstream of the modules we analysed the promoters of the 4285 module hub genes for the presence of transcription factor binding sites (TFBS) using oPOSSUM 3.0 single site analysis (Kwon et al, 2012). The promoter regions used in the analysis were from 2000 nucleotides upstream of the TSS to the TSS of each gene. All vertebrate JASPAR profiles with a minimum specificity of 8 bits were used for the analysis. TFs were selected showing significant binding site enrichment measured by both empirical Z score and Fisher score cutoffs (Z score ≥10 AND Fisher score ≥7).
The oPOSSUM results for each significantly enriched TF were parsed to create a directed network of TFs and their predicted targets. The TFs were also analysed separately using oPOSSUM to detect potential binding events between TFs. Here no Zscore or Fisher score cutoff was used since the goal was not to test for enrichment, but rather to identify potential TF-TF regulation. A directed network was created for each module-trait combination with

Confidential

genes as nodes and edges between nodes representing evidence of binding site prediction. Subsequent network analysis was performed in *R* using *iGraph* (Csardi & Nepusz, 2006).

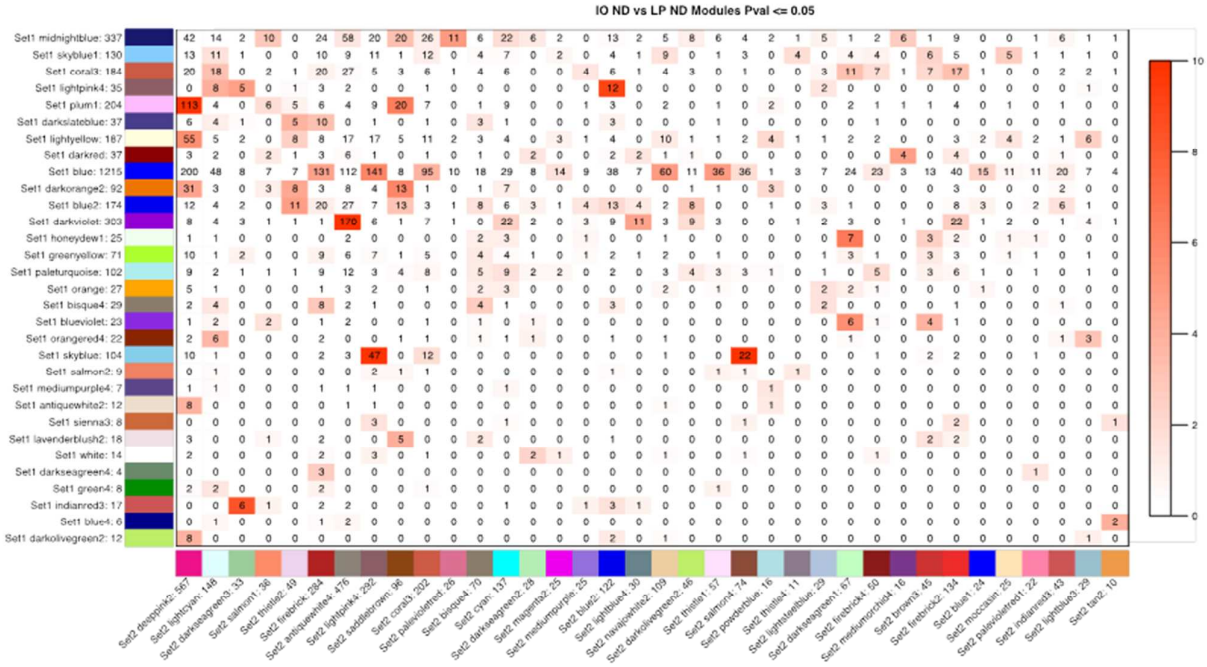
Modules and correlated traits used for the sequenced-based TF network generation

Module	Sample Source	Correlated trait
antiquewhite4	PPP	Fasting insulin
blue	OD	Insulin stimulation index (ISI)
darkviolet	OD	Insulin stimulation index (ISI)
deeppink2	PPP	Mg
lightpink4	PPP	Glycemia 2 hours
plum1	OD	Glibenclamide stimulation index
skyblue	OD	Glucose stimulation index

Generation of a literature-based Transcription Factor network. Literature-based networks were created for the same module-trait gene sets using Ingenuity upstream regulator analysis (Kramer et al, 2014). To do this, significant of overlap between the gene sets and known targets of transcriptional regulators from the literature were calculated using Fisher's exact test. Significant regulators were identified as those with an overlap p-value ≤0.01. The predicted upstream regulators were then filtered to select only those that were transcription factors. A directed network was created for each module-trait combination with genes as nodes and edges between nodes representing predicted transcriptional regulation. Subsequent network analysis was performed in *R* using *iGraph* (Csardi & Nepusz, 2006).

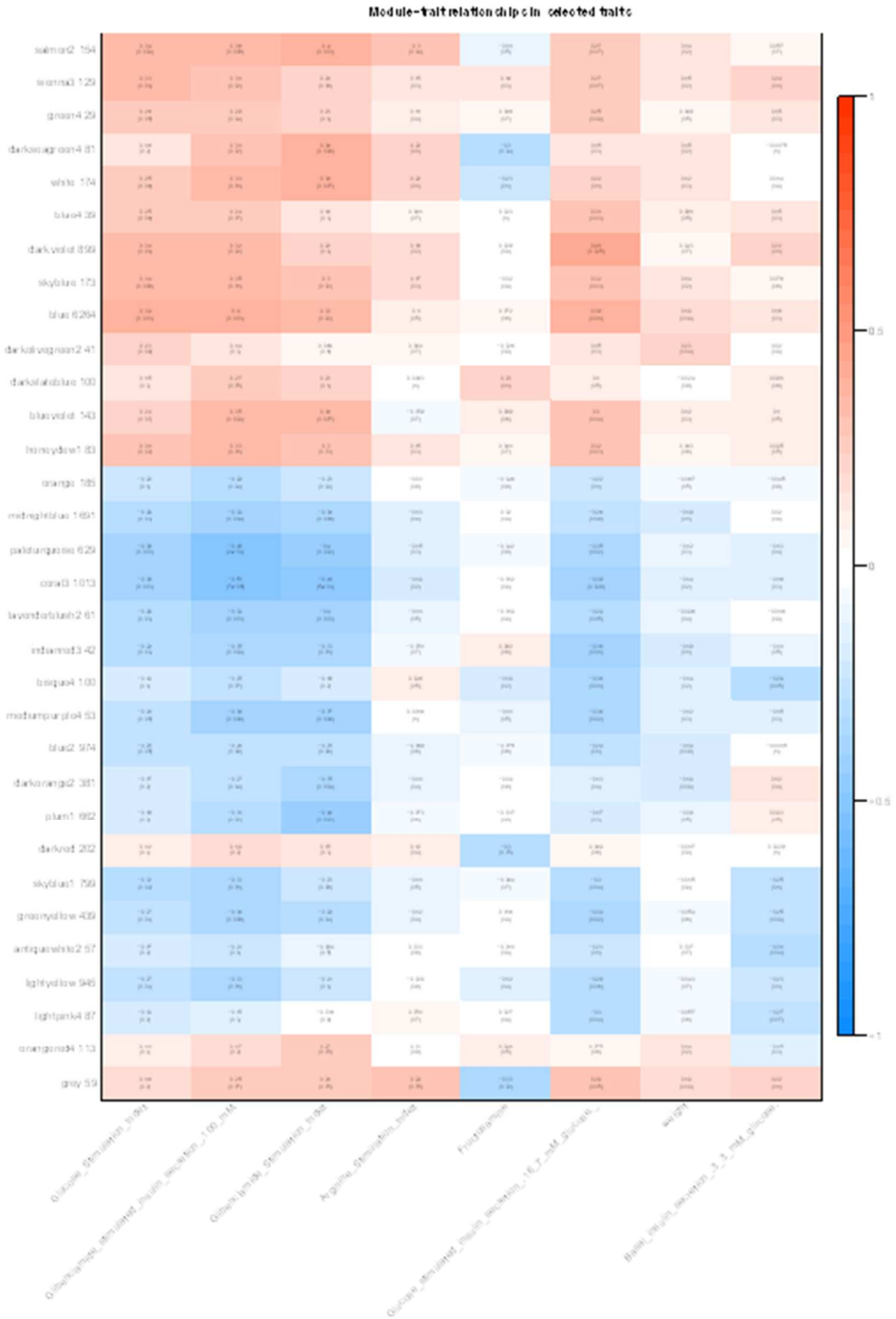
Merging of sequence-based and literature-based Transcription Factor networks. We reasoned that TF-target gene relationships that were predicted by both a sequence-based and a literature-based approach would constitute robust predictions of up-stream regulators of the trait-associated modules. We therefore created a network combining the information from the literature-based and sequence-based networks. To do this, the individual module networks were merged to create a single literature-based, and a single sequence-based network by taking the union of all of the edges in the individual module networks. The literature and sequence-based networks were then combined to create a network containing only the intersecting edges. Hive plots (Krzywinski et al, 2012) (Figure 5b) were created for the sequence-based, the literature-based and the intersection network using the *HiveR* package in R (https://github.com/bryanhanson/HiveR). Network visualization (Figure 5c) was performed using Gephi (http://gephi.github.io/).

Confidential

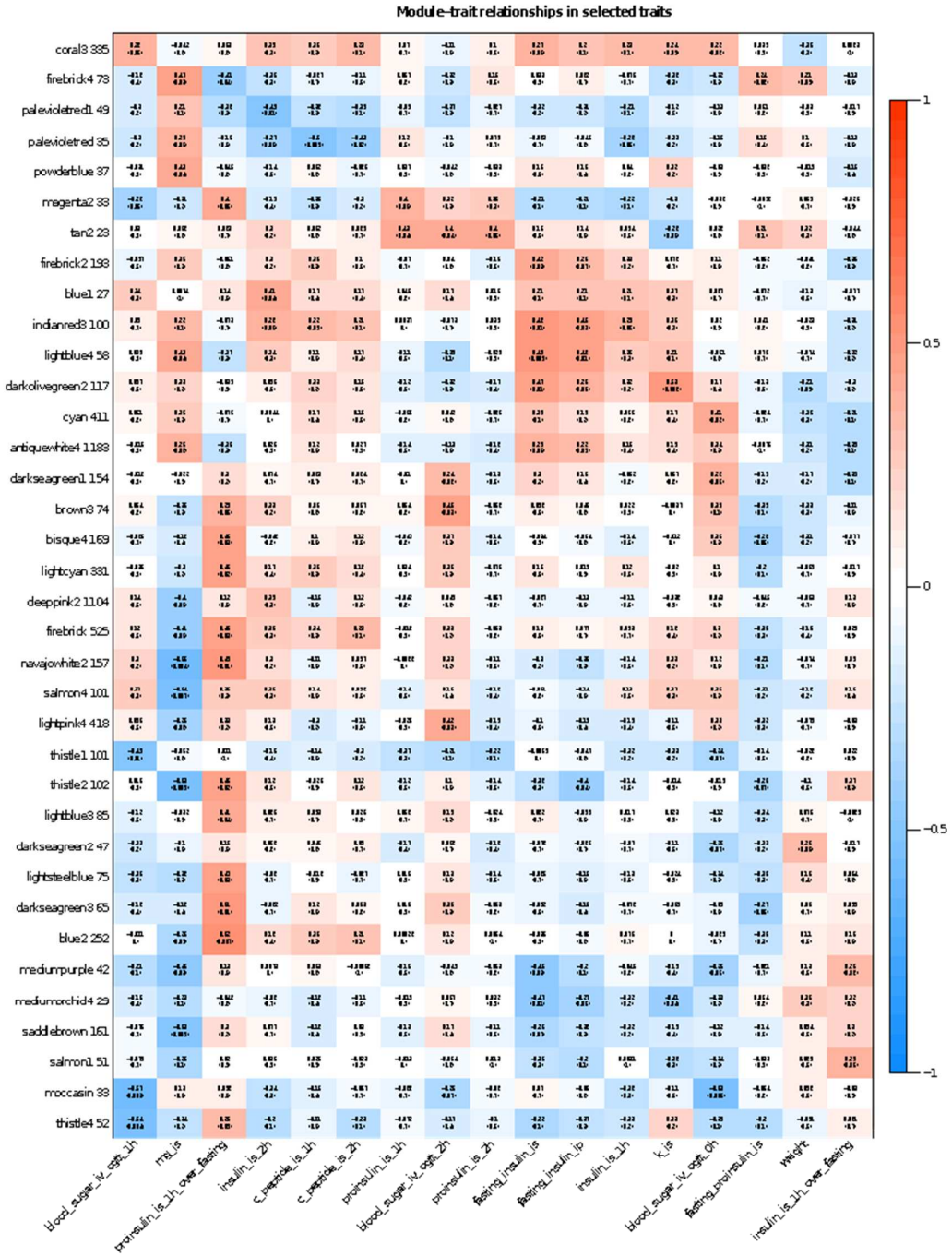


OD-Islet modules (Set1) comparison to PPP-Islet modules (Set2). Numbers indicate number of overlapping genes. The intensity of red indicates the significance: darker red=more significant (Fisher test). Scale (right) is –log10 (p-value).

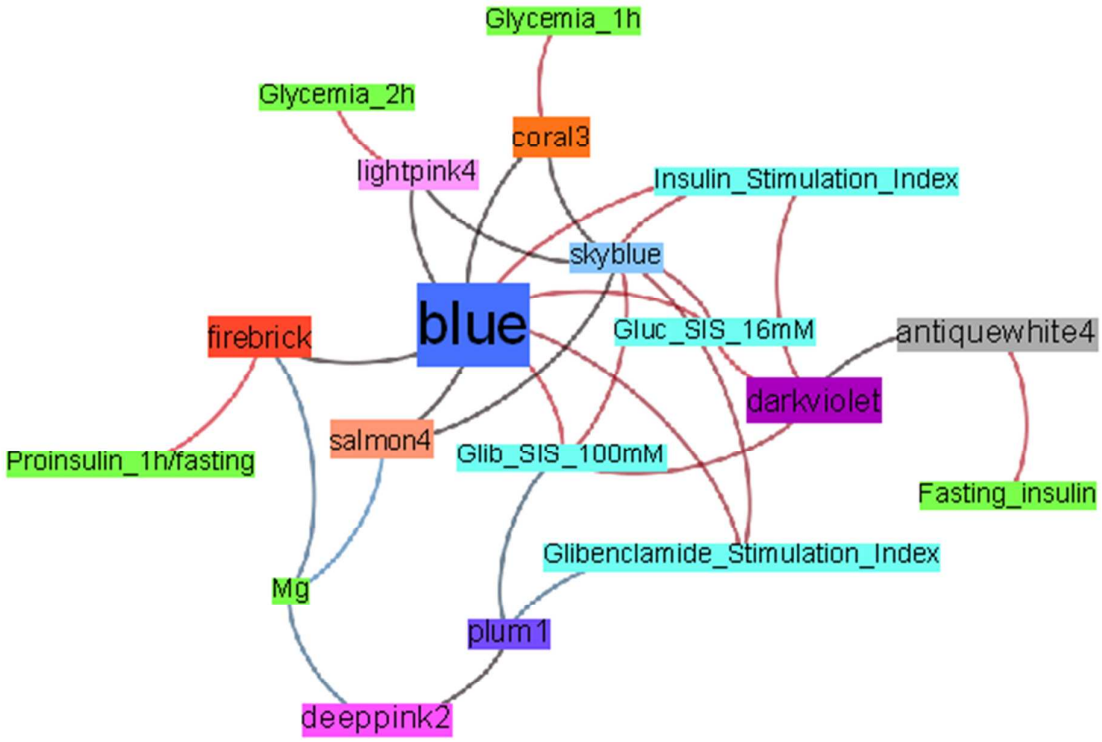
Confidential



OD-Islet co-expression module correlations with clinical and functional traits. Only module-trait correlations with p-value ≤0.05 are shown. The colors indicate the strength of the correlation (blue=strong negative correlation; red=strong positive correlation). Glucose/glibenclamide/arginine stimulation index refer to Glucose/Glibenclamide/Arginine-induced insulin stimulation index.



PPP-Islet co-expression module correlations with clinical and functional traits. Only module-trait correlations with p-value ≤0.05 are shown. The colors indicate the strength of the correlation (blue=strong negative correlation; red=strong positive correlation).



Module-trait heatmap showing OD and PPP module correlations with functional and clinical traits. The modules (blue, skyblue, darkviolet, antiquewhite4, coral3, lightpink4, firebrick, salmon4, plum1 and deeppink2) are colored according to their names. OD traits Glucose-induced insulin stimulation index (insulin_stimulation_index), Glucose induced insulin secretion at 16mM (Gluc_ISI_16mM), Glibenclamide stimulation index and Glibenclamide-induced insulin secretion at 100mM (Glib_ ISI_100mM) are colored in turquoise and are connected to OD modules (blue, skyblue, darkviolet, plum1). PPP traits Glycemia (OGTT) at 1 or 2 hours (Glycemia_1h/2h), fasting insulin, proinsulin at 1 hour/fasting proinsulin and magnesium (Mg) are colored in light green and are connected to PPP modules (firebrick, salmon4, lightpink4, coral3, deeppink2, antiquewhite4). Red edges indicate positive correlations between modules and traits; blue edges represent negative correlations between modules and traits. Dark grey edges between modules represent significant overlap between module genes.

For Review Only

Supplementary References

Bonifacio E (2015) Predicting type 1 diabetes using biomarkers. Diabetes Care 38**:** 989-996

Botticher G, Sturm D, Ehehalt F, Knoch KP, Kersting S, Grutzmann R, Baretton GB, Solimena M, Saeger HD (2011) Isolation of human islets from partially pancreatectomized patients. J Vis Exp

Bugliani M, Liechti R, Cheon H, Suleiman M, Marselli L, Kirkpatrick C, Filipponi F, Boggi U, Xenarios I, Syed F et al (2013) Microarray analysis of isolated human islet transcriptome in type 2 diabetes and the role of the ubiquitin-proteasome system in pancreatic beta cell dysfunction. Mol Cell Endocrinol 367**:** 1-10

Csardi G, Nepusz T (2006) The igraph software package for complex network research. InterJournal, Complex Systems 1695**:** 1-9

Falcon S, Gentleman R (2007) Using GOstats to test gene lists for GO term association. Bioinformatics 23**:** 257-258

Gentleman RC, Carey VJ, Bates DM, Bolstad B, Dettling M, Dudoit S, Ellis B, Gautier L, Ge Y, Gentry J et al (2004) Bioconductor: open software development for computational biology and bioinformatics. Genome Biol 5**:** R80

Johnson WE, Li C, Rabinovic A (2007) Adjusting batch effects in microarray expression data using empirical Bayes methods. Biostatistics 8**:** 118-127

Jorns A, Akin M, Arndt T, Terbish T, Zu Vilsendorf AM, Wedekind D, Hedrich HJ, Lenzen S (2014) Anti-TCR therapy combined with fingolimod for reversal of diabetic hyperglycemia by beta cell regeneration in the LEW.1AR1-iddm rat model of type 1 diabetes. J Mol Med (Berl) 92**:** 743-755

Jorns A, Gunther A, Hedrich HJ, Wedekind D, Tiedge M, Lenzen S (2005) Immune cell infiltration, cytokine expression, and beta-cell apoptosis during the development of type 1 diabetes in the spontaneously diabetic LEW.1AR1/Ztm-iddm rat. Diabetes 54**:** 2041-2052

Kirkpatrick CL, Marchetti P, Purrello F, Piro S, Bugliani M, Bosco D, de Koning EJ, Engelse MA, Kerr-Conte J, Pattou F et al (2010) Type 2 diabetes susceptibility gene expression in normal or diabetic sorted human alpha and beta cells: correlations with age or BMI of islet donors. PLoS One 5**:** e11053

Kramer A, Green J, Pollard J, Jr., Tugendreich S (2014) Causal analysis approaches in Ingenuity Pathway Analysis. Bioinformatics 30**:** 523-530

Krzywinski M, Birol I, Jones SJ, Marra MA (2012) Hive plots--rational approach to visualizing networks. Brief Bioinform 13**:** 627-644

Kwon AT, Arenillas DJ, Worsley Hunt R, Wasserman WW (2012) oPOSSUM-3: advanced analysis of regulatory motif over-representation across genes or ChIP-Seq datasets. G3 (Bethesda) 2**:** 987-1002

Confidential

Langfelder P, Horvath S (2008) WGCNA: an R package for weighted correlation network analysis. BMC Bioinformatics 9**:** 559

Lukowiak B, Vandewalle B, Riachy R, Kerr-Conte J, Gmyr V, Belaich S, Lefebvre J, Pattou F (2001) Identification and purification of functional human beta-cells by a new specific zinc-fluorescent probe. J Histochem Cytochem 49**:** 519-528

Marselli L, Bugliani M, Suleiman M, Olimpico F, Masini M, Petrini M, Boggi U, Filipponi F, Syed F, Marchetti P (2013) beta-Cell inflammation in human type 2 diabetes and the role of autophagy. Diabetes Obes Metab 15 Suppl 3**:** 130-136

Marselli L, Suleiman M, Masini M, Campani D, Bugliani M, Syed F, Martino L, Focosi D, Scatena F, Olimpico F et al (2014) Are we overestimating the loss of beta cells in type 2 diabetes? Diabetologia 57**:** 362-365

Parnaud G, Bosco D, Berney T, Pattou F, Kerr-Conte J, Donath MY, Bruun C, Mandrup-Poulsen T, Billestrup N, Halban PA (2008) Proliferation of sorted human and rat beta cells. Diabetologia 51**:** 91-100

Ravassard P, Hazhouz Y, Pechberty S, Bricout-Neveu E, Armanet M, Czernichow P, Scharfmann R (2011) A genetically engineered human pancreatic beta cell line exhibiting glucose-inducible insulin secretion. J Clin Invest 121**:** 3589-3597

Ravier MA, Rutter GA (2010) Isolation and culture of mouse pancreatic islets for ex vivo imaging studies with trappable or recombinant fluorescent probes. Methods Mol Biol 633**:** 171-184

Ritchie ME, Phipson B, Wu D, Hu Y, Law CW, Shi W, Smyth GK (2015) limma powers differential expression analyses for RNA-sequencing and microarray studies. Nucleic Acids Res 43**:** e47

Sturm D, Marselli L, Ehehalt F, Richter D, Distler M, Kersting S, Grutzmann R, Bokvist K, Froguel P, Liechti R et al (2013) Improved protocol for laser microdissection of human pancreatic islets from surgical specimens. J Vis Exp

Confidential

Comparison	Bailey2016 comparison	Genes DE in PPP comparison
PPP T2D vs ND	ADEX vs rest	161
PPP T2D vs ND	IMMUNO vs rest	161
PPP T2D vs ND	PROGEN vs rest	161
PPP T2D vs ND	SQUAMO vs rest	161
OD T2D vs ND	ADEX vs rest	459
OD T2D vs ND	IMMUNO vs rest	459
OD T2D vs ND	PROGEN vs rest	459
OD T2D vs ND	SQUAMO vs rest	459

Threshold for DE = FC ≥1.5 and FDR ≤0.05
P-value = hypergeometric (unadjusted)

Confidential

Genes UP in PPP comparison	Genes DOWN in PPP comparison
103	59
103	59
103	59
103	59
143	317
143	317
143	317
143	317

Confidential

Genes DE in Bailey2016 comparison	Genes UP in Bailey2016 comparison
250	242
442	370
309	274
2366	1061
250	242
442	370
309	274
2366	1061

Confidential

Genes DOWN in Bailey2016 comparison	Intersect DE genes	Intersect UP genes
8	5	2
72	7	5
35	2	1
1305	38	12
8	25	3
72	6	1
35	17	2
1305	101	23

Confidential

Intersect DOWN genes	Total expressed genes	P-value DE genes	P-value UP genes
0	16742	0.104497004	0.457395092
0	16742	0.15134588	0.08686764
0	16742	0.815705364	0.828553378
15	16742	0.000841593	0.029583237
0	16502	6.46E-08	0.369300965
3	16502	0.988458878	0.965167266
0	16502	0.00823866	0.707042554
53	16502	4.75E-06	4.07E-05

Confidential

P-value DOWN genes
1
1
1
3.32E-05
1
0.170821871
1
1.46E-07

Confidential

Intersect genes UP

IGFN1,SV2B

CD74,CYTIP,IRF8,PDE4B,PTPRC

TMEM132C

ADAM19,ARL4C,C3orf67,CD44,COL1A1,DPYD,ELFN1,PAPPA,RUNX2,SERPINB9,ST8SIA1,WNT3

FGL1,NR5A2,SLC30A2

SLC12A2

CDH6,KBTBD12

AGTRAP,ARNTL2,CA12,CALB2,CCL8,CD44,CLDN1,COL12A1,CXCR7,FOXC1,GAS1,GBP1,IL1B,IL1RAP,IRX3,KLF

Confidential

Intersect genes DOWN

ACRBP,ADH6,C8orf47,CAPN13,MYCN,NRG3,PCDH20,PDX1,PFKFB2,PLA1A,RDH10,SCTR,TMED6,TMEM37,TM

L1CAM,NCKAP5,TRIM9

ABCC8,ADRA2A,BMP5,CACNA2D2,CADPS,CAPN13,CAPN8,CASR,CDH17,CNTN1,DCX,DDC,EDN3,FAM222A,F

Confidential

NIK

GF9,GABRB3,GPD1,GRIA4,HMGCLL1,HPGD,ILDR2,KCNA5,KCNG3,KCNH2,KIAA1211,LRRC36,MLX

Confidential

IPL,NAALAD2,NPC1L1,PCDH20,PDK4,PLCB4,PLCE1,RAB39B,RAB3B,RALYL,RBP4,RGS7,RIMKLA,RC

Confidential

DBO2,RSPH1,SCIN,SCTR,SEZ6L,SGSM1,SLC4A8,SLC5A1,SMAD9,SYT13,TMEM37,USH1C,WSCD2,Z

Confidential

NF540

Confidential

ENTREZID	SYMBOL
55856	ACOT13
51205	ACP6
84519	ACRBP
57180	ACTR3B
116	ADCYAP1
22850	ADNP2
57085	AGTRAP
8574	AKR7A2
207	AKT1
64400	AKTIP
8846	ALKBH1
23600 /// 114899 /// 100534612	AMACR /// C1QTNF3 /// C1QTNF3-AMACR
139285	AMER1
51239 /// 200539	ANKRD23 /// ANKRD39
10541	ANP32B
384	ARG2
26084	ARHGEF26
10776	ARPP19
430	ASCL2
489	ATP2A3
493	ATP2B4
515	ATP5F1
518	ATP5G3
51382	ATP6V1D
529	ATP6V1E1
51606	ATP6V1H
25814	ATXN10
342371	ATXN1L
567	B2M
8702	B4GALT4
440465	BAIAP2-AS1
11177	BAZ1A
27241	BBS9
622	BDH1
54841	BIVM
388135	C15orf59
145853	C15orf61
112770	C1orf85
770	CA11
143384	CACUL1
92291	CAPN13
846	CASR
112942	CCDC104
960	CD44
1028	CDKN1C
8760	CDS2
10752	CHL1
1152	CKB
1267	CNP

Confidential

28958	COA3
22837	COBLL1
150684	COMMD1
29099	COMMD9
10980	COPS6
84987	COX14
64506	CPEB1
1500 /// 100528016	CTNND1 /// TMX2-CTNND1
113612	CYP2U1
1600	DAB1
1628	DBP
51181	DCXR
1644	DDC
8526	DGKE
79665	DHX40
2039	DMTN
54788	DNAJB12
7802	DNALI1
1774	DNASE1L1
124454	EARS2
29904	EEF2K
79813	EHMT1
23741	EID1
23587	ELP5
54859	ELP6
24139	EML2
23052	ENDOD1
2036	EPB41L1
2098	ESD
2110	ETFDH
284611	FAM102B
11170 /// 101059937	FAM107A /// LOC101059937
145483	FAM161B
8987 /// 100129583 /// 100631383	FAM47E /// FAM47E-STBD1 /// STBD1
26240	FAM50B
22868	FASTKD2
114907	FBXO32
55030	FBXO34
338557	FFAR4
55785	FGD6
2271	FH
128486	FITM2
55691	FRMD4A
10841	FTCD
8087	FXR1
486	FXYD2
486 /// 100533181	FXYD2 /// FXYD6-FXYD2
57818	G6PC2
2571	GAD1
2591	GALNT3
2596	GAP43

Confidential

54815	GATAD2A
2642	GCGR
23062	GGA2
169792	GLIS3
2743	GLRB
10691	GMEB1
2788	GNG7
10007	GNPDA1
9570	GOSR2
2805	GOT1
64412	GZF1
22927	HABP4
3033	HADH
3030	HADHA
10021	HCN4
57467	HHATL
3131	HLF
6927	HNF1A
3178	HNRNPA1
3184	HNRNPD
3638	INSIG1
3667	IRS1
170850	KCNG3
131096	KCNH8
3786	KCNQ3
5927	KDM5A
340533	KIAA2022
83746	L3MBTL2
100129361	LOC100129361
100505997	LOC100505997
100506098	LOC100506098
6638 /// 91380 /// 100033444 /// 100	LOC100506948 /// SNORD107 /// SNORD115-13
100507316	LOC100507316
9659 /// 728802 /// 100996724 /// 10	LOC100996724 /// LOC100996761 /// LOC10106
56981 /// 101060179	LOC101060179 /// PRDM11
27246 /// 101060478	LOC101060478 /// RNF115
346389	MACC1
9223	MAGI1
4124	MAN2A1
4130	MAP1A
5871	MAP4K2
51275	MAPKAPK5-AS1
4152	MBD1
55796	MBNL3
55283	MCOLN3
4190	MDH1
9442	MED27
51399 /// 100500840	MIR3656 /// TRAPPC4
23417	MLYCD
3110	MNX1
4338	MOCS2

Confidential

51660	MPC1
4354	MPP1
78988	MRP63
63875	MRPL17
63931	MRPS14
51023	MRPS18C
339287	MSL1
57509	MTUS1
23281	MTUS2
90634	N4BP2L1
8775	NAPA
152217	NCBP2-AS2
4714	NDUFB8
4717	NDUFC1
4719	NDUFS1
4758	NEU1
4775	NFATC3
4799	NFX1
51335	NGRN
4809	NHP2L1
8508	NIPSNAP1
4825	NKX6-1
29881	NPC1L1
27065	NSG1
84284	NTPCR
26578	OSTF1
5019	OXCT1
5066	PAM
5091	PC
5096	PCCB
64881	PCDH20
5110	PCMT1
8622	PDE8B
5166	PDK4
81572	PDRG1
5037	PEBP1
8504	PEX3
5204	PFDN5
5208	PFKFB2
55276	PGM2
93183	PIGM
5432	POLR2C
5502	PPP1R1A
5537	PPP6C
25824	PRDX5
51422	PRKAG2
5621	PRNP
5631	PRPS1
11168	PSIP1
5684	PSMA3
5701	PSMC2

Confidential

9491	PSMF1
5782	PTPN12
5774	PTPN3
754	PTTG1IP
29920	PYCR2
5860	QDPR
201475	RAB12
29098	RANGRF
5923	RASGRF1
10231	RCAN2
6004	RGS16
6041	RNASEL
22838	RNF44
79657	RPAP3
6134 /// 26778	RPL10 /// SNORA70
58528	RRAGD
51493	RTCB
23168	RTF1
51507	RTFDC1
84816	RTN4IP1
10284	SAP18
6304	SATB1
23314	SATB2
51119 /// 155370	SBDS /// SBDSP1
7857	SCG2
6344	SCTR
9037	SEMA5A
129049	SGSM1
140885	SIRPA
6514	SLC2A2
2542	SLC37A4
6541	SLC7A1
440957	SMIM4
10302	SNAPC5
6635	SNRPE
6647	SOD1
92521	SPECC1
121665	SPPL3
57731	SPTBN4
58477	SRPRB
55437	STRADB
6821	SUOX
258010	SVIP
55530	SVOP
375757	SWI5
6853	SYN1
10492	SYNCRIP
90196	SYS1
143425	SYT9
84897	TBRG1
96764	TGS1

Confidential

25917	THUMPD3
29087	THYN1
57458	TMCC3
55863	TMEM126B
92293	TMEM132C
85014	TMEM141
161291	TMEM30B
140738	TMEM37
23043	TNIK
54472	TOLLIP
7167	TPI1
27010	TPK1
7175	TPR
93587	TRMT10A
125488	TTC39C
25828	TXN2
9352	TXNL1
51619	UBE2D4
137970	UNC5D
10975	UQCR11
84749	USP30
57687	VAT1L
7419	VDAC3
79001	VKORC1
348793	WDR53
7466	WFS1
7473	WNT3
9589	WTAP
7528	YY1
7691	ZNF132
7693	ZNF134
7695	ZNF136
353355	ZNF233
163255	ZNF540
148254	ZNF555
386758	ZNF582-AS1
163049	ZNF791

Confidential

GENENAME	PROBE ID_OD
acyl-CoA thioesterase 13	204565_at
acid phosphatase 6, lysophosphatidic	218795_at
acrosin binding protein	223717_s_at
ARP3 actin-related protein 3 homolog B (yeast)	1555487_a_at
adenylate cyclase activating polypeptide 1 (pituitary)	230237_at
ADNP homeobox 2	203322_at
angiotensin II receptor-associated protein	238135_at
aldo-keto reductase family 7, member A2 (aflatoxin aldehyde reductase)	202139_at
v-akt murine thymoma viral oncogene homolog 1	207163_s_at
AKT interacting protein	223894_s_at
alkB, alkylation repair homolog 1 (E. coli)	205621_at
alpha-methylacyl-CoA racemase /// C1q and tumor necrosis factor related protein	209424_s_at
APC membrane recruitment protein 1	1552882_a_at
ankyrin repeat domain 23 /// ankyrin repeat domain 39	1553366_s_at
acidic (leucine-rich) nuclear phosphoprotein 32 family, member B	201305_x_at
arginase 2	203946_s_at
Rho guanine nucleotide exchange factor (GEF) 26	227197_at
cAMP-regulated phosphoprotein, 19kDa	221482_s_at
achaete-scute complex homolog 2 (Drosophila)	229215_at
ATPase, Ca++ transporting, ubiquitous	230453_s_at
ATPase, Ca++ transporting, plasma membrane 4	212136_at
ATP synthase, H+ transporting, mitochondrial Fo complex, subunit B1	211755_s_at
ATP synthase, H+ transporting, mitochondrial Fo complex, subunit C3 (subunit 9)	207508_at
ATPase, H+ transporting, lysosomal 34kDa, V1 subunit D	208899_x_at
ATPase, H+ transporting, lysosomal 31kDa, V1 subunit E1	208678_at
ATPase, H+ transporting, lysosomal 50/57kDa, V1 subunit H	221504_s_at
ataxin 10	208833_s_at
ataxin 1-like	226095_s_at
beta-2-microglobulin	232311_at
UDP-Gal:betaGlcNAc beta 1,4- galactosyltransferase, polypeptide 4	212876_at
BAIAP2 antisense RNA 1 (head to head)	1566558_x_at
bromodomain adjacent to zinc finger domain, 1A	217986_s_at
Bardet-Biedl syndrome 9	37549_g_at
3-hydroxybutyrate dehydrogenase, type 1	211715_s_at
basic, immunoglobulin-like variable motif containing	233255_s_at
chromosome 15 open reading frame 59	230475_at
chromosome 15 open reading frame 61	229742_at
chromosome 1 open reading frame 85	1558692_at
carbonic anhydrase XI	209726_at
CDK2-associated, cullin domain 1	225192_at
calpain 13	229499_at
calcium-sensing receptor	210577_at
coiled-coil domain containing 104	224968_at
CD44 molecule (Indian blood group)	212063_at
cyclin-dependent kinase inhibitor 1C (p57, Kip2)	213348_at
CDP-diacylglycerol synthase (phosphatidate cytidylyltransferase) 2	233630_at
cell adhesion molecule with homology to L1CAM (close homolog of L1)	204591_at
creatine kinase, brain	200884_at
2',3'-cyclic nucleotide 3' phosphodiesterase	1557943_at

Confidential

cytochrome c oxidase assembly factor 3	218026_at
cordon-bleu WH2 repeat protein-like 1	215393_s_at
copper metabolism (Murr1) domain containing 1	226024_at
COMM domain containing 9	218072_at
COP9 signalosome subunit 6	201405_s_at
cytochrome c oxidase assembly homolog 14 (S. cerevisiae)	225772_s_at
cytoplasmic polyadenylation element binding protein 1	219578_s_at
catenin (cadherin-associated protein), delta 1 /// TMX2-CTNND1 readthrough (NM	211240_x_at
cytochrome P450, family 2, subfamily U, polypeptide 1	226393_at
Dab, reelin signal transducer, homolog 1 (Drosophila)	228329_at
D site of albumin promoter (albumin D-box) binding protein	209782_s_at
dicarbonyl/L-xylulose reductase	217973_at
dopa decarboxylase (aromatic L-amino acid decarboxylase)	205311_at
diacylglycerol kinase, epsilon 64kDa	238694_at
DEAH (Asp-Glu-Ala-His) box polypeptide 40	222574_s_at
dematin actin binding protein	204505_s_at
DnaJ (Hsp40) homolog, subfamily B, member 12	202865_at
dynein, axonemal, light intermediate chain 1	205186_at
deoxyribonuclease I-like 1	203912_s_at
glutamyl-tRNA synthetase 2, mitochondrial	227374_at
eukaryotic elongation factor-2 kinase	225546_at
euchromatic histone-lysine N-methyltransferase 1	225461_at
EP300 interacting inhibitor of differentiation 1	211698_at
elongator acetyltransferase complex subunit 5	223286_at
elongator acetyltransferase complex subunit 6	223277_at
echinoderm microtubule associated protein like 2	204399_s_at
endonuclease domain containing 1	212573_at
erythrocyte membrane protein band 4.1-like 1	212336_at
esterase D	209009_at
electron-transferring-flavoprotein dehydrogenase	33494_at
family with sequence similarity 102, member B	226568_at
family with sequence similarity 107, member A /// uncharacterized LOC101059937	209074_s_at
family with sequence similarity 161, member B	235378_at
family with sequence similarity 47, member E /// FAM47E-STBD1 readthrough ///	203986_at
family with sequence similarity 50, member B	205775_at
FAST kinase domains 2	229135_at
F-box protein 32	225328_at
F-box protein 34	218539_at
free fatty acid receptor 4	240856_at
FYVE, RhoGEF and PH domain containing 6	226799_at
fumarate hydratase	214170_x_at
fat storage-inducing transmembrane protein 2	226805_at
FERM domain containing 4A	225163_at
formimidoyltransferase cyclodeaminase	224300_x_at
fragile X mental retardation, autosomal homolog 1	230201_at
FXYD domain containing ion transport regulator 2	205674_x_at
FXYD domain containing ion transport regulator 2 /// FXYD6-FXYD2 readthrough	207434_s_at
glucose-6-phosphatase, catalytic, 2	221453_at
glutamate decarboxylase 1 (brain, 67kDa)	206669_at
UDP-N-acetyl-alpha-D-galactosamine:polypeptide N-acetylgalactosaminyltransfera	203397_s_at
growth associated protein 43	204471_at

Confidential

GATA zinc finger domain containing 2A	218131_s_at
glucagon receptor	210565_at
golgi-associated, gamma adaptin ear containing, ARF binding protein 2	208913_at
GLIS family zinc finger 3	229435_at
glycine receptor, beta	244680_at
glucocorticoid modulatory element binding protein 1	235233_s_at
guanine nucleotide binding protein (G protein), gamma 7	206896_s_at
glucosamine-6-phosphate deaminase 1	202382_s_at
golgi SNAP receptor complex member 2	239159_at
glutamic-oxaloacetic transaminase 1, soluble	208813_at
GDNF-inducible zinc finger protein 1	225884_s_at
hyaluronan binding protein 4	209818_s_at
hydroxyacyl-CoA dehydrogenase	211569_s_at
hydroxyacyl-CoA dehydrogenase/3-ketoacyl-CoA thiolase/enoyl-CoA hydratase (tri	208630_at
hyperpolarization activated cyclic nucleotide-gated potassium channel 4	230208_at
hedgehog acyltransferase-like	223572_at
hepatic leukemia factor	204755_x_at
HNF1 homeobox A	210515_at
heterogeneous nuclear ribonucleoprotein A1	222040_at
heterogeneous nuclear ribonucleoprotein D (AU-rich element RNA binding protein	209330_s_at
insulin induced gene 1	201626_at
insulin receptor substrate 1	238933_at
potassium voltage-gated channel, subfamily G, member 3	1552897_a_at
potassium voltage-gated channel, subfamily H (eag-related), member 8	1552742_at
potassium voltage-gated channel, KQT-like subfamily, member 3	228579_at
lysine (K)-specific demethylase 5A	215698_at
KIAA2022	244370_at
l(3)mbt-like 2 (Drosophila)	223205_s_at
chromosome X open reading frame 69-like	238915_at
uncharacterized LOC100505997	1568625_at
uncharacterized LOC100506098	227985_at
uncharacterized LOC100506948 /// small nucleolar RNA, C/D box 107 /// small nuc	1559342_a_at
uncharacterized LOC100507316	235428_at
myomegalin-like /// myomegalin-like /// myomegalin-like /// uncharacterized LOC	213388_at
uncharacterized LOC101060179 /// PR domain containing 11	239763_at
E3 ubiquitin-protein ligase RNF115-like /// ring finger protein 115	226468_at
metastasis associated in colon cancer 1	232151_at
membrane associated guanylate kinase, WW and PDZ domain containing 1	225474_at
mannosidase, alpha, class 2A, member 1	235103_at
microtubule-associated protein 1A	203151_at
mitogen-activated protein kinase kinase kinase kinase 2	204936_at
MAPKAPK5 antisense RNA 1	219817_at
methyl-CpG binding domain protein 1	226862_at
muscleblind-like splicing regulator 3	230113_at
mucolipin 3	229797_at
malate dehydrogenase 1, NAD (soluble)	200978_at
mediator complex subunit 27	51176_at
microRNA 3656 /// trafficking protein particle complex 4	217959_s_at
malonyl-CoA decarboxylase	218869_at
motor neuron and pancreas homeobox 1	214614_at
molybdenum cofactor synthesis 2	218212_s_at

Confidential

mitochondrial pyruvate carrier 1	218024_at
membrane protein, palmitoylated 1, 55kDa	202974_at
mitochondrial ribosomal protein 63	204386_s_at
mitochondrial ribosomal protein L17	222216_s_at
mitochondrial ribosomal protein S14	203801_at
mitochondrial ribosomal protein S18C	220103_s_at
male-specific lethal 1 homolog (Drosophila)	212708_at
microtubule associated tumor suppressor 1	239576_at
microtubule associated tumor suppressor candidate 2	244676_s_at
NEDD4 binding protein 2-like 1	213375_s_at
N-ethylmaleimide-sensitive factor attachment protein, alpha	206491_s_at
NCBP2 antisense RNA 2 (head to head)	225657_at
NADH dehydrogenase (ubiquinone) 1 beta subcomplex, 8, 19kDa	201227_s_at
NADH dehydrogenase (ubiquinone) 1, subcomplex unknown, 1, 6kDa	232146_at
NADH dehydrogenase (ubiquinone) Fe-S protein 1, 75kDa (NADH-coenzyme Q red	203039_s_at
sialidase 1 (lysosomal sialidase)	208926_at
nuclear factor of activated T-cells, cytoplasmic, calcineurin-dependent 3	210555_s_at
nuclear transcription factor, X-box binding 1	202585_s_at
neugrin, neurite outgrowth associated	217722_s_at
NHP2 non-histone chromosome protein 2-like 1 (S. cerevisiae)	230443_at
nipsnap homolog 1 (C. elegans)	201709_s_at
NK6 homeobox 1	221366_at
NPC1-like 1	220106_at
neuron specific gene family member 1	213533_at
nucleoside-triphosphatase, cancer-related	223272_s_at
osteoclast stimulating factor 1	204479_at
3-oxoacid CoA transferase 1	202780_at
peptidylglycine alpha-amidating monooxygenase	202336_s_at
pyruvate carboxylase	204476_s_at
propionyl CoA carboxylase, beta polypeptide	212694_s_at
protocadherin 20	232054_at
protein-L-isoaspartate (D-aspartate) O-methyltransferase	210156_s_at
phosphodiesterase 8B	1554789_a_at
pyruvate dehydrogenase kinase, isozyme 4	1562321_at
p53 and DNA-damage regulated 1	225075_at
phosphatidylethanolamine binding protein 1	211941_s_at
peroxisomal biogenesis factor 3	203972_s_at
prefoldin subunit 5	210908_s_at
6-phosphofructo-2-kinase/fructose-2,6-biphosphatase 2	226733_at
phosphoglucomutase 2	225366_at
phosphatidylinositol glycan anchor biosynthesis, class M	236622_at
polymerase (RNA) II (DNA directed) polypeptide C, 33kDa	208996_s_at
protein phosphatase 1, regulatory (inhibitor) subunit 1A	235129_at
protein phosphatase 6, catalytic subunit	225429_at
peroxiredoxin 5	1560587_s_at
protein kinase, AMP-activated, gamma 2 non-catalytic subunit	233748_x_at
prion protein	201300_s_at
phosphoribosyl pyrophosphate synthetase 1	208447_s_at
PC4 and SFRS1 interacting protein 1	205961_s_at
proteasome (prosome, macropain) subunit, alpha type, 3	237300_at
proteasome (prosome, macropain) 26S subunit, ATPase, 2	201068_s_at

Confidential

proteasome (prosome, macropain) inhibitor subunit 1 (PI31)	236012_at
protein tyrosine phosphatase, non-receptor type 12	202006_at
protein tyrosine phosphatase, non-receptor type 3	227944_at
pituitary tumor-transforming 1 interacting protein	200677_at
pyrroline-5-carboxylate reductase family, member 2	224855_at
quinoid dihydropteridine reductase	209123_at
RAB12, member RAS oncogene family	239891_x_at
RAN guanine nucleotide release factor	218526_s_at
Ras protein-specific guanine nucleotide-releasing factor 1	210550_s_at
regulator of calcineurin 2	203498_at
regulator of G-protein signaling 16	209324_s_at
ribonuclease L (2',5'-oligoisoadenylate synthetase-dependent)	221287_at
ring finger protein 44	203286_at
RNA polymerase II associated protein 3	218842_at
ribosomal protein L10 /// small nucleolar RNA, H/ACA box 70	200724_at
Ras-related GTP binding D	221524_s_at
RNA 2',3'-cyclic phosphate and 5'-OH ligase	200042_at
Rtf1, Paf1/RNA polymerase II complex component, homolog (S. cerevisiae)	212301_at
replication termination factor 2 domain containing 1	234926_s_at
reticulon 4 interacting protein 1	224509_s_at
Sin3A-associated protein, 18kDa	208741_at
SATB homeobox 1	203408_s_at
SATB homeobox 2	213435_at
Shwachman-Bodian-Diamond syndrome /// Shwachman-Bodian-Diamond syndron	222669_s_at
secretogranin II	204035_at
secretin receptor	1565737_at
sema domain, seven thrombospondin repeats (type 1 and type 1-like), transmemb	229427_at
small G protein signaling modulator 1	230287_at
signal-regulatory protein alpha	202897_at
solute carrier family 2 (facilitated glucose transporter), member 2	206535_at
solute carrier family 37 (glucose-6-phosphate transporter), member 4	202830_s_at
solute carrier family 7 (cationic amino acid transporter, y+ system), member 1	212290_at
small integral membrane protein 4	229826_at
small nuclear RNA activating complex, polypeptide 5, 19kDa	213203_at
small nuclear ribonucleoprotein polypeptide E	231112_at
superoxide dismutase 1, soluble	200642_at
sperm antigen with calponin homology and coiled-coil domains 1	228900_at
signal peptide peptidase like 3	224639_at
spectrin, beta, non-erythrocytic 4	224145_s_at
signal recognition particle receptor, B subunit	227737_at
STE20-related kinase adaptor beta	223266_at
sulfite oxidase	1553030_a_at
small VCP/p97-interacting protein	226278_at
SV2 related protein homolog (rat)	229818_at
SWI5 recombination repair homolog (yeast)	226027_at
synapsin I	221914_at
synaptotagmin binding, cytoplasmic RNA interacting protein	1555427_s_at
SYS1 Golgi-localized integral membrane protein homolog (S. cerevisiae)	224668_at
synaptotagmin IX	1563658_a_at
transforming growth factor beta regulator 1	230320_at
trimethylguanosine synthase 1	236371_s_at

Confidential

THUMP domain containing 3	223804_s_at
thymocyte nuclear protein 1	218491_s_at
transmembrane and coiled-coil domain family 3	235146_at
transmembrane protein 126B	221622_s_at
transmembrane protein 132C	232313_at
transmembrane protein 141	225568_at
transmembrane protein 30B	213285_at
transmembrane protein 37	1554485_s_at
TRAF2 and NCK interacting kinase	211828_s_at
toll interacting protein	217930_s_at
triosephosphate isomerase 1	210050_at
thiamin pyrophosphokinase 1	223686_at
translocated promoter region, nuclear basket protein	228709_at
tRNA methyltransferase 10 homolog A (S. cerevisiae)	230243_at
tetratricopeptide repeat domain 39C	1552307_a_at
thioredoxin 2	209077_at
thioredoxin-like 1	235561_at
ubiquitin-conjugating enzyme E2D 4 (putative)	218837_s_at
unc-5 homolog D (C. elegans)	231325_at
ubiquinol-cytochrome c reductase, complex III subunit XI	223613_at
ubiquitin specific peptidase 30	227572_at
vesicle amine transport protein 1 homolog (T. californica)-like	226415_at
voltage-dependent anion channel 3	208845_at
vitamin K epoxide reductase complex, subunit 1	217949_s_at
WD repeat domain 53	227814_at
Wolfram syndrome 1 (wolframin)	1555270_a_at
wingless-type MMTV integration site family, member 3	229103_at
Wilms tumor 1 associated protein	203137_at
YY1 transcription factor	201901_s_at
zinc finger protein 132	207402_at
zinc finger protein 134	206182_at
zinc finger protein 136	206240_s_at
zinc finger protein 233	230919_at
zinc finger protein 540	242697_at
zinc finger protein 555	1553286_at
ZNF582 antisense RNA 1 (head to head)	231260_at
zinc finger protein 791	1553704_x_at

Confidential

Adj.P.Val._OD	RATIO_OD	reg_OD	PROBE ID_PPP	Adj.P.Val_PPP	RATIO_PPP	reg_PPP
0.000362726	0.75875845	down	204565_at	0.009943882	0.81465484	down
0.011802045	0.786748354	down	218795_at	0.048767881	0.79823825	down
0.044533361	0.77556529	down	223717_s_at	3.50E-05	0.63430864	down
0.005141658	0.779652938	down	1555487_a_at	0.042142797	0.71699186	down
0.011097281	0.606430801	down	230237_at	0.003993792	0.70661746	down
0.032007018	1.193153202	up	203321_s_at	0.019592389	0.86481962	down
0.010749202	1.651236011	up	1555736_a_at	0.020691654	0.79951234	down
0.000764088	0.709577867	down	202139_at	0.027726139	0.81957632	down
0.025215528	1.143848914	up	207163_s_at	6.29E-06	0.72160905	down
0.027650311	0.878032069	down	223894_s_at	0.023279059	0.83144638	down
0.010379345	0.843140265	down	205621_at	0.013929655	0.84147171	down
0.000764088	0.726353883	down	209424_s_at	0.004053502	0.71593151	down
0.01321911	1.260627586	up	1552882_a_at	0.045538915	0.83926433	down
0.00639406	0.721839718	down	1553366_s_at	0.001809347	0.59988603	down
0.028593219	1.081866316	up	201306_s_at	0.047055968	0.91418831	down
0.00032856	0.605466175	down	203946_s_at	1.47E-09	0.46273766	down
0.006780952	0.736108505	down	227197_at	0.039011615	0.77050945	down
0.023793601	0.870514279	down	214553_s_at	0.02160946	0.80290416	down
0.002520735	0.540306211	down	229215_at	1.74E-08	0.46280139	down
0.012619653	0.675906501	down	213036_x_at	0.000807185	0.76421912	down
0.02419565	1.178967866	up	212136_at	0.02223989	1.20243884	up
0.049283752	0.935670595	down	243501_at	0.047064562	0.8273049	down
0.002979675	0.891211677	down	228168_at	0.02160946	0.82384039	down
0.010614166	0.861947174	down	208899_x_at	0.024703256	0.81367107	down
0.003524416	0.834148051	down	208678_at	0.014145817	0.87574334	down
0.003197541	0.865646959	down	221504_s_at	0.005239258	0.83885853	down
0.022544167	0.920857982	down	208832_at	0.03874566	0.85189408	down
0.004507608	1.203947771	up	226095_s_at	0.047967554	0.87388137	down
0.019704199	1.498256778	up	201891_s_at	0.016393911	1.093978	up
0.03486566	0.89556167	down	212876_at	0.039682329	0.88565024	down
0.009266041	0.819855841	down	1558148_x_at	0.006363703	0.82544698	down
0.004177339	1.305212232	up	217986_s_at	0.048979426	1.36163448	up
0.017641258	0.782807999	down	209958_s_at	0.047465697	0.83168897	down
0.005218527	0.765358806	down	211715_s_at	0.001948679	0.72426507	down
0.008193734	0.840686412	down	229589_x_at	0.013025363	1.18224465	up
0.004051939	0.626042976	down	230475_at	0.03212996	0.69348301	down
0.01146588	0.779706167	down	229742_at	0.000324052	0.75900706	down
0.022160412	0.782620292	down	1558693_s_at	0.048945567	0.85977032	down
0.041703463	0.753218001	down	209726_at	0.037110507	0.81189501	down
0.010844158	1.103981618	up	227258_at	0.019513397	0.87461075	down
0.002520735	0.534821686	down	229499_at	0.004664133	0.61415087	down
0.003958867	0.582734324	down	210577_at	0.039852225	0.78037273	down
0.000764088	0.794077333	down	224968_at	0.038018433	0.88567447	down
0.008586011	1.187986778	up	1557905_s_at	0.018421407	1.68099566	up
0.038879837	0.779405953	down	213183_s_at	0.013731188	1.22904577	up
0.034350122	0.754055017	down	212864_at	0.004870179	0.84048413	down
0.001615186	0.411294281	down	204591_at	1.56E-05	0.44644135	down
0.016139835	0.811287788	down	200884_at	0.03885739	1.32901934	up
0.020110332	0.748471909	down	208912_s_at	0.001674855	0.79921408	down

Confidential

0.010868197	0.870135589	down	218026_at	0.0075111	0.83942531	down
0.048234374	1.213277113	up	229598_at	0.011693112	0.74433713	down
0.014693853	0.865988875	down	226024_at	0.027307249	0.86370014	down
0.021061401	0.869568771	down	218072_at	0.017612556	0.87318819	down
0.004248885	0.863913619	down	201405_s_at	0.011180221	0.8843086	down
0.001682378	0.815314466	down	225772_s_at	0.040645479	0.8917504	down
0.022894274	0.654477654	down	219578_s_at	0.004199848	0.70990804	down
0.007362884	1.353689633	up	211240_x_at	0.049012222	1.17295163	up
0.013838371	0.696720809	down	226393_at	0.007178599	0.683956	down
0.038991183	0.616404624	down	228329_at	0.045941926	1.55135392	up
0.007951197	0.689215824	down	209782_s_at	0.023360694	0.7358805	down
0.010145176	0.786898618	down	217973_at	0.032513608	0.79597311	down
0.009922084	0.607222597	down	214347_s_at	0.044019304	0.80534061	down
0.001542277	0.732385049	down	1554621_at	0.00458111	0.67343	down
0.025616242	0.868767128	down	222574_s_at	0.004434447	0.81599767	down
0.007137358	0.785091869	down	204505_s_at	0.002984048	0.75227057	down
0.027508954	1.323932707	up	202867_s_at	0.017440212	0.83888171	down
0.012263013	0.807628253	down	205186_at	0.038867902	0.83787015	down
0.035721199	0.839981088	down	203912_s_at	0.017934151	0.85380739	down
0.018804796	0.849655188	down	227374_at	0.00180359	0.77929533	down
0.02474026	1.272050943	up	225546_at	0.033324607	1.2837015	up
0.019486231	1.176657606	up	225461_at	0.037110507	1.19717342	up
0.041703463	0.910589047	down	208670_s_at	0.040219728	0.86513324	down
0.04523539	0.8548898	down	223286_at	0.047902205	0.87840952	down
0.019127208	0.869972205	down	229863_s_at	0.005004214	0.806359	down
0.037532766	0.887220992	down	204399_s_at	0.025964306	0.85283015	down
0.041794238	0.807103887	down	212573_at	0.000110589	0.7402127	down
0.001696579	0.757362774	down	212336_at	0.000167479	0.78793246	down
0.010064855	0.908252644	down	209009_at	0.004076666	0.87728892	down
0.002979675	0.758386825	down	205530_at	0.039578418	0.81951101	down
0.009056804	1.537976164	up	226568_at	0.021574242	1.63607605	up
0.020424435	0.642070663	down	207547_s_at	0.035694845	0.66752343	down
0.049234771	0.79407629	down	235378_at	0.044577677	0.79309851	down
0.00041512	0.780631099	down	203986_at	0.011359961	0.71356713	down
0.01045168	0.826025451	down	205775_at	0.039748229	0.82607554	down
0.007948091	0.846109313	down	229135_at	0.008307598	0.81744868	down
0.001116983	1.447799427	up	225328_at	0.007666423	1.50543848	up
0.032649645	1.248078535	up	218539_at	0.034703981	0.83141009	down
0.011086116	0.60436801	down	240856_at	0.00179547	0.56624459	down
0.006314982	1.46597988	up	226799_at	0.023759143	1.36285114	up
0.014196313	0.922546095	down	203033_x_at	0.012205241	0.86592491	down
0.043041118	0.867778697	down	232186_at	0.006780445	0.76614289	down
0.00032856	1.361022579	up	225163_at	0.013263041	1.42387468	up
0.002458675	0.712183519	down	223702_x_at	0.002209142	0.55666025	down
0.011470618	0.788687095	down	201635_s_at	0.023279059	0.77816163	down
0.001116983	0.601726218	down	205674_x_at	0.000233319	0.6941291	down
0.000764088	0.594207109	down	207434_s_at	0.000191316	0.70001223	down
0.034398746	0.616120014	down	221453_at	0.027726139	0.64263027	down
0.035138699	1.396885271	up	205278_at	0.000807185	3.08148079	up
0.04122221	1.201547242	up	203397_s_at	0.019045987	1.25433648	up
0.019389013	0.610768063	down	204471_at	0.023279059	1.87972886	up

Confidential

0.018190481	1.104661673	up	222526_at	0.046900689	0.86565697	down
0.006334404	0.777377703	down	210565_at	0.002465318	0.74408911	down
0.005298122	0.793044395	down	213772_s_at	0.011120206	0.84410519	down
0.026666686	1.184245476	up	230258_at	0.004171036	0.73896721	down
0.029833823	0.728382352	down	205279_s_at	0.015520394	0.78926725	down
0.013164623	1.140928314	up	230613_at	0.038724161	0.7676914	down
0.002060835	0.699579429	down	206896_s_at	2.29E-05	0.69775862	down
0.033258477	0.842956609	down	202382_s_at	0.020691654	0.81774681	down
0.018029091	0.768825317	down	213180_s_at	0.020767817	0.82153066	down
0.025187519	0.876829359	down	208813_at	6.78E-05	0.75819513	down
0.025607116	0.872964581	down	234055_s_at	0.048832168	0.84282504	down
0.024013623	0.840339768	down	233919_s_at	0.033700454	0.81925915	down
0.003712644	0.684866125	down	201035_s_at	0.021574242	0.74246903	down
0.034831766	0.895758348	down	208631_s_at	0.035169854	0.89540714	down
0.014340757	0.702556874	down	230208_at	0.000836924	0.56570421	down
0.000109785	0.388328422	down	223572_at	0.000444501	0.41470383	down
0.02250557	0.673280902	down	204755_x_at	0.045243299	0.80605437	down
0.031664727	0.887880875	down	210515_at	0.033700454	0.79641019	down
0.032526999	1.35178575	up	221919_at	0.046480575	1.27158275	up
0.034547237	1.127872011	up	213359_at	0.010159228	1.27813323	up
0.030354564	1.159014833	up	201626_at	0.015858218	1.26735429	up
0.001623508	1.535204265	up	238933_at	0.049719976	1.2940884	up
0.008353499	0.620110063	down	1552897_a_at	0.036389508	0.68775855	down
0.010945398	1.528756925	up	1552742_at	0.017440212	1.64378887	up
0.005083254	1.746098712	up	228579_at	0.048832168	0.68479388	down
0.029065848	1.188222942	up	226367_at	0.047622941	0.86370147	down
0.008477285	0.701023426	down	244076_at	0.018142362	0.66787643	down
0.016027538	0.85132748	down	1555815_a_at	0.04881115	0.83976576	down
0.007513885	0.791635506	down	221847_at	0.01985344	0.86291628	down
0.039243058	0.705879727	down	1568625_at	0.01755045	0.70438824	down
0.02542125	0.752424992	down	227985_at	0.032791427	1.29438805	up
0.002103372	0.483472896	down	1559546_s_at	0.042924611	0.69435372	down
0.047740556	0.770088662	down	243749_s_at	0.03874566	0.83610827	down
0.012811444	0.650576211	down	214130_s_at	0.04881115	0.81368626	down
0.018820098	0.770346637	down	239763_at	0.000388159	0.70500475	down
0.045558147	1.119976073	up	226468_at	0.000747873	0.7994285	down
0.013822822	1.438570814	up	1566766_a_at	0.042114984	1.34316183	up
0.045672652	1.090095746	up	222372_at	0.005956976	1.5972291	up
0.002060835	1.366823113	up	226538_at	0.001250028	1.18559054	up
0.014027871	0.65440405	down	203151_at	0.002257989	0.74284995	down
0.006780952	0.818984699	down	204936_at	0.009361376	0.81956532	down
0.031357672	0.883406253	down	1553987_at	0.048633161	0.85617562	down
0.004419113	0.790779413	down	208595_s_at	0.025410522	0.87104393	down
0.003903313	0.73835395	down	230113_at	0.000167479	0.69950677	down
0.031380227	0.780265865	down	229797_at	0.006016316	0.71573892	down
0.000107649	0.830673086	down	200978_at	0.009943882	0.88936765	down
0.002330798	0.853970065	down	51176_at	0.049177979	0.82249498	down
0.048718035	0.87276095	down	217959_s_at	0.016201736	0.82436584	down
0.025050925	0.843587613	down	218869_at	0.005172062	0.80305563	down
0.006061483	0.752082489	down	214614_at	0.024462747	0.79197666	down
0.001693251	0.836387104	down	236208_at	0.039682329	0.77549153	down

Confidential

0.032476999	0.90347663	down	218024_at	0.025964306	0.87251504	down
0.004324388	0.698073148	down	202974_at	0.00541924	0.82439361	down
0.009861547	0.867983435	down	224535_s_at	0.024340137	0.84969713	down
0.044662984	0.883024873	down	222216_s_at	0.017254019	0.85333797	down
0.049745843	0.832612682	down	203801_at	0.043481433	0.84311912	down
0.020545813	1.24601905	up	228019_s_at	0.016124945	0.82641675	down
0.036882274	0.888777974	down	224765_at	0.002462133	1.19581419	up
0.021636705	1.392005145	up	212095_s_at	0.026564692	1.47194054	up
0.006501177	0.635834785	down	1554755_a_at	0.02430375	0.72656564	down
0.040623971	1.16827563	up	213375_s_at	0.032871583	1.19257668	up
0.017641258	0.820498871	down	206491_s_at	0.023233557	0.82652254	down
0.014058927	0.857771018	down	225657_at	0.003134964	0.80922549	down
0.000362726	0.841577111	down	201226_at	0.036389508	0.86823852	down
0.037091789	0.758877762	down	232146_at	0.016045413	0.76234573	down
0.00797413	0.890832151	down	203039_s_at	0.046540194	0.88579418	down
0.035422535	0.863649647	down	208926_at	0.024331093	0.854388	down
0.047694868	1.14313198	up	225141_at	0.029585721	0.85825412	down
0.01631664	0.863805399	down	202584_at	0.018567785	0.85903773	down
0.000628638	0.841049038	down	224281_s_at	0.002700057	0.831584	down
0.011555232	0.712082011	down	230443_at	0.004870179	0.71383507	down
0.048940865	0.83117689	down	201708_s_at	0.044147641	0.85264868	down
0.021200808	0.804148936	down	221366_at	0.023279059	0.72772064	down
0.001210758	0.568077446	down	220106_at	0.04881115	0.68735488	down
0.00474865	0.685433952	down	209569_x_at	0.000859566	0.60952245	down
0.001885472	0.818894566	down	223272_s_at	0.027720792	0.83734348	down
0.014400375	0.811110669	down	204479_at	0.037110507	0.8434338	down
0.044662221	0.810177198	down	202780_at	0.03713019	0.8444867	down
0.049795622	0.849662534	down	202336_s_at	0.026904667	1.10076542	up
0.012464053	0.81642314	down	204476_s_at	0.000167479	0.70757152	down
0.014903202	0.848655532	down	212694_s_at	0.009570038	0.81421965	down
0.029867164	0.627543524	down	232054_at	0.040219728	0.61202635	down
0.005506882	0.873836893	down	210156_s_at	0.039011615	0.86512451	down
0.006236375	0.565960622	down	1554789_a_at	0.048767881	0.71782827	down
0.008371322	0.537087542	down	225207_at	0.036067412	1.31762984	up
0.003164747	0.816424122	down	225075_at	0.001511275	0.82956566	down
0.002520735	0.792332837	down	211941_s_at	0.019798048	0.81339562	down
0.020241831	0.881109565	down	203972_s_at	0.010159228	0.83329991	down
0.047020906	0.922702562	down	207132_x_at	0.022117813	0.94123177	down
0.008533104	0.722334557	down	209992_at	0.028327718	0.64409516	down
0.025199444	1.34154555	up	223738_s_at	0.0131702	0.7520895	down
0.011228198	1.439596518	up	223470_at	0.026454016	0.83048972	down
0.001693251	0.836050146	down	208996_s_at	0.003012657	0.85528957	down
0.000307316	0.418784329	down	235129_at	5.54E-06	0.47499525	down
0.017136065	1.179984807	up	225429_at	0.046900689	0.8588385	down
0.005112362	0.861662302	down	222994_at	0.036389508	0.86284134	down
0.010290822	0.794113622	down	233748_x_at	0.020345406	0.79646366	down
0.020382763	0.884901006	down	215707_s_at	0.045941926	0.80390397	down
0.03038177	0.850720766	down	208447_s_at	0.033324607	0.77180582	down
0.032308851	0.822780827	down	209337_at	0.048177707	0.88665113	down
0.040784184	0.810637602	down	201532_at	0.007327105	0.81984019	down
0.047740556	0.923979899	down	201068_s_at	0.011052665	0.88004881	down

Confidential

0.034398746	1.180009319	up	201052_s_at	0.004765777	0.84959192	down
0.001948309	1.383162021	up	202006_at	0.018421407	1.23870934	up
0.015125958	0.829375512	down	203997_at	0.00028931	0.72983115	down
0.028785752	1.089297002	up	200677_at	0.010302532	1.12854625	up
0.000568922	0.80973396	down	231715_s_at	0.045214319	0.84838307	down
0.011138596	0.769730314	down	238616_at	0.048845033	1.22991187	up
0.034491919	0.869391562	down	235059_at	0.044111992	0.74131314	down
0.003808763	0.799805142	down	218526_s_at	0.0131702	0.80900883	down
0.018525718	0.680729201	down	210550_s_at	0.03874566	0.68121786	down
0.00815566	0.730911837	down	203498_at	0.016426846	0.835239	down
0.022338975	0.663349297	down	209324_s_at	0.038018433	1.68690186	up
0.020297977	0.794174596	down	221287_at	0.028471808	0.8296039	down
0.002035979	1.301427241	up	203286_at	0.02160946	1.17481511	up
0.023555098	0.863344208	down	1557984_s_at	0.018670428	0.7656365	down
0.013164623	0.817232413	down	200724_at	0.016158782	0.85100837	down
0.003903313	0.780178669	down	221524_s_at	0.000633432	0.75711409	down
0.01596598	0.869218363	down	200042_at	0.001915434	0.83540029	down
0.003893582	1.207445633	up	230832_at	0.012205241	0.78750867	down
0.009424031	0.893468426	down	233842_x_at	0.016512858	0.89354376	down
0.03880597	0.888264455	down	1555679_a_at	0.041349076	0.75427103	down
0.008622011	0.770624953	down	208740_at	0.016218389	0.83647707	down
0.023278269	1.156184997	up	203408_s_at	0.017480958	1.20366498	up
0.013889268	1.318882231	up	213435_at	0.037779	1.48430871	up
0.045437858	0.931509978	down	1554089_s_at	0.03874566	0.86116067	down
0.005144576	0.712216447	down	204035_at	0.045243299	1.21575328	up
0.004681447	0.530992324	down	1565737_at	0.000830588	0.49491227	down
0.001895465	0.656966719	down	213169_at	0.007327105	0.78355283	down
0.006425432	0.643980026	down	1562239_at	0.009956781	0.67139055	down
0.028529126	1.201868614	up	202896_s_at	0.009956781	1.51787687	up
0.000165678	0.272505791	down	206535_at	1.74E-08	0.36188348	down
0.015772696	0.817310154	down	217289_s_at	0.011701185	0.71186576	down
0.01060942	1.246962132	up	215979_s_at	0.03340409	0.79859917	down
0.012314612	0.834564303	down	229826_at	0.040582908	0.82680812	down
0.041889236	0.895610209	down	1554093_a_at	0.007778399	0.79690782	down
0.021629795	0.742959089	down	231112_at	0.00263063	0.71972915	down
0.012177856	0.911227683	down	200642_at	0.027174567	0.8999287	down
0.001797169	1.424236903	up	244461_at	0.047293735	0.74401292	down
0.049729083	1.126877793	up	224638_at	0.005600533	0.80886244	down
0.019181606	0.881618741	down	224551_s_at	0.027726139	0.90105655	down
0.040630569	0.792622416	down	218140_x_at	0.048017948	0.84621774	down
0.019127208	1.134476952	up	223266_at	0.024842701	1.16848089	up
0.00606235	0.830287757	down	1553030_a_at	0.041394767	0.82719092	down
0.002458675	0.765369743	down	230006_s_at	0.001750554	0.77709876	down
0.006744731	0.579812997	down	229818_at	0.003993792	0.70823454	down
0.002750252	0.818081822	down	226027_at	0.009989861	0.85274717	down
0.003448263	0.563309552	down	1553264_a_at	0.040087556	0.84243643	down
0.046550685	1.257933493	up	217833_at	0.048832168	0.89302362	down
0.040152674	1.189703627	up	224668_at	0.001570924	0.76399938	down
0.019500599	0.729276306	down	1563658_a_at	0.003798678	0.70547769	down
0.027365648	0.870729156	down	225818_s_at	0.03497124	0.86660067	down
0.037787497	1.164914269	up	238346_s_at	0.023086083	0.84382281	down

Confidential

0.004221604	0.851509142	down	225741_at	0.049665366	0.86647214	down
0.039979829	0.871147658	down	223711_s_at	0.038800467	0.86446552	down
0.028122583	0.732229811	down	226489_at	0.022081432	0.76432987	down
0.001693251	0.855056554	down	221622_s_at	0.049012222	0.86672051	down
0.019704199	1.376368968	up	232313_at	0.010229799	1.6871888	up
0.024270406	0.809231875	down	225568_at	0.027595293	0.83291173	down
0.045953521	1.117807019	up	213285_at	0.011754956	0.85922502	down
0.003903313	0.653787177	down	227190_at	3.84E-09	0.50385956	down
0.026131182	0.747763952	down	239288_at	0.005076699	0.65490736	down
0.019587236	0.828238257	down	233881_s_at	0.043589302	0.84525439	down
0.041593435	0.837986256	down	213011_s_at	0.040087556	0.90993463	down
0.031380227	0.81300099	down	223686_at	0.035357752	0.73532967	down
0.006158636	0.783927374	down	201731_s_at	0.009361376	0.89978817	down
0.046608887	1.21414188	up	230243_at	0.01076636	1.29771502	up
0.032738702	0.796821574	down	1552307_a_at	0.02487245	0.64225844	down
0.034169168	0.881401532	down	209078_s_at	0.032754493	0.84647065	down
0.032457424	0.736953794	down	235561_at	0.019211851	0.76743178	down
0.010080029	0.851521181	down	221949_at	0.001514906	0.79410778	down
0.012940581	0.535335631	down	231325_at	0.012049363	0.58926933	down
0.002474492	0.823655254	down	223613_at	0.00908106	0.82600286	down
0.02726197	0.832176254	down	223602_at	0.045770097	0.86375793	down
0.003530864	0.553405809	down	226415_at	0.03874566	0.73729541	down
0.002458675	0.904069817	down	208846_s_at	0.03713019	0.88011628	down
0.031869998	0.871763085	down	217949_s_at	0.03212996	1.17844502	up
0.045673227	0.910729232	down	227814_at	0.018381742	0.80243407	down
0.009346535	0.725695097	down	1555270_a_at	0.027536734	0.78454441	down
0.034398746	1.294824771	up	229103_at	0.004053502	1.71073244	up
0.044832185	1.129041776	up	203137_at	0.036635214	0.87071167	down
0.042165734	1.151033678	up	201902_s_at	0.013929655	0.76415452	down
0.007232404	0.673214337	down	207402_at	0.042823153	0.74391259	down
0.044940734	0.864887327	down	206182_at	0.015515613	0.78358119	down
0.009127681	0.838923613	down	206240_s_at	0.006363703	0.79468069	down
0.033067385	0.66115883	down	232986_at	0.008479664	0.70721027	down
0.001559339	0.630024603	down	242697_at	0.0232671	0.75743314	down
0.049965295	0.844421298	down	1553286_at	0.025964306	0.81526356	down
0.008616409	0.715203176	down	238708_at	0.002467787	0.73615461	down
0.030974964	0.836046202	down	1553703_at	0.04881115	0.81918891	down

Confidential